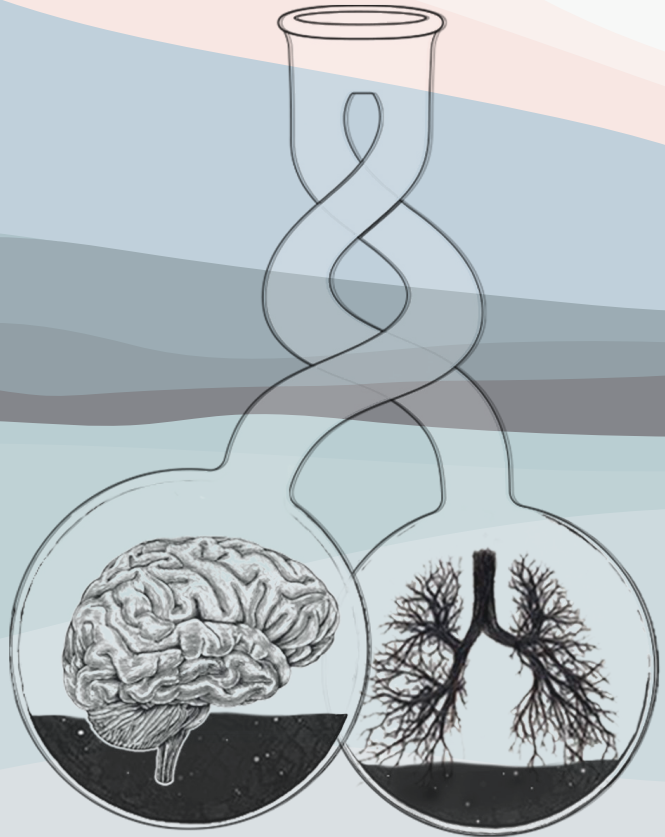
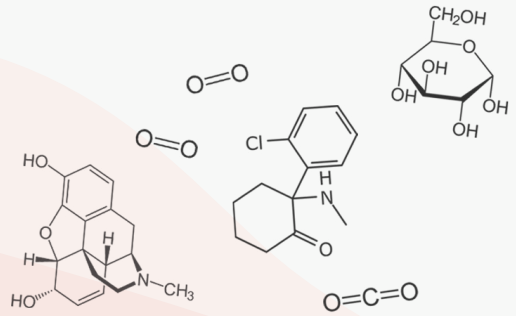


# Pharmacotherapy and Ventilatory Control in Health and Disease

Pieter Simons





---

**Pharmacotherapy  
and  
Ventilatory Control**  
in Health and Disease

Pieter Simons

---

The investigations described in chapters 2-5 of this thesis were performed in the Anesthesia & Pain Research Unit, Leiden University Medical Center, under the supervision of prof. dr. A. Dahan and dr. R. van der Schrier.

Copyright © 2024 *Pieter Simons*.

ISBN 978-94-6506-095-8

No part of this publication may be reproduced, stored in a retrieval system, or transmitted, in any form or by any means, electronic, mechanical, photocopying, recording, or otherwise, without prior permission of the author.

Typeset by L<sup>A</sup>T<sub>E</sub>X

Cover design by Anneriek Simons

Printed by Ridderprint, the Netherlands

The printing of this thesis was financially supported by: ChipSoft and Trevena.

---

# Pharmacotherapy and Ventilatory Control

in Health and Disease

PROEFSCHRIFT

ter verkrijging van  
de graad van Doctor aan de Universiteit Leiden,  
op gezag van Rector Magnificus Prof. dr. ir. H. Bijl,  
hoogleraar in de Faculteit der Wiskunde en Natuurwetenschappen,  
volgens besluit van het College voor Promoties  
te verdedigen op *5 juni 2024*  
klokke *11:15* uur

door

Pieter Simons  
geboren te Enschede  
in 1991

---

## Promotiecomissie

Promotor: Prof. dr. A. Dahan

Copromotores: Dr. M. Niesters  
Dr. M. van Velzen

Commissie: Prof. dr. E.Y. Sarton  
Prof. dr. S. B. Karan (Rochester Medical Center)  
Prof. dr. dr. M.W. Hollmann (Amsterdam UMC)  
Prof. dr. H. Pijl  
Prof. dr. J. Swen

---

*The marriage of breath and beat is critical for life.*

Ken D. O'Halloran - 2023





# Contents

1	Introduction	1
2	<i>S</i> -ketamine oral thin film pharmacokinetics	13
3	<i>S</i> -ketamine oral thin film pharmacodynamics	41
4	Oliceridine respiratory effects	65
5	Diabetes, hyperinsulinemia, and the hypoxic ventilatory response	99
6	Summary, conclusions, and perspectives	121
7	Nederlandse samenvatting	131
	Addenda	135



# List of Figures

2.1	<i>S</i> -ketamine PK - Plasma concentrations . . . . .	22
2.2	<i>S</i> -ketamine PK - Final PK model . . . . .	26
2.3	<i>S</i> -ketamine PK - Goodness of Fit (GOF) plots . . . . .	30
2.4	<i>S</i> -ketamine PK - Simulations . . . . .	31
2.5	<i>S</i> -ketamine PK - Simulations HNK . . . . .	35
3.1	<i>S</i> -ketamine PD - Pharmacokinetic data . . . . .	49
3.2	<i>S</i> -ketamine PD - Antinociceptive data . . . . .	49
3.3	<i>S</i> -ketamine PD - Goodness-of-Fit plots . . . . .	52
3.4	<i>S</i> -ketamine PD - Drug high data . . . . .	53
3.5	<i>S</i> -ketamine PD - Visual Predictive Checks . . . . .	54
3.6	<i>S</i> -ketamine PD - Steady-state concentration-effect relationships .	55
4.1	Oliceridine respiratory effects - $\dot{V}_{E55}$ for four treatment arms . .	74
4.2	Oliceridine respiratory effects - Mean pharmacokinetic data . . .	76
4.3	Oliceridine respiratory effects - Goodness-of-Fit PK data . . . . .	77
4.4	Oliceridine respiratory effects - Population PK model outcome .	78
4.5	Oliceridine respiratory effects - Population PD model outcome .	81
4.6	Oliceridine respiratory effects - Goodness-of-Fit PD data . . . . .	82
4.7	Oliceridine respiratory effects - Simulation multiple dosing . . . .	85
4.8	Oliceridine respiratory effects - Queried adverse events . . . . .	87
5.1	CB Hypoxia - Strobe diagram . . . . .	105
5.2	CB Hypoxia - HVR . . . . .	108
5.3	CB Hypoxia - Dejour . . . . .	109
5.4	CB Hypoxia - Hemodynamics . . . . .	111



# List of Tables

2.1	<i>S</i> -ketamine PK - Subject characteristics . . . . .	20
2.2	<i>S</i> -ketamine PK - Pharmacokinetic parameters OTF . . . . .	23
2.3	<i>S</i> -ketamine PK - Adverse effects . . . . .	24
2.4	<i>S</i> -ketamine PK - OTF pharmacokinetics . . . . .	27
3.1	<i>S</i> -ketamine PD - Pharmacodynamic parameter estimates . . . . .	51
4.1	Oliceridine respiratory effects - PK parameter estimates . . . . .	79
4.2	Oliceridine respiratory effects - PD parameter estimates . . . . .	83
4.3	Oliceridine respiratory effects - Adverse effects . . . . .	86
5.1	CB Hypoxia - Subject characteristics . . . . .	106



## Chapter 1

# Introduction

---

## Background

Inherently dangerous, anesthesia has matured into an essentially safe practice due to major advancements in the field. Over the decades, even since the 1950s, the field of anesthetic and perioperative care has witnessed a continuous decline in mortality rates.<sup>1</sup> These advancements can be attributed to the utilization of safer anesthetic agents, the development of advanced technical instruments and techniques, and comprehensive training programs, among other pivotal factors. Despite these remarkable progressions, challenges and gaps in our understanding persist.

The evolution of drug use in anesthesiology is particularly noteworthy. Initially focused on facilitating surgical procedures and enhancing patient health outcomes, in the current landscape of 2023, anesthetics have expanded their applications well beyond the confines of the operating room. They are now integral in diverse medical contexts, including trauma care, resuscitation, sedation, intensive care, and the management of acute and chronic pain.<sup>2</sup> Furthermore, the exploration of unconventional agents, such as psychedelics for pain, and the use of anesthetic agents in other disciplines, underscores the dynamic nature of modern medical practice and interdisciplinary research.<sup>3</sup>

For instance, consider ketamine, an *N*-methyl-D-aspartate receptor (NMDAR) blocker, introduced as an intravenous anesthetic in 1965. Since the 1990s its applications have extended to include the management of acute and chronic pain. More recently, since the early 2000s, nasal *S*-ketamine marketed as Spravato, has also found utility in psychiatry, offering an alternative treatment for therapy-resistant depression and post-traumatic stress disorder. This presents a potential replacement for traditional treatments like electroconvulsive therapy or antipsychotic therapy in specific cases.<sup>4,5</sup> Studies on this fascinating drug can be advantageous for both the fields of psychiatry and anesthesiology.

One persistent challenge of drugs in anesthesiology revolves around the efficacy and side-effect profile of contemporary analgesics. Both non-opioid and opioid analgesics, while indispensable in pain management, exhibit limitations in certain patient groups, particularly those suffering from chronic pain. Conversely, these drugs have adverse effects, including the potential for abuse, as observed with ketamine and opioids, as well as the life-threatening risk of opioid-induced respiratory depression. The combination of addiction and respiratory depression stands at the core of the current opioid epidemic in the United States, characterized by more than 100,000 deaths from opioid overdose in 2022.<sup>6</sup>

Both the efficacy and side-effect profile of these analgesics are intertwined with the critical role played by the patient's phenotype. "*One Size Fits All*" is a thing of the past and research and guidelines are increasingly tailored to



individual factors due to the heterogeneity of clinical effects. Notably, a recent observational study involving over 1,300 patients highlighted that factors such as male sex, older age, opioid naivety, sleep-disordered breathing, and heart failure are associated with an increased risk of opioid-induced respiratory depression.<sup>7</sup> Additional risk factors encompass the presence of comorbidities, concomitant use of systemic opioids and sedatives, and higher BMI.<sup>8,9</sup> While clinical trials, typically conducted on young and healthy subjects, illuminate drug effects, questions are raised about the applicability of their findings. Therefore, we focus on studying a new opioid in a representative study sample comprising male and female volunteers of older age, including overweight participants.

Of particular interest is the role of obesity as a risk factor for opioid-induced respiratory depression. Obesity's global prevalence is staggering, and it directly heightens the risk of opioid-induced respiratory depression due to obesity-related changes in the respiratory system, alterations in respiratory drive, and breathing abnormalities during sleep.<sup>9,10</sup> Furthermore, obesity increases the likelihood of developing insulin resistance and type 2 diabetes. Intriguingly, studies indicate that insulin resistance can modulate ventilatory drive, and type 2 diabetes can lead to the development of sleep-disordered breathing, independent of obesity.<sup>11,12,13</sup> While speculative, these factors may contribute to an elevated risk of premature mortality among individuals with type 2 diabetes who use opioids over an extended period.<sup>14</sup>

In this thesis, I will present a series of studies conducted in our laboratory, focusing on the pharmacology of ketamine oral and buccal thin film, intravenous oliceridine and morphine, and type 2 diabetes. The studies encompass pharmacological aspects (ketamine, oliceridine, and morphine) and their effects on ventilatory control (morphine, oliceridine, and type 2 diabetes), spanning the important effects of these drugs in clinical practice.

### Thesis overview

While ketamine has been used for nearly six decades, ongoing developments have led to new indications and new formulations are still being developed. As an analgesic, ketamine is employed in the prehospital setting, emergency ward, perioperatively, and for chronic pain syndromes.<sup>15,16,17,18</sup> Substantial gaps persist in our understanding of its efficacy and safety when considering different routes of administration, varied durations, dosages, and distinct enantiomers in diverse clinical contexts.

This thesis delves into the pharmacology of a novel *S*-ketamine oral and buccal thin film in **Chapters 2 and 3**, exploring its pharmacokinetics and pharmacodynamics, respectively. To achieve this, we employ a population pharmacokinetic/pharmacodynamic model, which integrates the changes in

---

concentration over time with the relationship between the concentration at the effect site and the intensity of the observed response, while considering multiple covariables.<sup>19</sup> While the precise clinical indications for *S*-ketamine films remain undefined, our research primarily centers on evaluating its analgesic efficacy and its profile of side effects. It is conceivable that this thin film formulation may eventually find application as a potential treatment for therapy-resistant depression, akin to its intranasal counterpart.

In **Chapter 4**, we compare the respiratory effects of oliceridine, a *mu*-opioid receptor agonist with biased characteristics, to morphine, a prototypical *mu*-opioid receptor agonist. The concept of biased agonism, or functional selectivity, underscores the origins of these distinctive characteristics.<sup>20</sup> The respiratory effects of opioids are exerted via *mu*-opioid receptors in important brainstem respiratory centers. Upon binding to the *mu*-opioid receptor, opioids trigger the activation of distinct intracellular pathways. Earlier studies pointed towards the role of *beta*-arrestin recruitment in adverse effects of opioids, including respiratory depression.<sup>21</sup> This understanding paved the way for the development of oliceridine, a *mu*-opioid receptor agonist exhibiting a pronounced bias in favor of G-protein signaling.<sup>22</sup> The resultant net effect is an opioid that mitigates the extent of respiratory depression, offering a potential therapeutic advantage.

Finally, in **Chapter 5**, we explore the effect of type 2 diabetes and hyperinsulinemia on ventilatory control. Only recently, a link between metabolic disorders and changes in ventilatory control has been established in animal and preclinical studies.<sup>23,24,25</sup> These changes comprise changes in chemoreflex sensitivity, modifications in breathing patterns, and adjustments in carotid-body mediated sympathetic outflow.<sup>26,27,28</sup> Given the increased incidence, morbidity, and mortality associated with SARS-COV-2 among individuals with type 2 diabetes, our particular interest was the ventilatory effect of hypoxia in this group of patients. The hypoxic ventilatory response is crucial in determining an individual's predisposition to hypoxia-related pathologies. Therefore, this response was obtained in individuals with type 2 diabetes and compared to healthy controls, both during fasting conditions and under the influence of a hyperinsulinemic-euglycemic clamp. This study provides insight into the effects of metabolic dysregulation on ventilatory control. Given the large increase in patients with type 2 diabetes worldwide, this is an important study that may guide our approach to type 2 diabetics, particularly under conditions of changes in ventilatory control, such as those encountered perioperatively or following opioid administration.

## Ventilatory control

Two chapters in this thesis are dedicated to ventilatory control and the effect of drugs (morphine and oliceridine in **Chapter 4**) and type 2 diabetes (**Chapter 5**) on the ventilatory control system. In the field of anesthesiology, the study of ventilatory control has been of particular interest due to its implications for patient safety. Comprehending its underlying mechanisms is crucial, since disturbances in the normal respiratory rhythm generation may have severe cardiorespiratory consequences.

The generation of respiratory rhythms occurs in specialized respiratory networks located in the pons and medulla. These networks receive afferent input from various sources, including the central and peripheral chemoreceptors, mechanoreceptors, and behavioral control from higher centers.<sup>29</sup> The central chemoreceptors, dispersed in the hindbrain, sense minor changes in  $\text{CO}_2/\text{H}^+$  within the cerebrospinal fluid.<sup>30</sup> The carotid bodies, the main peripheral chemoreceptors located in the fork of the carotid arteries, monitor hypoxia, hypercapnia as well as a variety of metabolic stimuli including arterial blood glucose concentrations.<sup>31</sup> These chemoreceptors work together in an additive fashion. Upon metabolic acidosis, the input from the chemoreceptors activates the respiratory networks causing a hyperventilatory response, aimed at compensating the metabolic acidosis. A similar response is triggered by the exogenous administration of carbon dioxide, the hypercapnic ventilatory response or HCVR, and is used to determine the sensitivity of the ventilatory control system to  $\text{CO}_2$ . The HCVR is particularly sensitive to the effects of opioids.

In case of hypoxia, the carotid bodies are activated and a hyperventilatory response occurs that is biphasic.<sup>32</sup> An initial acute response is followed by a slow decline, the hypoxic ventilatory decline. The secondary adaptation has a central origin, although its exact mechanism has yet to be elucidated. Apart from inducing a brisk hypoxia-induced hyperventilatory response, the carotid bodies induce an arousal response, as is observed in patients with obstructive sleep apnea. The obstruction and ensuing hypoxia stimulate the carotid bodies, causing an arousal response that clears the upper airways, followed by a short hyperventilatory response.

In **Chapter 4**, we obtain hypercapnic ventilatory responses induced by  $\text{CO}_2$  rebreathing according to the method developed by the Australian investigator D.J.C Read in the mid-1960s. Inhalation of 7%  $\text{CO}_2$  (in 93%  $\text{O}_2$ ) from a 4-6 liter rebreathing bag results in a linear increase in ventilation. We used the ventilation at an extrapolated end-tidal  $\text{PCO}_2$  of 55 mmHg as the main endpoint in our study. Recent studies from our laboratory indicate that this is the most sensitive parameter when determining the effect of drugs on ventilatory control.<sup>33</sup>

In **Chapter 5**, we use the more sophisticated dynamic end-tidal forcing

---

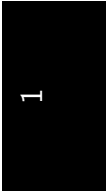
technique to obtain the ventilatory response to acute (5 min) hypoxia. This technique uses computer-controlled feedforward input to a series of mass flow controllers that allow manipulation of the inspired gas concentrations to induce a change in end-tidal gas concentration (and thus also arterial gas concentration) independent of the content of the venous return.

### Study objectives

The objectives of this thesis are:

1. To quantify the pharmacokinetics and pharmacodynamics (pain relief and psychomimetic adverse effects) of a novel *S*-ketamine oral thin film;
2. To quantify the pharmacokinetics and respiratory pharmacodynamics of the biased ligand oliceridine, in comparison to morphine;
3. Explore the effects of insulin on the hypoxic ventilatory response in type 2 diabetics compared to healthy controls.





## References

1. Bainbridge D, Martin J, Arango M, Cheng D. Perioperative and anaesthetic-related mortality in developed and developing countries: a systematic review and meta-analysis. *The Lancet*. 2012; **380**: 1075–1081  
DOI: 10.1016/S0140-6736(12)60990-8.
2. Nagrebetsky A, Gabriel RA, Dutton RP, Urman RD. Growth of Nonoperating Room Anesthesia Care in the United States: A Contemporary Trends Analysis. *Anesthesia & Analgesia*. 2017; **124**: 1261–1267  
DOI: 10.1213/ane.0000000000001734.
3. Goel A, Rai Y, Sivadas S, Diep C, Clarke H, Shanthanna H, Ladha KS. Use of Psychedelics for Pain: A Scoping Review. *Anesthesiology*. 2023; **139**: 523–536  
DOI: 10.1097/aln.0000000000004673.
4. Anand A et al. Ketamine versus ECT for Nonpsychotic Treatment-Resistant Major Depression. *New England Journal of Medicine*. 2023; **388**: 2315–2325  
DOI: 10.1056/nejmoa2302399.
5. Reif A, Bitter I, Buyze J, Cebulla K, Frey R, Fu DJ, Ito T, Kambarov Y, Llorca PM, Oliveira-Maia AJ, Messer T, Mulhern-Haughey S, Rive B, Holt C von, Young AH, Godinov Y. Esketamine Nasal Spray versus Quetiapine for Treatment-Resistant Depression. *New England Journal of Medicine*. 2023; **389**: 1298–1309  
DOI: 10.1056/nejmoa2304145.
6. Humphreys K, Shover CL, Andrews CM, Bohnert ASB, Brandeau ML, Caulkins JP, Chen JH, Cuellar MF, Hurd YL, Juurlink DN, Koh HK, Krebs EE, Lembke A, Mackey SC, Larrimore Ouellette L, Suffoletto B, Timko C. Responding to the opioid crisis in North America and beyond: recommendations of the Stanford-Lancet Commission. *The Lancet*. 2022; **399**: 555–604  
DOI: 10.1016/S0140-6736(21)02252-2.

## References

---

7. Khanna AK et al. Prediction of Opioid-Induced Respiratory Depression on Inpatient Wards Using Continuous Capnography and Oximetry: An International Prospective, Observational Trial. *Anesthesia & Analgesia*. 2020; **131**: 1012–1024  
DOI: 10.1213/ane.0000000000004788.
8. Overdyk FJ, Dowling O, Marino J, Qiu J, Chien HL, Ersilon M, Morrison N, Harrison B, Dahan A, Gan TJ. Association of Opioids and Sedatives with Increased Risk of In-Hospital Cardiopulmonary Arrest from an Administrative Database. *PLOS ONE*. 2016; **11**: e0150214  
DOI: 10.1371/journal.pone.0150214.
9. Dahan A, Aarts L, Smith TW. Incidence, Reversal, and Prevention of Opioid-induced Respiratory Depression. *Anesthesiology*. 2010; **112**: 226–238  
DOI: 10.1097/ALN.0b013e3181c38c25.
10. Piper AJ, Grunstein RR. Big breathing: the complex interaction of obesity, hypoventilation, weight loss, and respiratory function. *Journal of Applied Physiology*. 2010; **108**: 199–205  
DOI: 10.1152/jappphysiol.00713.2009.
11. Ramadan W, Dewasmes G, Petitjean M, Wiernsperger N, Delanaud S, Geloën A, Libert JP. Sleep Apnea Is Induced by a High-fat Diet and Reversed and Prevented by Metformin in Non-obese Rats\*. *Obesity*. 2007; **15**: 1409–1418  
DOI: 10.1038/oby.2007.169.
12. Lecube A, Simó R, Pallayova M, Punjabi NM, López-Cano C, Turino C, Hernández C, Barbé F. Pulmonary Function and Sleep Breathing: Two New Targets for Type 2 Diabetes Care. *Endocrine Reviews*. 2017; **38**: 550–573  
DOI: 10.1210/er.2017-00173.
13. Sánchez E, Sapiña-Beltrán E, Gavaldà R, Barbé F, Torres G, Sauret A, Dalmases M, López-Cano C, Gutiérrez-Carrasquilla L, Bermúdez-López M, Fernández E, Purroy F, Castro-Boqué E, Farràs-Sallés C, Pamplona R, Mauricio D, Hernández C, Simó R, and AL. Prediabetes Is Associated with Increased Prevalence of Sleep-Disordered Breathing. *Journal of Clinical Medicine*. 2022; **11**: 1413  
DOI: 10.3390/jcm11051413.
14. Nalini M, Khoshnia M, Kamangar F, Sharafkhah M, Poustchi H, Pourshams A, Roshandel G, Gharavi S, Zahedi M, Norouzi A, Sotoudeh M, Nikmanesh A, Brennan P, Boffetta P, Dawsey SM, Abnet CC, Malekzadeh R, Etemadi A. Joint effect of diabetes and opiate use on all-cause and cause-specific mortality: the Golestan cohort study. *International Journal of Epidemiology*. 2020; **50**: 314–324  
DOI: 10.1093/ije/dyaa126.



15. Niesters M, Dahan A, Swartjes M, Noppers I, Fillingim RB, Aarts L, al. et. Effect of ketamine on endogenous pain modulation in healthy volunteers. *Pain*. 2011; **152**: 656–663  
DOI: 10.1016/j.pain.2010.12.015.
16. Jonkman K, Dahan A, Donk T van de, Aarts L, Niesters M, Velzen M van. Ketamine for pain. *F1000Research*. 2017;  
DOI: 10.12688/f1000research.11372.1.
17. Brinck E, Tiippana E, Heesen M, Bell RF, Straube S, Moore RA, Kontinen V. Perioperative intravenous ketamine for acute postoperative pain in adults. *Cochrane Database of Systematic Reviews*. 2018;  
DOI: 10.1002/14651858.cd012033.pub4.
18. Bansal A, Miller M, Ferguson I, Burns B. Ketamine as a Prehospital Analgesic: A Systematic Review. *Prehospital and Disaster Medicine*. 2020; **35**: 314–321  
DOI: 10.1017/s1049023x20000448.
19. Olofsen E, Dahan A. Population pharmacokinetics/pharmacodynamics of anesthetics. *The APPS Journal*. 2005; **7**: E383–9  
DOI: 10.1208/aapsj070239.
20. Smith JS, Lefkowitz RJ, Rajagopal S. Biased signalling: from simple switches to allosteric microprocessors. *Nature Reviews Drug Discovery*. 2018; **17**: 243–260  
DOI: 10.1038/nrd.2017.229.
21. Raehal KM, Walker JKL, Bohn LM. Morphine side effects in -arrestin 2 knockout mice. *J Pharmacol Ther*. 2005; **314**: 1195–2001  
DOI: 10.1124/jpet.105.087254.
22. Stahl EL, Bohn LM. Low intrinsic efficacy alone cannot explain the improved side effect profiles of new opioid agonists. *Biochem*. 2021;  
DOI: 10.1021/acs.biochem.1c00466.
23. Ribeiro MJ, Sacramento JF, Gonzalez C, Guarino MP, Monteiro EC, Conde SV. Carotid body denervation prevents the development of insulin resistance and hypertension induced by hypercaloric diets. *Diabetes*. 2013; **62**: 2905–16  
DOI: 10.2337/db12-1463.
24. Cunha-Guimaraes JP, Guarino MP, Timoteo AT, Caires I, Sacramento JF, Ribeiro MJ, Selas M, Santiago JCP, Mota-Carmo M, Conde SV. Carotid body chemosensitivity: early biomarker of dysmetabolism in humans. *European Journal of Endocrinology*. 2020; **182**: 549–557  
DOI: 10.1530/EJE-19-0976.

## References

---

25. Sacramento JF, Chew DJ, Melo BF, Donega M, Dopson W, Guarino MP, Robinson A, Prieto-Lloret J, Patel S, Holinski BJ, Ramnarain N, Pikov V, Famm K, Conde SV. Bioelectronic modulation of carotid sinus nerve activity in the rat: a potential therapeutic approach for type 2 diabetes. *Diabetologia*. 2018; **61**: 700–710  
DOI: 10.1007/s00125-017-4533-7.
26. Lecube A, Sampol G, Hernández C, Romero O, Ciudin A, Simó R. Characterization of Sleep Breathing Pattern in Patients with Type 2 Diabetes: Sweet Sleep Study. *PLOS ONE*. 2015; **10**: e0119073  
DOI: 10.1371/journal.pone.0119073.
27. Gutiérrez-Carrasquilla L, López-Cano C, Sánchez E, Barbé F, Dalmases M, Hernández M, Campos A, Gaeta AM, Carmona P, Hernández C, Simó R, Lecube A. Effect of Glucose Improvement on Nocturnal Sleep Breathing Parameters in Patients with Type 2 Diabetes: The Candy Dreams Study. *Journal of Clinical Medicine*. 2020; **9**: 1022  
DOI: 10.3390/jcm9041022.
28. Sacramento JF, Andrzejewski K, Melo BF, Ribeiro MJ, Obeso A, Conde SV. Exploring the Mediators that Promote Carotid Body Dysfunction in Type 2 Diabetes and Obesity Related Syndromes. *International Journal of Molecular Sciences*. 2020; **21**:  
DOI: 10.3390/ijms21155545.
29. Feldman JL, Mitchell GS, Nattie EE. Breathing: rhythmicity, plasticity, chemosensitivity. *Annual Review of Neuroscience*. 2003; **26**: 239–66  
DOI: 10.1146/annurev.neuro.26.041002.131103.
30. Nattie E, Li A. Central chemoreceptors: locations and functions. *Comprehensive Physiology*. 2012; **2**: 221–54  
DOI: 10.1002/cphy.c100083.
31. Lopez-Barneo J. Neurobiology of the carotid body. *Handbook of Clinical Neurology*. 2022; **188**: 73–102  
DOI: 10.1016/B978-0-323-91534-2.00010-2.
32. Pamerter ME, Powell FL. Time Domains of the Hypoxic Ventilatory Response and Their Molecular Basis. *Comprehensive Physiology*. 2016; **6**: 1345–1385  
DOI: 10.1002/cphy.c150026.
33. Hellinga M, Algera MH, Schrier R van der, Sarton E, Velzen M van, Dahan A, Olofsen E, Niesters M. A Biomarker of Opioid-induced Respiratory Toxicity in Experimental Studies. *iScience*. 2023; **24**: 106520  
DOI: 10.1016/j.isci.2023.106520.

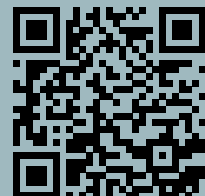
## Chapter 2

# ***S*-ketamine oral thin film – Part I: population pharmacokinetics of *S*-ketamine, *S*-norketamine and *S*-hydroxynorketamine**

Pieter Simons<sup>1</sup>, Erik Olofsen<sup>1</sup>, Monique van Velzen<sup>1</sup>, Maarten van Lemmen<sup>1</sup>, René Mooren<sup>1</sup>, Tom van Dasselaar<sup>1</sup>, Patrick Mohr<sup>2</sup>, Florian Hammes<sup>2</sup>, Rutger van der Schrier<sup>1</sup>, Marieke Niesters<sup>1</sup>, Albert Dahan<sup>1,3</sup>

*Front Pain Res (Lausanne)* 2022; 3:946486

1. Department of Anesthesiology, Leiden University Medical Center, 2300 RC Leiden, The Netherlands
2. LTS Lohmann Therapie-Systeme AG, Andernach, D-56626 Germany
3. PainLess Foundation, Leiden, the Netherlands



---

## Introduction

Over the last decade, low-dose ketamine has gained in popularity for treatment of chronic pain and therapy-resistant depression.<sup>1</sup> Since its discovery in the early 1960s, ketamine has been administered mostly *via* the parenteral route for the induction of anesthesia and procedural sedation. With a broader range of indications and pre-hospital and out-of-hospital use of ketamine, the need for skilled venipunctures is a hurdle for chronic and repeated ketamine administrations.

To overcome this problem, different routes of ketamine administration have been studied extensively, including inhaled, oral, sublingual, nasal, subcutaneous, intramuscular and rectal administrations. All of these routes have advantages, such as simplicity of administration, and drawbacks. For example, oral dosing results in slow absorption and is largely subject to intestinal and first-pass metabolism, with unpredictable bioavailability (7-25%). Others, such as the subcutaneous or intramuscular administration routes, are invasive and also result in a relatively slow absorption.<sup>2,3</sup> Here we study the pharmacokinetics (and in part 2 of this study,<sup>4</sup> the pharmacodynamics) of sublingual and buccal fast-dissolving oral-thin-films (OTFs) that contain 50 mg of *S*-ketamine, one of the stereoisomers of ketamine. In this report, we present the results of a pharmacokinetic analysis of the concentration-time curves following sublingual or buccal administration of 50 mg or 100 mg *S*-ketamine OTF in healthy volunteers. Apart from the simplicity of application, the use of an *S*-ketamine OTF may, depending on its bioavailability and first-pass effect, be advantageous in the treatment of pain and depression. An acceptable level of *S*-ketamine bioavailability will make it suitable for pain treatment in an acute setting,<sup>2,5</sup> while a large first-pass effect with high concentrations of hydroxynorketamine will make the *S*-ketamine OTF an interesting alternative for the management of therapy-resistant depression as there is evidence that this metabolite is a potent antidepressant.<sup>6,7</sup>

We performed a population pharmacokinetic analysis of the *S*-ketamine OTF in healthy volunteers, and considered the parent compound and its metabolites, *S*-norketamine and *S*-hydroxynorketamine in the analysis.

## Methods

### Ethics and Subjects

The protocol was approved by the Central Committee on Research Involving Human Subjects (Competent authority: Centrale Commissie Mensgebonden Onderzoek (CCMO), The Hague, the Netherlands; registration number NL75727.058.20) and the Medical Research Ethics Committee at Leiden University Medical Center (Medische Ethische Toetsingscommissie Leiden-Den Haag-Delft, the Netherlands; identification number P20.111). The study was registered at the trial register of the Dutch Cochrane Center ([www.onderzoekmetmensen.nl](http://www.onderzoekmetmensen.nl)) under identifier NL9267 and at the European Union Drug Regulating Authorities Clinical Trials (EudraCT) database under number 2020-005185-33. All procedures were performed in compliance with the latest version of the Declaration of Helsinki and followed Good Clinical Practice guidelines.

Healthy male and female volunteers, aged 18-45 years and with a body mass index  $\geq 19$  kg/m<sup>2</sup> and  $\leq 30$  kg/m<sup>2</sup>, were recruited. After recruitment, all subjects gave written and oral informed consent, after which they were screened. Additional inclusion criteria were the ability to communicate with the research staff, non-smoking for at least 3 months prior to screening, and deemed suitable by the investigators. Exclusion criteria included: presence or history of any medical or psychiatric disorder (including a history of substance abuse, anxiety, or a chronic pain syndrome), use of medication in the three months prior to screening (including vitamins and herbs, excluding oral contraceptives), use of more than 21 units of alcohol per week, use of illicit substances (including cannabis) in the 4 weeks prior to the study, a positive urine drug test or an alcohol breath test at screening or on the morning of test drug dosing, pregnancy, lactating or a positive pregnancy test at screening or on the morning of dosing, participation in another (drug) trial in the 60 days prior to dosing. Eating, drinking, tooth brushing or gum chewing was not allowed on the morning of oral thin film application to avoid changes/variabilities in saliva pH, which could potentially affect the mucosal permeability and *S*-ketamine uptake.

### Study Design

#### ***S*-Ketamine Oral Thin Film Placement – Randomization – Intravenous *S*-ketamine Infusion**

This phase 1 study had an open-label randomized crossover design. The subjects were randomized to receive one oral thin film on one occasion (50 mg *S*-ketamine) and two on another visit (100 mg *S*-ketamine) with at least 7 days between visits. The thin film is a rectangular 4.5 cm<sup>2</sup> orodispersible

---

film containing 57.7 mg *S*-ketamine hydrochloride (*S*-ketamine HCL). The *S*-ketamine HCL is dispersed within a matrix to produce a film corresponding to 50 mg *S*-ketamine free base. The film(s) was/were placed either under the tongue or buccally on the mucosa. After placement of the films, the subject was not allowed to swallow for 10 min. The randomization sequence was determined by the randomization option in the Electronic Data Capture system CASTOR ([www.castoredc.com](http://www.castoredc.com)). The oral thin films were provided by LTS Lohmann Therapie-Systeme AG (Andernach, Germany) and were dispensed by the hospital trial pharmacy on the morning of dosing. To calculate the bioavailability of the OTF, six hours after placement of the oral thin film, all subjects received an intravenous *S*-ketamine (Ketanest-S, Pfizer, the Netherland) infusion of 20 mg over 20 min. The intravenous dose of 20 mg given was based on a previous study on the pharmacokinetics of inhaled *S*-ketamine in which a 20 mg intravenous dose was administered over 20 min. This dose was well accepted by the volunteers.<sup>8</sup> We waited 6 h before giving the intravenous dose to ensure that most of the pharmacodynamic effects (*i.e.* the topic of our accompanying paper)<sup>4</sup> had dissipated.

### Blood Sampling and *S*-Ketamine Measurement

Blood samples were obtained at  $t = 0$  (= oral thin film placement) 5, 10, 20, 40, 60, 90, 120, 180, 240, 300, 360 min, and at the following time periods following the start of the intravenous administration: 2, 4, 10, 15, 20, 30, 40, 60, 75, 90 and 120 min. 3-mL samples were obtained from a 22G arterial line placed in the radial artery of the non-dominant arm and collected in lithium heparin tubes. All heparin samples were centrifuged at 1,500 g for 10 min, within 15 min after withdrawal and plasma was separated and stored in two aliquots at  $-80\text{ }^{\circ}\text{C}$  until analysis.

For analysis the samples were thawed and 200  $\mu\text{L}$  was transferred into glass tubes and 10  $\mu\text{L}$  internal standard was added. After mixing, 250  $\mu\text{L}$  buffer was added. After again mixing, 4 mL methyl-tertiar-butylether followed by 15 min and 15 min centrifugation. The upper organic layer was pipetted into another tube that contained 0.6 mL of 0.4 mol/L hydrochloric acid in methanol, and dried under a gentle stream of nitrogen at  $35\text{ }^{\circ}\text{C}$ . The residue was re-dissolved in 100  $\mu\text{L}$  mobile phase (6.8 % methanol in water with 0.1 % formic acid) by vortexing and ultrasonication for 3 min and 5  $\mu\text{L}$  sample was injected on the chromatographic system with a C18 column.

All reference standards (ketamine and norketamine) and internal standards ketamine-D4 (K-D4), norketamine-D4 (NK-D4) were HCl salts and purchased from LGC Standards GmbH (Germany); cis-6-hydroxynorketamine (6-HNK) was purchased from Syncom BV (the Netherlands); and the internal standard hydroxy- norketamine- $^{13}\text{C}6$  (HNK-13C6) was purchased from Alsachim SAS (France).

*S*-ketamine and its metabolites, *S*-norketamine and *S*-hydroxynorketamine, were measured at the Department of Pharmacy and Toxicology using liquid chromatography coupled to QTOF-MS (hybrid quadrupole time-of-flight mass spectrometry) as detection technique (*i.e.* LC-QTOF-MS/MS). The LC-QTOF-MS/MS system consisted of a Thermo Scientific double pump 3000 gradient system gradient with Bruker IL-2 QTOF.A column (Xterra MS C18 3.5 $\mu$ m x 2.1 mm x 100 mm) and precolumn (Xterra MS C18 Vanguard cartridge 3.5  $\mu$ m x 2.1 mm) and was purchased from Waters Chromatography Europe BV (the Netherlands). For separation the mobile phase was methanol/water with 0.1 % formic acid with a gradient from 6.8-96 % methanol from 1 until 8.5 min. The total separation time was 15 min with a flow rate of 0.3 ml/min. The eluent was directed to the QTOF-MS from 1.2 until 7 min while the other part was directed to waste by a valve to avoid contamination of the QTOF. The system was controlled by Chromeleon Chromatography Data System software (Thermo Fisher Scientific, the Netherlands) for the LC part and Hystar (Bruker Nederland BV, the Netherlands) for the QTOF/MS part. In the positive ionization mode, the masses of the M+H ions were respectively 224.084, 228.109, 238.0993, 242, 124, 240.0786 and 246.099 Da for norketamine, norketamine-D4, ketamine, ketamine-D4, Cis-6-hydroxynorketamine and hydroxynorketamine-<sup>13</sup>C6.

Quant Analysis (Bruker Nederland BV, the Netherlands) was used for quantification of all analytes with a weighed (1/X\*X) calibration line. The lower limits of quantitation were 6 ng/ml (0.025 nmol/mL), 6 ng/ml (0.026 nmol/mL) and 4 ng/ml (0.01 nmol/mL), for *S*-ketamine, *S*-norketamine and *S*-hydroxynorketamine, respectively. The upper limits of quantitation were, respectively, 500 ng/ml (2.1 nmol/ml), 1,000 (4.4 nmol/ml) and 200 ng/mL (0.72 nmol/ml) for *S*-ketamine, *S*-norketamine and *S*-hydroxynorketamine.

### **Adverse Events**

Reported adverse events related to treatment were collected and were split up into events related to the 50 or 100 mg oral thin film or to the intravenous administration of *S*-ketamine. Additionally, the subjects were queried for dissociative side effects using the Bowdle questionnaire.<sup>9</sup> The Bowdle questionnaire allows derivation of three factors of psychedelic ketamine effects: drug high and changes in internal and external perception. All three were measured on a visual analog score from 0 (no effect) to 10 cm (maximum effect). The questionnaire was first published in 1998 as a hallucinogen rating scale to quantify ketamine-induced psychedelic symptoms in volunteers and has been used in multiple studies on the effect of various psychedelics on dissociative symptoms. Blood pressure was obtained from the arterial-line using the FloTrac and Hemosphere system (Edwards Lifesciences, Irvine USA).

---

## Population Pharmacokinetic Analysis

Data analysis was performed using NONMEM version 7.5.0 (ICON Development Solutions, Hanover, MD, USA). To account for the differences in molecular weight between *S*-ketamine and the metabolites, concentration data were converted from ng/ml to nmol/ml. Data were analyzed in a stepwise fashion. First, *S*-ketamine data were analyzed, followed by the addition of *S*-norketamine and subsequently *S*-hydroxynorketamine. The routing of *S*-ketamine consists of two parts: one direct pathway from the OTF into plasma, and one indirect pathway in which some *S*-ketamine is stored in saliva which is ingested and absorbed *via* the gastrointestinal tract. Since *S*-norketamine was not administered, theoretically, the volume of the central *S*-norketamine compartment (VN1) was not identifiable. However, since we assumed that 80% of *S*-ketamine was metabolized VN1 is identifiable.<sup>2</sup> The same applies for *S*-hydroxynorketamine: since we assumed that 70% of *S*-norketamine is transformed into *S*-hydroxynorketamine,<sup>10</sup> the volume of the central *S*-hydroxynorketamine compartment is identifiable. The number of *S*-ketamine, *S*-norketamine and *S*-hydroxy-norketamine compartments as well as the intermediary metabolism compartments was determined by goodness-of-fit criteria, *i.e.*, a significant decrease in objective function value (OFV) calculated as  $-2 \log$  likelihood ( $\chi^2$  test), visual inspection of the data fits and goodness-of-fit plots (normalized prediction distribution error *vs* time plots, normalized prediction distribution error *vs* predicted plots, and predicted *vs* measured plots). Moreover, prediction-variance-corrected visual predictive checks (VPCs) were performed by simulating 1,000 data sets based on the model parameters and comparing the simulated quantiles with those of the true data.  $P < 0.01$  were considered significant.

FOCE-I (first-order conditional estimation with interaction) was used to estimate model parameters. To account for inter-individual and inter-occasion variability (IOV), random effects were included in the model with an exponential relation:  $\theta_i = \theta \times \exp(\eta_i + \eta_{ioV})$ , where  $\theta_i$  is the parameter for individual  $i$ ,  $\theta$  is the population parameter,  $\eta_i$  is the random difference between the population and individual parameter, and  $\eta_{ioV}$  is the difference between  $\theta_i$  and  $\theta$  as a result of IOV. In addition, proportional and additive errors were evaluated for each separate analyte to account for residual variability. The proportional and combined proportional and additive error models were described by  $Y_{ij} = P_{ij} \times (1 + \epsilon_{ij})$  and  $Y_{ij} = P_{ij} \times (1 + \epsilon_{1ij}) + \epsilon_{2ij}$ , respectively, where  $Y_{ij}$  is the  $j$ th observed plasma concentration for individual  $i$ ,  $P_{ij}$  is the corresponding model prediction, and  $\epsilon_{ij}$  is the residual error. Inter-occasion variability was determined for the *S*-ketamine and *S*-norketamine absorption parameters, while it was determined for all *S*-hydroxynorketamine model parameters.



## Simulations

*In-silico* simulations were performed to determine the effect of changes in the duration that the 50 mg *S*-ketamine oral thin film stayed sublingually (before the subjects was allowed to swallow) on plasma concentrations of *S*-ketamine and its metabolites. To that end, factor D1 was either increased or decreased by a factor (F) of 2, F1 was adjusted assuming it converges to 1 exponentially with D1 (*i.e.* F1 approaches 1 in case the OTF remains sublingually and is not swallowed), F2 was adjusted so that total bioavailability remains constant, and changes in D2 followed changes in D1 assuming D2 is the sum of D1 and gastrointestinal lag times. D1 is the duration of absorption, D2 is the duration of absorption from the gastrointestinal tract. F1 and F2 are the *S*-ketamine bioavailability from the oral mucosa and gastrointestinal tract, respectively.

---

## Results

Twenty-three subjects were screened, of which three subjects were excluded from participation because of psychological issues ( $n = 2$ ) or earlier alcohol abuse ( $n = 1$ ). Twenty subjects were dosed at least once (see Table 2.1 for their demographic characteristics), 19 subjects were dosed twice (once OTF with 50 mg *S*-ketamine, once with 100 mg *S*-ketamine).

**Table 2.1:** Subject characteristics

Characteristic	Total population $n = 20$	Sublingual OTF $n = 15$	Buccal OTF $n = 5$
Age (yr) $\pm$ SD (range)	$24 \pm 3$ (19-32)	$24 \pm 3$ (21-30)	$25 \pm 5$ (19-32)
Sex (M/F $n$ )	10/10	8/7	2/3
Mean weight (kg) $\pm$ SD (range)	$73 \pm 12$ (53-93)	$72 \pm 13$ (53-93)	$74 \pm 8$ (64-85)
Mean height (cm) $\pm$ SD (range)	$179 \pm 10$ (161-197)	$179 \pm 12$ (161-197)	$177 \pm 6$ (170-183)
Mean BMI ( $\text{kg}/\text{m}^2$ ) $\pm$ SD (range)	$23 \pm 2$ (19-27)	$22 \pm 2$ (19-27)	$24 \pm 3$ (21-27)

BMI = body mass index

One subject declined further participation after completing the first session, receiving 100 mg *S*-ketamine OTF sublingually, due to psychotomimetic side effects that occurred during the intravenous *S*-ketamine infusion. The mean and individual *S*-ketamine, *S*-norketamine and *S*-hydroxynorketamine data for both the sublingual and buccal OTF and intravenous infusion are given in Figure 2.1 on page 22. Since no differences were observed in plasma concentrations for the sublingual ( $n = 15$ ) or buccal ( $n = 5$ ) locations of the OTF (individual data in Figure 2.1 panels D-I with in red buccal administration and in black sublingual administration) and in the subject characteristics (Table 2.1), we merged the two subgroups in the pharmacokinetic model analyses. Peak concentration ( $C_{MAX}$ ), time of peak concentration ( $T_{MAX}$ ) and area-under-the-concentration-time curves (AUC) of *S*-ketamine and its metabolites are given in Table 2.2 on page 23. These data indicate that increasing the *S*-ketamine OTF dose produces dose dependent increase in  $C_{MAX}$  for *S*-ketamine and its metabolites, with a delay in  $C_{MAX}$  for the downstream metabolites. Comparing these data to the values observed after the intravenous *S*-ketamine in Figure 1, panels A-C, administration indicate the greater metabolism of the *S*-ketamine from the OTF compared to the 20 mg intravenous *S*-ketamine. Peak *S*-ketamine concentrations after the intravenous infusion were 273 (259-287) ng/mL (mean (95% confidence interval)) after treatment with the 50 mg *S*-ketamine OTF and 260 (251-269) ng/mL after treatment with the 100 mg *S*-ketamine OTF (Figure 2.1).

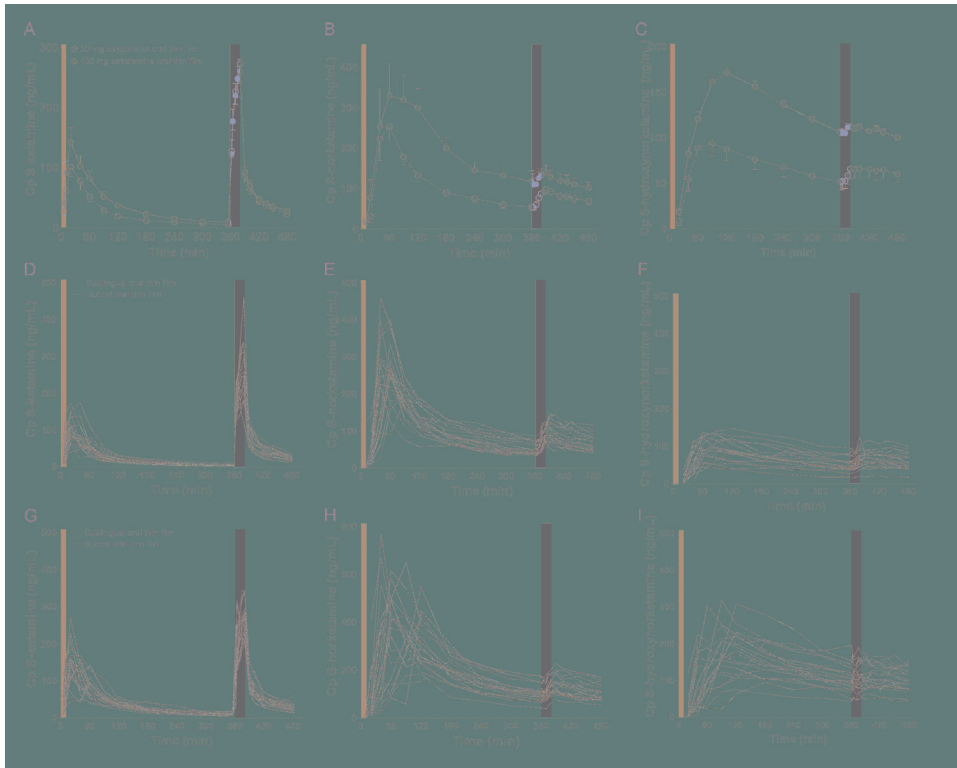


**Figure 2.1:** Mean measured plasma concentrations following application of the 50 and 100 mg S-ketamine oral thin film (OTF): (A) *S*-ketamine, (B) *S*-norketamine and (C) *S*-hydroxynorketamine. Individual concentrations are given in panels D-F for the 50 mg oral thin film, and G-I for the 100 mg oral thin film. In black the results of placement below the tongue, in red buccal placement. The OTF was administered at  $t = 0$  min for 10 min (green bars); at  $t = 360$  min, an intravenous dose of 20 mg *S*-ketamine was administered over 20 min (light orange bars).

## S-ketamine oral thin film pharmacokinetics

**Table 2.2:** Peak concentration ( $C_{MAX}$ ), time of  $C_{MAX}$  ( $T_{MAX}$ ), and area-under-the time-concentration curve (AUC) of *S*-ketamine, *S*-norketamine and *S*-hydroxynorketamine following 50 and 100 mg *S*-ketamine oral thin film (OTF).

	50 mg <i>S</i> -ketamine OTF	100 mg <i>S</i> -ketamine OTF
<b><i>S</i>-ketamine</b>		
$C_{MAX}$ (ng/ml)	96 (81 – 111)	144 (127 – 161)
$C_{MAX}$ (nM)	420 (360 – 480)	600 (500 – 700)
$T_{MAX}$ (min)	18.8 (16.6 – 21.2)	19.1 (17.1 – 21.2)
AUC (0-6 h) (ng/ml.min)	8,363 (7,263 – 9,464)	13,347 (11,933 – 14,760)
<b><i>S</i>-norketamine</b>		
$C_{MAX}$ (ng/ml)	276 (243-308)	426 (362-489)
$C_{MAX}$ (nM)	1,130 (970 – 1300)	1,475 (1,122 – 2,237)
$T_{MAX}$ (min)	61 (53-68)	78 (66-91)
AUC (0-6 h) (ng/ml.min)	38,497 (34,131 – 42,863)	67,959 (60,045 – 75,872)
<b><i>S</i>-hydroxynorketamine</b>		
$C_{MAX}$ (ng/ml)	101 (89 – 115)	189 (160 – 218)
$C_{MAX}$ (nM)	340 (293 – 387)	619 (594 – 644)
$T_{MAX}$ (min)	81 (69-92)	109 (89 – 130)
AUC (0-6 h) (ng/ml.min)	24,087 (20,694 – 27,480)	44,972 (38,563 – 51,382)

Values are mean ( $\pm$  95% confidence interval).

### Adverse Events

Eighteen subjects reported at least one adverse event. In total, there were 97 adverse events. None were serious adverse events. See for the prevalence of events Table 2.3 on page 24. We relate one adverse event (numbness of the tongue) directly to the application of the oral thin film, the remaining events were drug-associated. All subjects experienced dissociative side effects (drug high, changes in internal and external perception) as derived from the Bowdle questionnaire. The accompanying paper on the OTF pharmacodynamic effects presents these data in detail.<sup>4</sup> During the first hour after application of the OTF, blood pressure increased with mean arterial pressure  $92 \pm 11$  mmHg (mean  $\pm$  SD),  $97 \pm 7$  mmHg and  $104 \pm 6$  mmHg at baseline (prior to application) and 10 and 60 min after the application of the 50 mg *S*-ketamine OTF, respectively, and  $95 \pm 15$  mmHg,  $97 \pm 11$  mmHg and  $108 \pm 10$  mmHg at baseline and 10 and 60 min after the application of the 100 mg *S*-ketamine OTF.

---

**Table 2.3:** Adverse effects

	50 mg <i>S</i> -ketamine OTF	100 mg <i>S</i> -ketamine OTF	20 mg <i>S</i> -ketamine Intravenous
Blurred vision	1		
Feeling drunk	2		
Bradykinesia	1	1	
Whistling sound in the ears			1
Vertigo/dizziness	1	3	4
Drowsiness			3
Nausea	1	1	2
Headache	1	2	3
Numbness of the tongue		2	
Hypertension (SBP > 180 mmHg)			2
Perspiration			1
Dry eyes			1
Dissociative effects*	20	20	20
Total	27	29	37

\* Dissociative effects included drug high and changes in internal and external perception.

## Population Pharmacokinetic Analysis

The schematic diagram of the final pharmacokinetic model of the absorption of *S*-ketamine from the OTF and disposition of *S*-ketamine, with three compartments, and its metabolites *S*-norketamine and *S*-hydroxynorketamine, with each 2 compartments, is given in Figure 2.2 on page 26. Model parameter estimates are given in Table 2.4 on page 27; *S*-ketamine and *S*-norketamine distribution- and clearance-related parameters are in close correspondence with earlier data derived from a pooled-analysis of data from the literature.<sup>11</sup> Gastrointestinal absorption of *S*-ketamine and the metabolism of *S*-ketamine and *S*-norketamine were best described by two delay or metabolism compartments. The model parameters given in Table 2.4 are explained in Figure 2.2. All pharmacokinetic data fits are presented in Supplementary Figure 1 online; the goodness-of-fit plots (individual predicted concentration *vs.* measured concentration; individual weighted residuals over time; normalized prediction discrepancy errors) are given in Figure 2.3 on page 30. Inspection of these plots together with the individual data fits indicate that the final model adequately described the plasma concentration-time data of *S*-ketamine and its two measured metabolites.

The bioavailability of *S*-ketamine from the OTF was  $26.3 \pm 1.0\%$ , with a duration of absorption (D1) of 13 min and an absorption rate constant of  $0.04 \text{ min}^{-1}$  (KA1), with one outlier (subject #4) who had a KA1 value of  $0.012 \text{ min}^{-1}$ . The bioavailability for the 50 mg and 100 mg OTF differed by about 20% (F1 50 mg = 29%, F1 100 mg = 23%), but this did not reach the level of significance ( $p \approx 0.01$ ). The *S*-ketamine that was not absorbed in the mouth was ingested and was absorbed in the remainder of the gastrointestinal system into the portal vein. This process was modeled by two delay compartments defined by an absorption rate constant KA2 and a mean transit time (MTTG, Figure 2.4). The gastrointestinal absorption (F2) took 30 min. Around 75% of the initial amount of *S*-ketamine was directly metabolized into *S*-norketamine without participating in the distribution of *S*-ketamine in the systemic circulation. Metabolism into *S*-norketamine was modeled by two delay compartments with the delay defined by two mean transit times (MTT  $K \rightarrow NK$ , Table 2.2 and Figure 2.2), which has a population value of around 20 min (again with outlier subject #4 who had a value of 9 min). Twenty percent of *S*-ketamine was not metabolized into *S*-norketamine but was either metabolized into other metabolites (*e.g.* hydroxyketamine) or was lost in the gut. *S*-norketamine was metabolized into *S*-hydroxynorketamine via two metabolism compartments with the delay defined by two mean transit times ( $NK \rightarrow HNK$ , Table 2.2 and Figure 2.2), which had a population value of around 1 min. Thirty percent of *S*-norketamine was not metabolized into *S*-hydroxynorketamine but was metabolized to other metabolites such as *S*-dehydronorketamine.

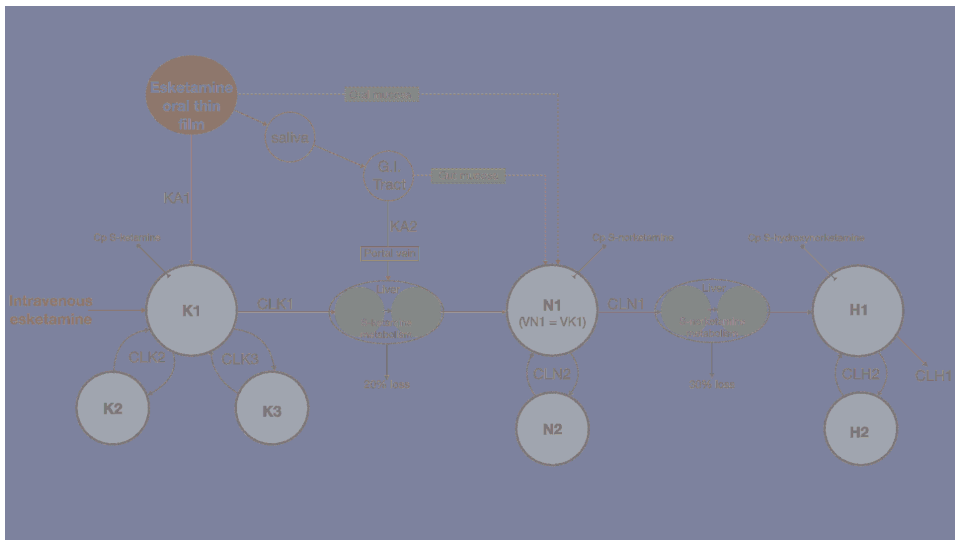


**Figure 2.2:** Final pharmacokinetic model. K = *S*-ketamine, N = *S*-norketamine and H = *S*-hydroxynorketamine. KA1 and KA2 are *S*-ketamine rate constants. G.I. tract = gastrointestinal tract. Cp = plasma concentration. K1, N1 and H1 are the central compartments for *S*-ketamine, *S*-norketamine and *S*-hydroxynorketamine, respectively. VN1 and VK1 are the volumes of the central compartments of *S*-ketamine and *S*-norketamine, respectively. Kx, Nx and Hx are the peripheral compartments for *S*-ketamine, *S*-norketamine and *S*-hydroxynorketamine, respectively, with x = compartment 2 or 3. CL = clearance with CLK1 and CLN1 *S*-ketamine and *S*-norketamine clearances from the central compartment towards the metabolism compartment, respectively and CLK2, CLK3, CLN2 and CLH2 intercompartmental clearances. CLH1 is the terminal *S*-hydroxynorketamine clearance. MTT = mean transit (or delay) time with MTTG the mean transit time from the gut to the liver.



**Table 2.4:** S-ketamine OTF pharmacokinetics

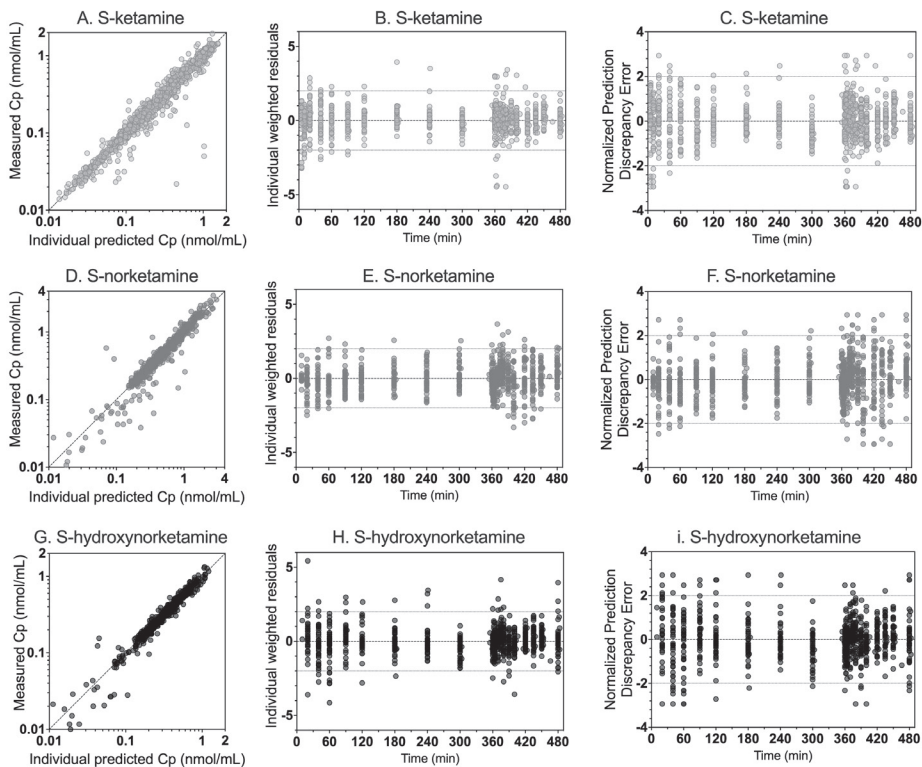
Parameter	Estimate	SEE	Inter-subject variability ( $\omega^2$ )	SEE	Inter-occasion variability ( $\nu^2$ )	SEE
<b><i>S-ketamine mucosal absorption from OTF</i></b>						
F1 (bioavailability) %	26.3	1.2			0.060	0.019
D1 (duration of absorption) min	13.1	1.0			0.154	0.033
Absorption rate constant; KA1 (min <sup>-1</sup> )	0.04	0.002			0.062	0.014
Outlier (id = 4, occ = 2) for KA1 (min <sup>-1</sup> )	0.012	0.0004				
Volume of S-ketamine compartment 1; VK1 (L @ 70 kg)	11.6	0.9	0.057	0.019		
Volume of S-ketamine compartment 2; VK2 (L @ 70 kg)	39.0	2.9				
Volume of S-ketamine compartment 3; VK3 (L @ 70 kg)	174	11				
Clearance from VK1 towards metabolism compartment MK; CLK1 (L/min @ 70 kg)	1.48	0.06	0.029	0.012		
Clearance from VK1 to VK2; CLK2 (L/min @ 70 kg)	2.43	0.24				
Clearance from VK1 to VK3; CLK3 (L/min @ 70 kg)	1.21	0.08	0.026	0.014		
sRelative (relative within subject variability)	0.012	0.0004				
<b><i>S-ketamine absorption from the gastrointestinal tract</i></b>						
F2 (bioavailability) %	116	6			0.057	0.031
D2 (duration of infusion) min	29.9	3.5			0.611	0.120
Absorption rate constant; KA2 (min <sup>-1</sup> )	0.049	0.007			0.376	0.150
Mean transit time GUT (min)	10.7	1.7			0.937	0.312

Table 2.4 continued from previous page

Parameter	Estimate	SEE	Inter-subject variability ( $\omega^2$ )	SEE	Inter-occasion variability ( $\nu^2$ )	SEE
<b>S-norketamine</b>						
Volume of S-norketamine compartment 1; VN1	11.6	0.9	0.057	0.019	11.6	
Volume of S-norketamine compartment 2; VN2 (L @ 70 kg)	221	13				
Clearance of S-norketamine compartment 1; CLN1 (L/min @ 70 kg)	1.00	0.04	0.050	0.012		
Clearance of S-norketamine compartment 2; CLN2 (L/min @ 70 kg)	2.63	0.15				
Mean transit time K $\text{\textcircled{R}}$ NK (min)	20.1	1.0	0.021	0.122		
Outlier mean transit time (id = 4) (min)	8.72	0.19				
sRelative (relative within-subject variability)	0.102	0.007				
sAdditive (additive within-subject variability)	0.058	0.018			0.751	0.349
<b>S-hydroxynorketamine</b>						
Volume of S-hydroxynorketamine compartment 1; VH1 (L @ 70 kg)	4.4	2.0	1.22	0.91		
Volume of S-hydroxynorketamine compartment 2; VH2 (L @ 70 kg)	87.5	6.5			0.152	0.031
Clearance of S-hydroxynorketamine compartment 1; CLH1 (L/min @ 70 kg)	0.933	0.068	0.103	0.042	0.008	0.004
Clearance of S-hydroxynorketamine compartment 2; CLH2 (L/min @ 70 kg)	1.70	0.25	0.287	0.124		

Table 2.4 continued from previous page

Parameter	Estimate	SEE	Inter-subject variability ( $\omega^2$ )	SEE	Inter-occasion variability ( $\nu^2$ )	SEE
Outlier (id = 9; occ = 2)						
CLH2 (L/min @ 70 kg)	0.36	0.02				
Mean transit time NK $\rightarrow$ HNK (min)	1.12	0.51				
$\sigma_{\text{Relative}}$ (relative within subject variability)	0.079	0.005				
$\sigma_{\text{Additive}}$ (additive within subject variability)	0.020	0.003				



**Figure 2.3:** Goodness-of-fit plots for *S*-ketamine (A-C), *S*-norketamine (D-F) and *S*-hydroxynorketamine (G-I). A, D and G: measured concentration versus individual predicted. B, E and H: individual weighted residuals versus time. C, F and I: Normalized discrepancy errors versus time.

## Simulations

The results of the *in-silico* simulations are given in Figure 2.4 on page 31. Increasing the duration of 50 mg oral thin film application in the mouth increased peak *S*-ketamine concentration by a factor of 2, while reducing the duration of the film in the mouth reduced peak *S*-ketamine concentration accordingly (Figure 2.4A). Both *S*-norketamine and *S*-hydroxynorketamine peak concentrations changed reciprocally to the changes in *S*-ketamine (Figure 2.4B,C) due to changes in the first-pass effect.

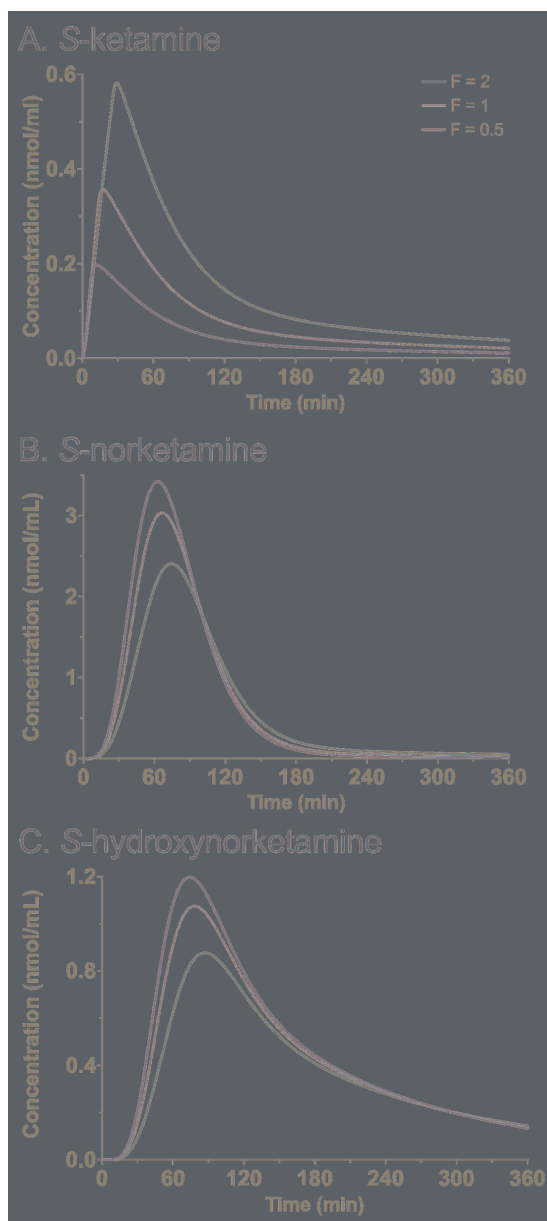


**Figure 2.4:** Simulations showing the effect of changing the duration of placement of the 50 mg oral thin file in the mouth by changing both F1 (bioavailability) and D (duration of absorption) on the plasma concentrations of *S*-ketamine (A), *S*-norketamine (B) and *S*-hydroxynorketamine (C). F is a factor by which D1 is adjusted and ranges from 0.5 (red lines) to 1 (blue lines) and 2 (green lines).



---

## Discussion

The main findings from our pharmacokinetic study on the *S*-ketamine oral thin film are summarized as follows: (i) the oral thin film was safe and the participants experienced mild adverse events infrequently related to the application of the film; (ii) *S*-ketamine bioavailability from the OTF was on average 26%; (iii) a 20% lower bioavailability of the 100 mg OTF relative to the 50 mg OTF was observed although this difference did not reach the level of significance; (iv) due to the large first pass-effect, 80% of *S*-ketamine was metabolized into *S*-norketamine leading to high concentrations of *S*-norketamine following sublingual or buccal film application for at least 6 h; (v) 56% of *S*-ketamine was finally metabolized into *S*-hydroxynorketamine, similarly, giving high plasma concentration for at least 6-hours; (vi) no differences in pharmacokinetics were observed for the sublingual or buccal administration routes; (vii) pharmacokinetic parameter estimates are in agreement with earlier findings.

The OTF is rapidly, that is within 2 min, dissolved in saliva. Subjects were not allowed to swallow for 10 min after the oral film was applied, and retained the dissolved *S*-ketamine in their mouth. The process of local absorption took on average 13 min (Table 2.4), indicative that some *S*-ketamine remained on the mucosa after swallowing. The majority of the *S*-ketamine was swallowed after 10 min, and moved into the gastrointestinal tract, where it was absorbed and transported *via* the portal vein to the liver, where further biotransformation occurred. We remain uninformed regarding the 20% loss of *S*-ketamine.<sup>2</sup> This may be related to loss in the gut, or metabolism into other metabolites than *S*-norketamine. It is thought that about 10% of ketamine is eliminated unchanged in the gut. A minor metabolic pathway is the hydroxylation of *S*-ketamine into 4-hydroxyketamine and some other metabolites (*e.g.* hydroxyphenylketamine).<sup>12</sup> The majority of *S*-ketamine (80%) undergoes hepatic *N*-demethylation into *S*-norketamine by cytochrome P450 (CYP) enzymes 2B6 and 3A4.<sup>12,13</sup> We cannot exclude that some part of the *S*-ketamine is metabolized in extrahepatic tissues, such as oral or gut mucosal cells.<sup>14,15,16</sup> This possibility is represented in the pharmacokinetic model (Figure 2.2) by the dotted red lines, which symbolize metabolic pathways of the oral and gut mucosa. Cytochrome P450 enzymes such as CYP3A4 but not CYP2D6 are expressed in the oral mucosal lining.<sup>15</sup> Similarly, the intestinal mucosa contains CYP3A4 and may possibly be an important route for first-pass conversion of *S*-ketamine and production of *S*-norketamine.<sup>15</sup> However, previous studies showed just a minor role for gut wall clearance in the overall metabolism of *S*-ketamine with a ratio of intestinal mucosal clearance to hepatic clearance of 1:253.<sup>17</sup> Because of this reason and the fact that we cannot discriminate between first-pass hepatic clearance and gut wall clearance, we modeled the *S*-ketamine first-pass effect through parenchymal liver metabolism

only. In the liver, *S*-norketamine is metabolized *via* cyclohexanone ring hydroxylation to form 4-, 5- and 6-hydroxynorketamine by CYP2B6 and CYP2A6 enzymes.<sup>12</sup> A small amount of *S*-norketamine is dehydrogenated into dehydronorketamine by CYP2B6, while some dehydronorketamine may additionally be produced from *S*-hydroxynorketamine by dehydration.<sup>12</sup> In the current analysis we just modeled the major metabolic pathways and assumed that 70% of *S*-norketamine was metabolized into *S*-hydroxynorketamine. This is based on earlier modeling studies that showed that a hydroxynorketamine to dehydronorketamine metabolic ratio of 70%:30% reflected best their measured plasma concentrations.<sup>10</sup> Finally, all hydroxy products are glucuronidated in the liver and subsequently eliminated via bile and kidney.<sup>12</sup>

Bioavailability of the oral thin film was on average 26% with a somewhat higher bioavailability for the 50 mg film than for the 100 mg film (F1 50 mg = 29%, F1 100 mg = 23%). Similar dose-dependency of bioavailability was observed for intranasal *S*-ketamine formulation that showed a decrease in bioavailability from 63% for a 28 mg *S*-ketamine dose to 50% for a 112 mg *S*-ketamine dose.<sup>18</sup> Possibly a saturation in absorption is observed here. Alternatively, a longer absorption time by expanding the “do not swallow” period following film application would have increased F1 at the expense of the first-pass effect. In other words, *S*-ketamine bioavailability following OTF application is reciprocally related to the *S*-norketamine and *S*-hydroxynorketamine concentrations (Figure 2.4). This is also reflected in the ratio *S*-norketamine over *S*-ketamine. Earlier studies indicated that this ratio equals 5 following oral ketamine administration and 2 after sublingual application of a ketamine lozenge.<sup>19</sup> In our study the ratio equals 4.6 after the 50 mg OTF and 5.1 after the 100 mg film. This and our model analysis indicate a large first-pass effect related to the transition of the *S*-ketamine into the gut after the ingestion of the remaining *S*-ketamine from the film after the 10-min “do not swallow” period and subsequently into the portal vein, or to metabolism directly in the mucosa of either the oral cavity or the remaining intestinal tract. As indicated above, we are unable to discriminate among these first-pass metabolic pathways. It is important to realize that depending on the clinical need, a large first-pass effect may be advantageous as it results in relatively high plasma concentrations of the ketamine metabolites. Particularly, high concentrations of hydroxynorketamine may be of interest when treating patients suffering from therapy-resistant depression.<sup>6</sup> Figure 2.1 shows that OTF 50 and 100 mg *S*-hydroxynorketamine concentrations (as observed from  $t = 0$  to 6 h) exceed the increase in *S*-hydroxynorketamine concentration from  $t = 6$  to 8 h following the 20 mg intravenous *S*-ketamine infusion. To obtain similar concentration of *S*-hydroxynorketamine following intravenous *S*-ketamine administration would require much higher intravenous doses that would coincide with a higher probability of unwanted side effects.<sup>5</sup> Whether hydroxynorketamine is analgesic

---

in humans has not yet been tested as no hydroxynorketamine is available for human use. One animal study did find analgesic efficacy from (*2R,6R*)-hydroxynorketamine in several acute and chronic pain animal models.<sup>20</sup> In part 2 of our analysis, we performed a pharmacokinetic-pharmacodynamic analysis and took, apart from *S*-ketamine, both metabolites into account in the pharmacodynamic model. This (indirect) approach could not substantiate any effect of *S*-norketamine or *S*-hydroxynorketamine in the antinociceptive behavior of the *S*-ketamine OTF.<sup>4</sup>

The level of the sublingual/buccal *S*-ketamine bioavailability we observed fits well with earlier findings on sublingual ketamine formulations that ranged from 24 to 29%.<sup>2,21</sup> Bioavailability after oral administration is more variable and ranges from 8 to 24%.<sup>2,3,22,23</sup> A recent report on the population pharmacokinetics of *S*-ketamine nasal spray indicate a bioavailability of 54% from passage through the nasal cavity with about 19% of the swallowed dose reaching the systemic circulation.<sup>18</sup> Finally, inhalation of *S*-ketamine has a bioavailability of 70% but is depending on the ketamine plasma concentration.<sup>7</sup> At higher concentrations, due to sedation, ketamine is lost to the environment, and bioavailability decreases (at 275 and 375 ng/ml bioavailability is 50% and 38%, respectively). So, in comparison, bioavailability for the different administration routes are oral < sublingual < intranasal < inhalation (albeit dose-dependent) < intravenous administration.

As indicated extending the sublingual or buccal absorption time of the OTF would likely have increased the *S*-ketamine concentration in plasma in our study (Figure 2.4). This may be an important consideration when treating acute pain with the OTF. Additionally, the *S*-ketamine oral thin film metabolic profile differs from other administration forms that exhibit a lesser first-pass effect (including intravenous administration, Figure 2.5; the greater the first pass effect, the more norketamine and hydroxynorketamine is formed). This together with the differences in bioavailability will evidently affect the efficacy profile of the formulation for treatment of pain and depression.

Finally, since *S*-ketamine is an important treatment option for therapy-resistant depression,<sup>1</sup> we simulated the *S*-ketamine and *S*-hydroxynorketamine profiles following 0.5 mg/kg intravenous ketamine given over 40 min to a 70 kg individual, which is the usual treatment dose for depression, and compared these profiles to those observed after the 100 mg *S*-ketamine oral thin film. The results indicate greater *S*-ketamine concentrations after the intravenous infusion but lower *S*-hydroxynorketamine concentrations compared to the oral thin film (Figure 2.5 on page 35). Since the role of the various ketamine metabolites such as hydroxynorketamine remain unknown in producing the antidepressant effects of ketamine,<sup>1,12</sup> a study on the effect of the *S*-ketamine oral thin film in patients with depression may shed light on this matter.



In conclusion, the *S*-ketamine oral thin film is a safe and practical alternative to intravenous *S*-ketamine administration that results in relatively high concentrations of *S*-ketamine and its two metabolites.

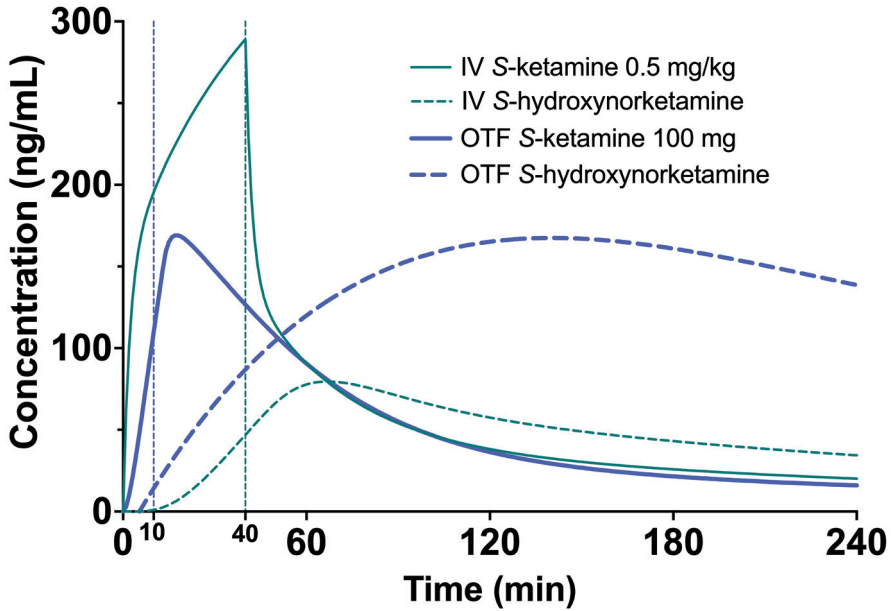


**Figure 2.5:** Simulation showing the *S*-ketamine (continuous green line) and *S*-hydroxynorketamine (broken green line) concentration profiles following a 0.5 mg/kg *S*-ketamine infusion, given for 40 min in a 70-kg individual. As comparator the equivalent concentrations are given following the 100 mg *S*-ketamine oral thin film (blue continuous = *S*-ketamine, and broken blue line = *S*-hydroxynorketamine).





## References

1. Abdallah CG, Sanacora G, Duman RS, Krystal JH. Ketamine and rapid-acting antidepressants: a window into a new neurobiology for mood disorder therapeutics. *Annu Rev Med.* 2015; **66**: 509–523  
DOI: 10.1146/annurev-med-053013-062946.
2. Peltoniemi MA, Hagelberg NM, Olkkola KT, Saari TI. Ketamine: a review of clinical pharmacokinetics and pharmacodynamics in anesthesia and pain therapy. *Clin Pharmacokinet.* 2016; **55**: 1059–1077  
DOI: 10.1007/s40262-016-0383-6.
3. Grant IS, Nimmo WS, Clements JA. Pharmacokinetics and analgesic effects of i.m. and oral ketamine. *Br J Anaesth.* 1981; **63**: 805–810  
DOI: 10.1093/bja/53.8.805.
4. Simons P, Olofsen E, Velzen M van, Lemmen M van, Dasselaar T van, Mohr P, Hammes F, Schrier R van der, Niesters M, Dahan A. S-Ketamine oral thin film-Part 2: Population pharmacodynamics of S-ketamine, S-norketamine and S-hydroxynorketamine. *Front Pain Res (Lausanne).* 2022; **3**: 946487  
DOI: 10.3389/fpain.2022.946487.
5. Kamp J, Velzen M van, Olofsen E, Boon M, Dahan A, Niesters M. Pharmacokinetic and pharmacodynamic considerations for NMDA-receptor antagonist ketamine in the treatment of chronic neuropathic pain: an update of the most recent literature. *Exp Opin Drug Metab Toxicol.* 2019; **15**: 1033–1041  
DOI: 10.1080/17425255.2019.1689958.
6. Zanos P, Moaddel R, Morris PJ, Georgiou P, Fischell J, Elmer GI, al. et. NMDAR inhibition-independent antidepressant actions of ketamine metabolites. *Nature.* 2016; **533**: 481–486  
DOI: 10.1038/nature17998.
7. Highland JN, Zanos P, Riggs LM, Georgiou P, Clark SM, Morris PJ, al. et. Hydroxynorketamine: pharmacology and potential therapeutic applications. *Pharmacol Rev.* 2021; **73**: 763–791  
DOI: 10.1124/pharmrev.120.000149.

## References

---

8. Jonkman K, Duma A, Olofsen E, Henthorn T, Velzen M van, Mooren R, al. et. Pharmacokinetics and bioavailability of inhaled esketamine in healthy volunteers. *Anesthesiology*. 2017; **127**: 675–683  
DOI: 10.1097/ALN.0000000000001798.
9. Bowdle TA, Radant AD, Cowley DS, Kharasch ED, Strassman RJ, Roy-Byrne PP. Psychedelic effects of ketamine in healthy volunteers: relationship to steady-state plasma concentrations. *Anesthesiology*. 1998; **88**: 82–88  
DOI: 10.1097/00000542-199801000-00015.
10. Kamp J, Jonkman K, Velzen M van, Aarts L, Niesters M, Dahan A, al. et. Pharmacokinetics of ketamine and its major metabolites norketamine, hydroxynorketamine and dehydronorketamine: a model-based analysis. *Br J Anaesth*. 2020; **125**: 750–761  
DOI: 10.1016/j.bja.2020.06.067.
11. Kamp J, Olofsen E, Henthorn T, Velzen M van, Niesters M, Dahan A. Ketamine pharmacokinetics. *Anesthesiology*. 2020; **133**: 1192–1213  
DOI: 10.1097/ALN.0000000000003577.
12. Zanos P, Moadell R, Morris PJ, Riggs LM, Highland JN, Georgiou P, al. et. Mechanism of ketamine action as antidepressant. *Mol Psychiatry*. 2018; **23**: 801–811  
DOI: 10.1038/mp.2017.255.
13. Adams JDJ, Baillie TA, Trevor AJ, Castagnoli N. Studies on the biotransformation of ketamine. 1-Identification of metabolites produced in vitro from rat liver microsomal preparations. *Biomed Mass Spectrom*. 1981; **8**: 527–538  
DOI: 10.1002/bms.1200081103.
14. Weiss M, Siegmund W. Pharmacokinetic modeling of ketamine enantiomers and their metabolites after administration of prolonged-release ketamine with emphasis on 2,6-hydroxynorketamines. *Clin Pharmacol Drug Develop*. 2022; **11**: 194–206  
DOI: 10.1002/cpdd.993.
15. Vondracek M, Xi Z, Larsson P, Baker V, Mace K, Pfeifer A, al. et. Cytochrome P450 expression and related metabolism in human buccal mucosa. *Carcinogenesis*. 2001; **22**: 481–488  
DOI: 10.1093/carcin/22.3.481.
16. Herwaarden AE van, Wagenaar E, Kruijssen CM van der, Waterschoot RA van, Smit JW, Song JY, al. et. Knockout of cytochrome P450 3A yields new mouse models for understanding xenobiotic metabolism. *J Clin Invest*. 2007; **117**: 3583–3592  
DOI: 10.1172/JCI33435.

17. Ashraf MW, Peltoniemi MA, Olkkola KT, Neuvonen PJ, Saari TI. Semimechanistic population pharmacokinetic model to predict the drug-drug interaction between S-ketamine and ticlopidine in healthy human volunteers. *CPT Pharmacometrics Syst Pharmacol.* 2018; **7**: 687–697  
DOI: 10.1002/psp4.12346.
18. Perez-Ruixo C, Rossenu S, Zannikos P, Nandy P, Singh J, Drevets WC, al. et. Population pharmacokinetics of esketamine nasal spray and its metabolite norketamine in healthy subjects and patients with treatment resistant depression. *Clin Pharmacokin.* 2021; **60**: 501–516  
DOI: 10.1007/s40262-020-00953-4.
19. Chong C, Schug SA, Page-Sharp M, Jenkins B, Ilett K. Development of a sublingual/oral formulation of ketamine for use in neuropathic pain. *Clin Drug Invest.* 2009; **29**: 317–324  
DOI: 10.2165/00044011-200929050-00004.
20. Kroin JS, Das V, Moric M, Buvanendran A. Efficacy of ketamine metabolite (2R,6R)-hydroxynorketamine in mice models of pain. *Reg Anesth Pain Med.* 2019; **44**: 111–117  
DOI: 10.1136/rapm-2018-000013.
21. Rolan P, Lim S, Sunderland V, Liu Y, Molnar V. The absolute bioavailability of racemic ketamine from a novel sublingual formulation. *Br J Clin Pharmacol.* 2013; **77**: 1011–1016  
DOI: 10.1111/bcp.12264.
22. Peltoniemi MA, Saari TL, Hagelberg NM, Laine K, Kurkinen KJ, Neuvonen PJ, al. et. Rifampicin has a profound effect on the pharmacokinetics of oral S-ketamine and less on intravenous S-ketamine. *Basic Clin Pharmacol Toxicol.* 2021; **111**: 325–332  
DOI: 10.1111/j.1742-7843.2012.00908.x.
23. Fanta S, Kinnunen M, Backman JT, Kalso E. Population pharmacokinetics of S-ketamine and norketamine in healthy volunteers after intravenous and oral dosing. *Eur J Clin Pharmacol.* 2015; **71**: 441–447  
DOI: 10.1007/s00228-015-1826-y.



## Chapter 3

# ***S*-ketamine oral thin film – Part II: population pharmacodynamics of *S*-ketamine, *S*-norketamine and *S*-hydroxynorketamine**

Pieter Simons<sup>1</sup>, Erik Olofsen<sup>1</sup>, Monique van Velzen<sup>1</sup>, Maarten van Lemmen<sup>1</sup>, René Mooren<sup>1</sup>, Tom van Dasselaar<sup>1</sup>, Patrick Mohr<sup>2</sup>, Florian Hammes<sup>2</sup>, Rutger van der Schrier<sup>1</sup>, Marieke Niesters<sup>1</sup>, Albert Dahan<sup>1,3</sup>

*Front Pain Res (Lausanne)* 2022; 3:946487

1. Department of Anesthesiology, Leiden University Medical Center, 2300 RC Leiden, The Netherlands
2. LTS Lohmann Therapie-Systeme AG, Andernach, D-56626 Germany
3. PainLess Foundation, Leiden, the Netherlands



---

## Introduction

The *N*-methyl-D-aspartate receptor antagonist ketamine experiences a clinical renaissance due to the introduction of various new indications.<sup>1</sup> While initially developed as an anesthetic and a substitute for phencyclidine, it later gained popularity as an analgesic and currently is available as a rapid-acting antidepressant.<sup>1</sup> Ketamine has multiple administration routes that may be divided into those that require a sometimes painful injection or venipuncture (intravenous and subcutaneous delivery) and those that circumvent the disadvantages of delivery by injection and allow an easy and painless treatment. The latter route includes delivery by oral, intranasal, transcutaneous, or rectal routes. Here, we study the pharmacodynamics [and in part 1 of this study, the pharmacokinetics, see chapter 2]<sup>2</sup> of sublingual and buccal fast-dissolving oral-thin-films (OTFs) that contain 50 mg of *S*-ketamine, one of the isomers of ketamine. The OTF is a rectangular 4.5 cm<sup>2</sup> thin film that is loaded with an active substance that immediately dissolves in the mouth and is rapidly absorbed through the mucosa. Ketamine is a complex drug for various reasons; it is a racemic mixture of *S*- and *R*-isomers and is metabolized into active compounds such as norketamine and hydroxynorketamine.<sup>3,4</sup> All these differ in pharmacokinetics and dynamics, and consequently may influence the ultimate effect of the drug and consequently the *S*-ketamine OTF.<sup>3,4</sup>

In the current study, we present the results of a pharmacodynamic analysis of the effect of one and two OTFs, containing, respectively, 50 and 100 mg *S*-ketamine, administered sublingually or buccally. In the accompanying report, we showed that the *S*-ketamine OTF undergoes a large first-pass effect causing relatively high concentrations of *S*-norketamine and *S*-hydroxynorketamine.<sup>3</sup> We studied the OTF on two end-points, nociception, by testing three distinct pain assays (pressure pain, electrical pain, and thermal pain), and drug high, one of the psychotomimetic effects of *S*-ketamine. Our main interest is the description of the pharmacodynamic effects of *S*-ketamine in the *S*-ketamine OTF. Additionally, we quantified the contribution of the *S*-ketamine metabolites in the production of antinociception and drug high. Earlier studies demonstrated that *S*-norketamine has a little analgesic effect in humans and is possibly even pro-algesic,<sup>5</sup> while animal data indicate that *S*-hydroxynorketamine has potent analgesic and antidepressant properties.<sup>6,7</sup>

We performed a population pharmacodynamic analysis of the *S*-ketamine OTF in a group of healthy volunteers and built a pharmacodynamic model that incorporates the contribution of *S*-norketamine and *S*-hydroxynorketamine. Pharmacokinetic–pharmacodynamic modeling is an important tool in the development of new therapies (including new administration modes of existing therapies) to quantify the therapeutic index or utility in terms of wanted and unwanted effects and determine the contribution of metabolites.



## Methods

This report is accompanied by a report on the population pharmacokinetics of the *S*-ketamine OTF, in chapter 2.<sup>8</sup> Here we describe the pharmacodynamic endpoints that were collected simultaneously with the pharmacokinetic data.

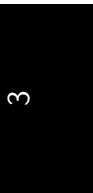
## Ethics and Subjects

The protocol was approved by the Central Committee on Research Involving Human Subjects (Competent authority: Centrale Commissie Mensgebonden Onderzoek (CCMO), The Hague, the Netherlands; registration number NL75727.058.20) and the Medical Research Ethics Committee of Leiden University Medical Center (Medisch Ethische Toetsingscommissie Leiden-Den Haag-Delft, The Netherlands; identifier P20.111) and was registered at the trial register of the Dutch Cochrane Center ([www.onderzoekmetmensen.nl](http://www.onderzoekmetmensen.nl)) under identifier NL9267. Healthy male and female volunteers (aged 18-45 years, body mass index 19 and 30 kg.m<sup>-2</sup>) were recruited. All recruited subjects gave written and oral informed consent, after which they were screened. Inclusion and exclusion criteria are given in chapter 2. Eating, drinking, brushing teeth or gum chewing was not allowed in the morning of the OTF application to avoid changes/variabilities in saliva pH, which could potentially affect the mucosal permeability and *S*-ketamine plasma concentration variability.

## Study Design

This phase 1 study had an open-label randomized crossover design. The subjects were randomized to receive one OTF on one occasion (50 mg *S*-ketamine) and two on another (100 mg *S*-ketamine) with at least 7 days between visits. The thin film is a rectangular 4.5 cm<sup>2</sup> orodispersible film containing 57.7 mg *S*-ketamine hydrochloride (*S*-ketamine HCL). The *S*-ketamine HCL is dispersed within a matrix to produce a film corresponding to 50 mg *S*-ketamine free base. The film(s) was/were placed either under the tongue or buccally on the mucosa. After placement of the films, the subject was not allowed to swallow for 10 min. The randomization sequence was determined by the randomization option in the Electronic Data Capture system CASTOR ([www.castoredc.com](http://www.castoredc.com)). The OTFs were obtained from LTS Lohmann Therapie-Systeme AG (Andernach, Germany) and were dispensed by the pharmacy on the morning of dosing. Measurement of pharmacodynamic endpoints lasted for 6 h. For blood sampling and measurement of *S*-ketamine, *S*-norketamine and *S*-hydroxynorketamine, see the accompanying report.<sup>2</sup>

In all subjects, on both occasions, an intravenous *S*-ketamine infusion followed the 6 h OTF test phase and was included in the pharmacokinetic



---

analysis to determine the *S*-ketamine bioavailability. Here we only present the pharmacodynamic data obtained during the OTF test phase.

### Noxious assays

Three independent pain assays, namely thermal noxious pain, electrical noxious pain and pressure pain, were randomly applied around predefined time intervals:  $t = 0, 10, 20, 30, 40, 60, 80, 100, 120, 150, 180, 240, 300$  and 360 min after placement of the OTF(s) with 3-5 min in between tests.

Electrical pain was induced by an in-house manufactured transcutaneous electrical current stimulator.<sup>9</sup> A constant current electrical stimulus train (stimulation at 20 Hz, pulse duration 0.2 ms) was applied on the skin over the tibial bone on the non-dominant side of the body through two surface electrodes. The location of the electrodes was such that muscle contractions did not occur. The current that it induced a numerical pain rating score (NRS) of 8 on a pain scale from 0 (no pain) to 10 (worst pain imaginable) at baseline was used in the remainder of the study. The search for the correct current was performed three times before any drug administration at 5-10 min intervals in steps of 0.5 mA.

Thermal noxious stimulation was applied on the volar side of the non-dominant forearm using a 3 cm<sup>2</sup> Peltier element or thermal probe of the Pathway device (Medoc Ltd., Israel) that allows computer-controlled changes in contact heat changes in steps of  $\pm 0.5$  °C.<sup>9</sup> In the current study a heat level was chosen that at baseline caused an NRS of 8 on the above-mentioned 11-point pain scale. The correct heat level was derived from three tests at 5-10 min intervals.

Pressure pain was induced using an Algometer (FDN 200 series, Wagner Instruments Inc., Greenwich, CT).<sup>10</sup> Pressure pain was delivered on a 1 cm<sup>2</sup> skin area between the thumb and index finger of the non-dominant hand. The device has a force capacity ( $\pm$  accuracy) of  $200 \pm 2$  N ( $= 20 \pm 0.2$  kgf) and graduation of 1 N (100 gf), respectively. A gradually increasing pressure was applied and the subjects indicated when the pressure became painful (pressure pain threshold). Three tests were applied at baseline; the obtained pressure values were averaged and served as the baseline value. A researcher well trained in this assay performed the pressure pain tests throughout the study visit days.

### Questionnaire

The Bowdle questionnaire was taken at regular intervals to determine the effect of treatment on mental and psychotomimetic side effects.<sup>11</sup> The timing of the questionnaires was at baseline (prior to any drug administration) and at 30 min intervals until 6 h after thin film application. In case the querying coincided with pain testing, the questionnaires were taken prior to pain testing. The Bowdle questionnaire allows the derivation of three factors of psychedelic ketamine effects: drug high and changes in internal and external perception. All

three were measured on a visual analogue score from 0 (no effect) to 10 cm (maximum effect). In the pharmacokinetic-pharmacodynamic data analysis, we included the effect of the OTF on drug high derived from the Bowdle questionnaire. The description of the effect of the *S*-ketamine OTF on the other endpoints, internal and external perception, is given in the in Supplementary Figure 1 online.

## Population pharmacodynamic analysis

Data were analyzed in a stepwise fashion. First, the pharmacokinetic data were analyzed using a population-based approach (see chapter 2). Next, the pharmacodynamic data were analyzed with individual concentration profiles of *S*-ketamine and its metabolites (based on the empirical Bayesian estimates of the pharmacokinetic parameters) as input of the sigmoid  $E_{MAX}$  pharmacodynamic models. The metabolites were assumed to be agonists or antagonists, with the total effect, EFF, modeled as:

$$EFF = EFF(K) + EFF(NK) + EFF(HNK)$$

With

$$EFF(K) = C_{E,K}/C_{50,K}$$

$$EFF(NK) = C_{E,NK}/C_{50,NK}$$

$$EFF(HNK) = C_{E,HNK}/C_{50,HNK}$$

or

$$EFF = EFF(K) = C_{E,K}/C_{50}$$

with

$$C_{50} = C_{50,K} \times [1 + EFF(NK) + EFF(HNK)]$$

and

$$EFF(NK) = C_{E,NK}/C_{100,NK}$$

$$EFF(HNK) = C_{E,HNK}/C_{100,HNK}$$

under the agonistic and antagonistic assumptions, respectively.  $C_{E,K}$ ,  $C_{E,NK}$  and  $C_{E,HNK}$  are the effect-site concentrations of *S*-ketamine, *S*-norketamine and

---

*S*-hydroxynorketamine, respectively;  $C_{50,K}$ ,  $C_{50,NK}$  and  $C_{50,HNK}$  are the steady-state or effect-site concentrations causing 50% of the pharmacodynamic effect; and  $C_{100,NK}$  and  $C_{100,HNK}$  are the *S*-norketamine and *S*-hydroxynorketamine concentrations causing a 100% increase of *S*-ketamine  $C_{50}$ .

An effect compartment was postulated to account for the hysteresis between the *S*-ketamine plasma concentrations (and possibly its metabolites) and its effect. This effect compartment equilibrates with the plasma compartment with plasma-effect-site equilibration half-life ( $t_{1/2k_{e0}}$ ).

The results of the electrical and thermal noxious assays were analyzed using the following inhibitory sigmoid  $E_{MAX}$  model:

$$NRS(t) = NRS_0 \times [1 + (C_E(t)/C_{50})^\gamma]^{-1}$$

where  $NRS(t)$  is the NRS in response to the noxious stimulation at time  $t$  and  $NRS_0$  is the NRS at baseline (pre-drug condition), and  $\gamma$  is a dimensionless shape parameter.

For pressure pain, we assume that *S*-ketamine (and possibly its metabolites) attenuates the response to the applied noxious pressure stimulus by the inhibition of signal propagation and central nociceptive processing. As a consequence, stronger stimuli are needed before the subjects indicate that he or she experiences pain. The attenuation ( $A$ ) is described by an inhibitory sigmoid  $E_{MAX}$  model:<sup>12</sup>

$$A = [1 + C_E(t)/C_{50}]^{-1}$$

Since a response of the subjects occurs just above the response threshold, we use the following equation for the pressure pain threshold at time  $t$ :

$$P(t) = P_0 \times 1/A = P_0 \times [1 + C_E(t)/C_{50}]^\gamma$$

where  $P_0$  is the baseline or pre-drug pressure that elicited a pain threshold response.

Drug high was modeled using a sigmoid  $E_{MAX}$  model:

$$VAS \text{ drug high } (t) = [E_{max} \times C_E(t)^\gamma] / [C_{50}^\gamma + C_E(t)^\gamma]$$

where  $C_{50}$  is the *S*-ketamine concentration that causes a drug high of 50% of  $E_{MAX}$ , and  $E_{MAX}$  the maximum possible effect on drug high (10 cm).

Data analysis was performed using NONMEM version 7.5.0 (ICON Development Solutions, Hanover, MD, USA). Inter-occasion variability ( $\nu^2$ ) was determined for baseline values only, as we assumed that other parameter values would not differ between the two occasions and were drug-dose independent. Determining whether the metabolites contributed to the measured effect and the level of significance of model parameters were based on the log-likelihood criterion (-2LL; a decrease of more than 6.6 is significant at the  $p < 0.01$  level for one additional parameter). The Goodness-of-Fit was based on the visual inspection of the model fits and Goodness-of-Fit plots (individual predicted *versus* measured, individual weighted residuals *vs.* time and normalized prediction discrepancy error *vs.* time). Additionally, visual predictive checks (PVCs) were generated to ensure that the models were able to reproduce the data used for model building. Although no pharmacokinetic differences were observed in the sublingual and mucosal applications, we compared the location of the application on the pharmacodynamic parameter estimates.

---

## Results

Twenty subjects participated in the study to receive, in random order, a single OTF (50 mg) or, on a second occasion, two OTFs applied simultaneously (100 mg) sublingually ( $n = 15$ ) or on the buccal mucosa ( $n = 5$ ). One subject participated only once (receiving 100 mg *S*-ketamine), due to side effects experienced from the intravenous *S*-ketamine infusion. Since no differences were observed in the sublingual and mucosal application regarding pharmacokinetics and pharmacodynamics of *S*-ketamine and its metabolites, we combined the two in the pharmacokinetic and pharmacodynamic model analyses. The mean age of the volunteers was 24 years (with range 19-32 years), mean weight 73 kg (53-93 kg), and mean body mass index 23 kg/m<sup>2</sup> (19-27 g/m<sup>2</sup>) with an equal number of men and women participating (10/10).

To summarize the pharmacokinetic data that stands at the basis of the pharmacodynamic analyses, we give the average plasma concentrations for *S*-ketamine, *S*-norketamine and *S*-hydroxynorketamine following 50 and 100 mg *S*-ketamine OTF in Figure 3.1 on page 49. It shows the large first-pass effect, with relatively high concentrations of the *S*-ketamine metabolites. No serious adverse events occurred during the study (see chapter 2 for a description of adverse events). The effects of the 50 and 100 mg *S*-ketamine OTF on pain responses are given in Figure 3.2 on page 49 for the three assays: electrical pain, heat pain and pain pressure. The data indicate that the OTF produces antinociception in all three assays, but irrespective of the pain assay a clear dose-response relationship was absent. Among subjects, pain relief was most variable in the pain pressure test compared to the other pain test with pain relief lasting two hours (heat pain test) or longer (electrical pain test). Comparing Figures 3.1 and 3.2, gives rise to the suggestion that the *S*-ketamine effect is pharmacokinetically-driven, *i.e.* that the pain responses closely follow the *S*-ketamine concentration profile, without any effect of the metabolites. In Figure 3.4, panels A and B, the individual median drug high visual analogue scores are given in gray and red, respectively. The peak median effect is higher for the 100 mg *S*-ketamine OTF compared to the lower dose OTF.

## S-ketamine oral thin film pharmacodynamics

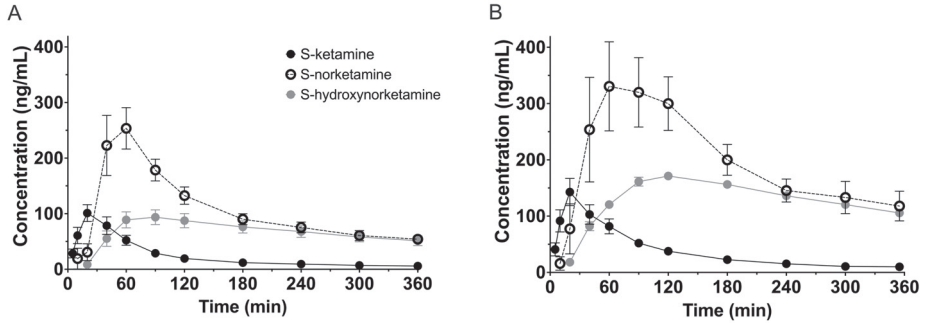


**Figure 3.1:** Pharmacokinetic data. Average plasma concentrations  $\pm$  95% confidence intervals for *S*-ketamine, *S*-norketamine and *S*-hydroxynorketamine following administration of 50 mg (A) and 100 mg (B) *S*-ketamine oral thin film.

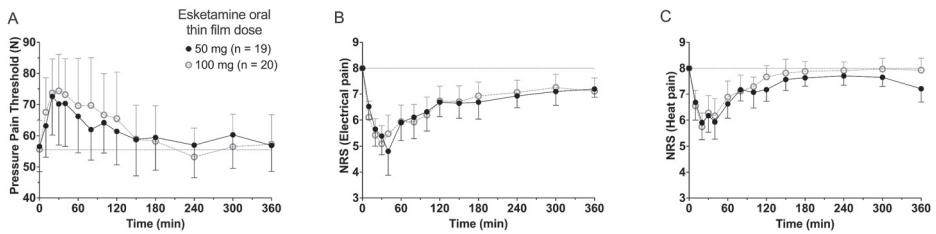


**Figure 3.2:** Antinociceptive data. The effects of the 50 mg and 100 mg *S*-ketamine oral thin film on pain responses for the three pain assays, pressure pain threshold (A), electrical pain numerical rating scale (B), and heat pain numerical rating scale (C). Data are mean  $\pm$  95% confidence interval.

---

## Population pharmacodynamic analysis

Population parameters estimates are given in Table 3.1 on page 51, the best median and worst fits (based on  $R^2$ ) for all 4 endpoints are given in Supplementary Figure 1 online. The Goodness-of-Fit plots are given in Figure 3.3 and Figure 3.4 on page 52 and 53, panels C-E. Visual Predictive Checks (VPCs), comparing observations with model predictions, are given in Figure 3.5 on page 54. Inspection of the fits, Goodness-of-Fit plots and VPCs indicate that the PKPD models adequately describe the data with no differences between the 50 and 100 mg OTF-related data. No contribution of either *S*-norketamine or *S*-hydroxynorketamine could be detected, *i.e.* EFF(NK) and EFF(HNK) approached zero. Consequently, the antinociceptive and drug high effects are attributed solely to *S*-ketamine. *S*-ketamine potency was about 3- to 5-fold lower for antinociception than for drug high:  $C_{50}$  1.2-1.7 nmol/mL *vs.* 0.3 nmol/mL for the nociceptive tests and for drug high, respectively. The onset/offset of the *S*-ketamine effect was similarly fast for all tests, nociceptive and drug high, and ranged from a value not different from zero (Table 3.1), indicative of an instantaneous effect to 5 min. In Figure 3.6 on page 55, the steady-state or effect-site concentration-effect relationships are given for the four pharmacodynamic endpoints. The dots in the figure depict the  $C_{50}$  values. No effect of the location of the OTF on parameter estimates was observed ( $p > 0.05$ ).

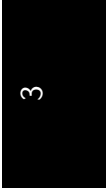


S-ketamine oral thin film pharmacodynamics

**Table 3.1:** Pharmacodynamic parameter estimates

	Estimate $\pm$ SEE	$\omega^2 \pm$ SEE	$\nu^2 \pm$ SEE
<b>Electrical pain NRS (0-10)</b>			
Baseline NRS	7.2 $\pm$ 0.2		0.025 $\pm$ 0.010
$t_{1/2}k_{e0}$ (min)	3.4 $\pm$ 0.4	1.13 $\pm$ 0.81	
$C_{50}$ (nmol/mL)	1.3 $\pm$ 0.2	1.01 $\pm$ 0.32	
$\gamma$	1 (FIX)		
$\sigma$	0.75 $\pm$ 0.07		
<b>Heat pain NRS (0 -10)</b>			
Baseline NRS	7.9 $\pm$ 0.2		0.011 $\pm$ 0.006
$t_{1/2}k_{e0}$ (min)	-		
$C_{50}$ (nmol/mL)	1.2 $\pm$ 0.32	0.57 $\pm$ 0.27	
$\gamma$	1 (FIX)	0.57 $\pm$ 0.31	
$\sigma$	0.66 $\pm$ 0.08		
<b>Pressure pain</b>			
Baseline (N)	56 $\pm$ 5	0.09 $\pm$ 0.03	0.03 $\pm$ 0.01
$t_{1/2}k_{e0}$ (min)	-		
$C_{50}$ (nmol/mL)	1.7 $\pm$ 0.29	0.27 $\pm$ 0.11	
$\gamma$	1 (FIX)		
$\sigma$ (N)	9.26 $\pm$ 1.18		
<b>Drug high VAS (0-10 cm)</b>			
$t_{1/2}k_{e0}$ (min)	5.4 $\pm$ 0.2	1.1 $\pm$ 0.69	
$C_{50}$ (nmol/mL)	0.31 $\pm$ 0.03	0.16 $\pm$ 0.08	
$\gamma$	2.8 $\pm$ 0.3	0.15 $\pm$ 0.05	
$\sigma$	0.89 $\pm$ 0.10		

NRS = numerical rating scale;  $t_{1/2}k_{e0}$  is blood-effect-site equilibration half-life;  $C_{50}$  is the concentration at steady-state causing 50% effect;  $\gamma$  is a shape parameter and  $\sigma$  a measure of residual noise.



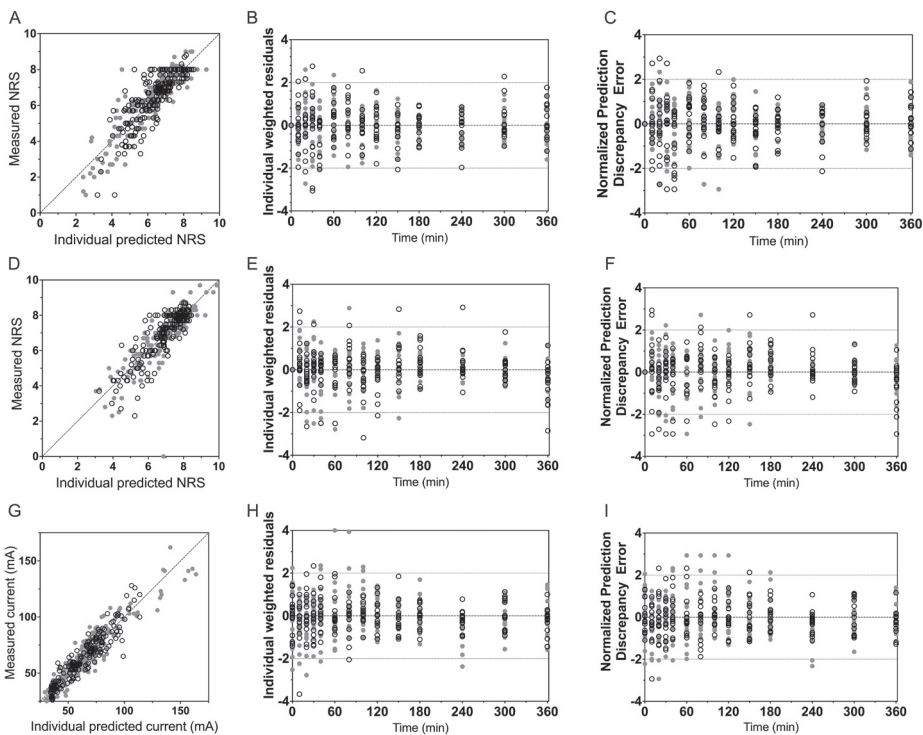


**Figure 3.3: Goodness-of-Fit plots.** A-C electrical pain numerical rating scale; D-F heat pain numerical rating scale; G-I pressure pain threshold. A, D, and G: measured versus individual predicted; B, E, and H: individual weighted residuals versus time. C, F and I: normalized prediction discrepancy errors versus time. Dashed lines are the 95% confidence intervals. Open circles denote data from the 50 mg *S*-ketamine oral thin film, closed circles data from the 100 mg *S*-ketamine oral thin film.

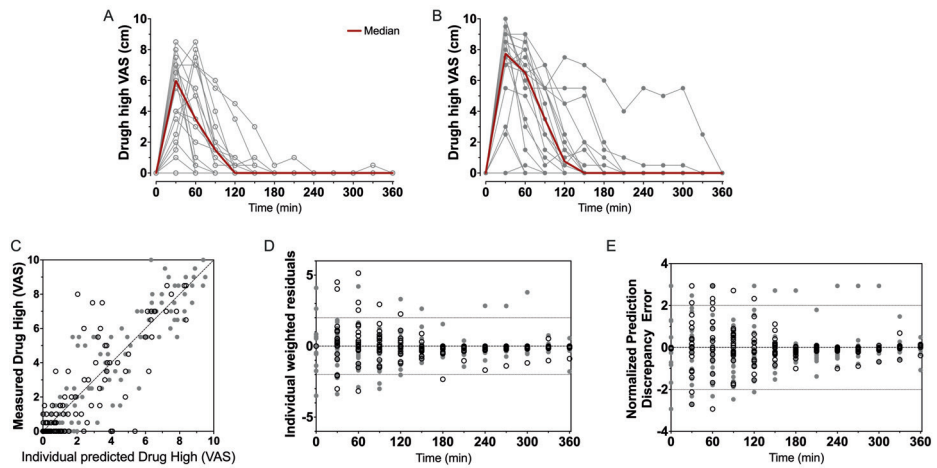


**Figure 3.4: drug high data.** Individual and median drug high visual analogue scores following the 50 mg (A) and 100 mg (B) *S*-ketamine oral thin film. C-E: Goodness-of-Fit plots, C. measured versus individual; D. individual weighted residuals versus time; E. normalized prediction discrepancy errors versus time. Dashed lines are the 95% confidence intervals. Open circles denote data from the 50 mg *S*-ketamine oral thin film, closed circles data from the 100 mg *S*-ketamine oral thin film.

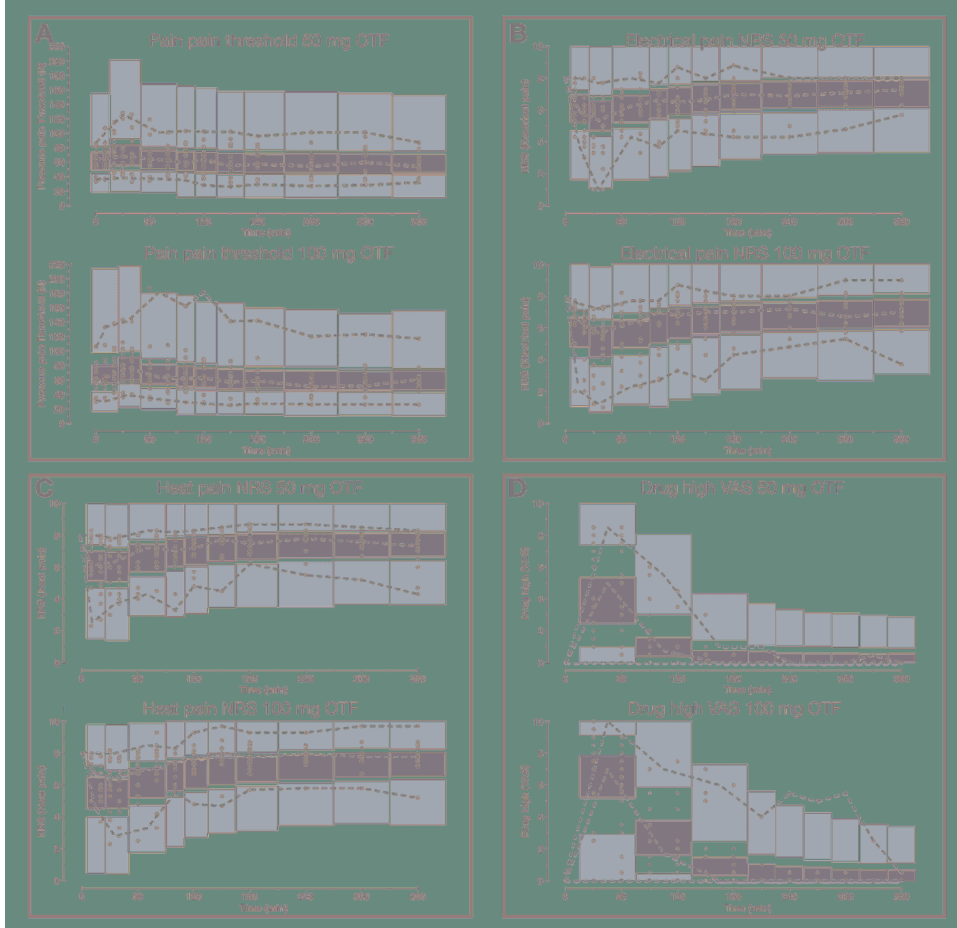


**Figure 3.5: Visual predictive checks of the pharmacodynamic model in for the two *S*-ketamine OTF doses.** The circles are the measured data points; the broken lines are the observed percentiles (dark red: median, dark blue: 2.5th and 97.5th percentiles); the bins are the 95% confidence intervals of simulated percentiles (orange bins: median, blue bins: 2.5th and 97.5th percentiles). **A.** Pain threshold; **B.** Electrical pain numerical rating scale (NRS); **C.** Heat pain NRS; **D.** Drug high visual analog scale (VAS).

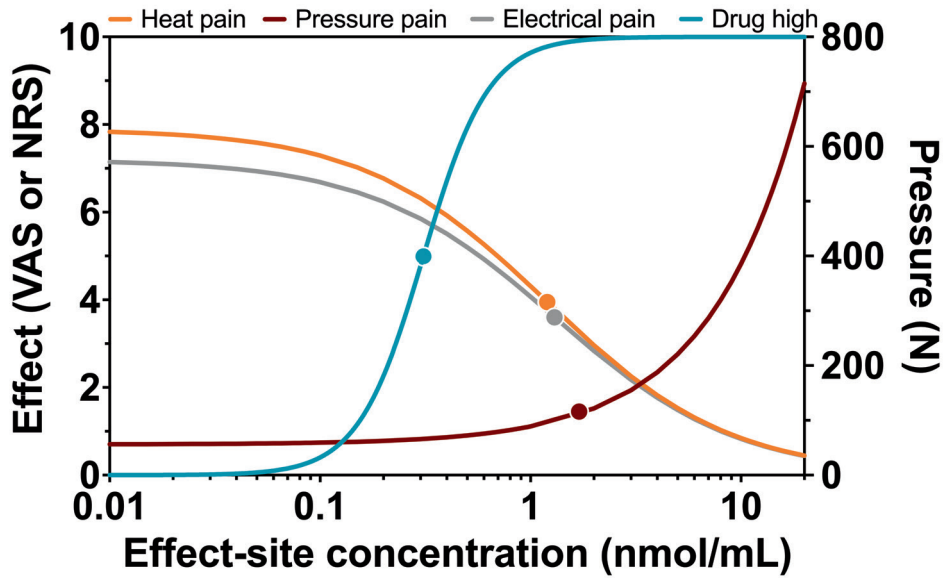
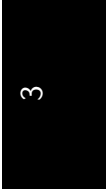


Figure 3.6: Steady-state concentration-effect relationships for heat pain, pressure pain, electrical pain, and drug high. Relationship between steady-state or effect-site *S*-ketamine plasma concentrations and effect with dots representing 50 values or half-effect concentration values.



---

## Discussion

The main findings from our population pharmacodynamic modeling study of an *S*-ketamine OTF are summarized as follows: (i) the sublingual and buccal 50 and 100 mg *S*-ketamine OTFs are antinociceptive with effects lasting at least 2 h; (ii) the onset of effect is rapid with peak effects within 30 to 45 min; (iii) drug high had a peak effect at 30 min and lasted at least 2 h; (iv) *S*-ketamine potency was lower for antinociception than for drug high by a factor of 3 to 5; (v) there were no contributions of *S*-norketamine and *S*-hydroxynorketamine to the antinociceptive or drug high *S*-ketamine effects detected in our model.

A clear dose-response relationship was not observed in the nociceptive data. For all three pain assays, the effect of doubling the dose of the OTF did not produce a significant increase in antinociception. Several mechanisms may be involved: (i) this may be related to a 20% lower *S*-ketamine bioavailability for 100 mg OTF compared to 50 mg OTF (bioavailability 50 mg = 29% *vs.* 100 mg 23%);<sup>2</sup> (ii) as observed in Figure 3.6, for electrical and heat pain, the effect-site concentration-effect curve becomes ultimately flat at high concentrations; for pressure pain, the slope of the response is initially not particularly steep and some overlap in the response data may be expected; (iii) The high concentrations of the measured and non-measured metabolites may have an antagonistic effect on the antinociceptive response.<sup>5</sup> High concentrations of *S*-norketamine and *S*-hydroxynorketamine were observed after the 50 and 100 mg *S*-ketamine OTFs due to the high first-pass effect. We earlier showed that *S*-norketamine counteracts the effects of *S*-ketamine,<sup>5</sup> but see below; (iv) possibly some noise in the data and variability in the day-to-day analgesic drug efficacy may have caused the overlap of antinociceptive response; (v) since we applied several noxious stimuli in a relatively short period of time to the volunteers, this may have altered the discriminatory ability of the nociception signaling pathways. Such an effect was earlier observed for volunteers treated with an opioid;<sup>13</sup> (vi) and finally, theoretically, there may be a ceiling in the ability of the nociceptive assays at higher drug doses. In a *post hoc* analysis, we observed that the separately estimated  $C_{50s}$  following the two *S*-ketamine OTFs did not differ, indicative that the absence of a dose-dependency of antinociceptive effect is probably related to the following items (i) reduced bioavailability for the higher dose OTF, (ii) flat concentration-effect relationship, and (iii) lesser discriminatory ability of the pain signaling pathways when multiple stimuli are administered. An effect of metabolites on the antinociceptive and drug high responses is further discussed below.

## Norketamine and hydroxynorketamine

Due to the large first-pass effect, plasma concentrations of *S*-norketamine and *S*-hydroxynorketamine were relatively high compared to intravenous ketamine administration (chapter 2 and Figure 3.1). Our modeling approach detected no contribution of these two *S*-ketamine metabolites to the antinociceptive and drug high effects of the *S*-ketamine OTF. Animal studies do show an antinociceptive effect from both ketamine and norketamine,<sup>14,15</sup> while we earlier observed a small negative contribution of *S*-norketamine to the antinociceptive and hemodynamic effects of *S*-ketamine in healthy volunteers.<sup>5</sup> We argued that this is one of the main reasons for the observation of pain facilitation after ketamine treatment, when norketamine concentrations exceed ketamine concentrations in plasma. Such observations are sometimes observed both clinically and in experimental studies.<sup>16,17,18</sup> The absence of a negative *S*-norketamine contribution to the antinociception from the OTF, suggests that *S*-norketamine has either no antinociceptive effect in humans, or the effect is small and was not detected from the noise in the data in our current study. Still, the absence of treatment arms that received *S*-norketamine precludes a definite conclusion regarding the effect of either metabolite on the pharmacodynamic responses in our study. For now, we cautiously infer from our modeling approach that *S*-norketamine has no or just little effect on either analgesia or drug high in human volunteers. The excitatory phenomena observed after ketamine infusion in other studies may then be related to the rebound activation of *N*-methyl-D-aspartate receptor and non-*N*-methyl-D-aspartate receptor glutamate receptors from accumulated excitatory amino acids in the synaptic cleft.<sup>18</sup>

In an animal study, Kroin et al.<sup>7</sup> showed earlier that (*2R,6R*)-hydroxynorketamine is an efficacious analgesic in mice. In three pain models, nerve-injury neuropathic pain, tibia fracture complex regional pain syndrome, and plantar incision postoperative pain, (*2R,6R*)-hydroxynorketamine was effective and superior to ketamine in terms of efficacy and side effect profile. Hence, we anticipated a long-term analgesic effect from *S*-hydroxynorketamine in our model with sustained and relatively high *S*-hydroxynorketamine concentrations in plasma. While after intravenous *S*-ketamine the ratio peak concentration *S*-hydroxynorketamine to *S*-ketamine equals 0.3,<sup>3</sup> this ratio  $\approx 1$  after application of the *S*-ketamine OTF, irrespective of dose (Figure 3.1). The absence of an *S*-hydroxynorketamine contribution may be dose-related (*i.e.* at higher concentration an effect may become visible), related to the stereoselectivity in the effect of hydroxynorketamine (*S*-hydroxynorketamine in our study *vs.* *R*-hydroxynorketamine in the study of Kroin et al.,<sup>7</sup> and finally it may be due to the cancellation of an antinociceptive effect from *S*-hydroxynorketamine by a pronociceptive rebound effect from the accumulated excitatory amino acids following the decline in *S*-ketamine plasma concentration



---

and reduced blockade of NMDA glutamatergic receptors.<sup>19</sup> This later mechanism would then suggest that *S*-ketamine and *S*-hydroxynorketamine act at different receptor systems to induce analgesia. Zanos et al.<sup>6</sup> showed indeed that (*2R,6R*)-hydroxynorketamine, but not ketamine, acts at the non-NMDA glutamate -amino-3-hydroxy-5-methyl-4-isoxazolepropionic acid (AMPA) receptor. Moreover, a recent study from Bonaventura et al.,<sup>19</sup> showed that (*2R,6R*)-hydroxynorketamine displays minimal brain uptake and rapid clearance from the brain, without any affinity for opioid receptors or any other known ketamine targets. Evidently, we need to consider the stereoselective effects of ketamine's metabolites. We argue therefore that, similar to *S*-norketamine, *S*-hydroxynorketamine needs to be administered to humans, in future studies to quantify its analgesic effect.

## Drug high *vs.* analgesia

For drug high, a dose dependent *S*-ketamine effect was observed (Figure 3.4A,B), without any contribution from its metabolites. Relative to the *S*-ketamine antinociception, *S*-ketamine was about 3-5 times more potent in producing its drug high effects with a  $C_{50}$  (*S*-ketamine concentration causing a drug high of 5 on an 11-point scale from 0 to 10) of 0.31 nmol/ml. Interestingly, earlier studies showed that the racemic ketamine  $C_{50}$  for drug high is at least a factor 2 greater than that of *S*-ketamine, indicative of a greater *S*-ketamine potency compared to the *R*-isomer and the racemic mixture in producing drug high effects with some studies finding that *R*-ketamine does not produce any psychotypical effects.<sup>19,20</sup>

Drug high effects were predominantly present during the analgesic period, suggestive of a connection between drug high and pain relief. A connection or association between the various ketamine endpoints such as analgesia and its psychotomimetic effects has been a matter of debate and has recently been refuted.<sup>20,21,22</sup> However, the current data set and earlier studies from our laboratory support an intricate association between analgesia and psychotomimetic side effects.<sup>20</sup> What this means is still unclear. It may relate to a similar site of action within the brain, or more probably, a connection between distinct brain areas that fire together upon exposure to ketamine. The latter would cause similar dynamics of the response (*i.e.* with similar onset/offset times), although potency between the two endpoints may differ. We plan further studies to increase our insights into this matter.



## Conclusions

In this pharmacokinetic-pharmacodynamic modeling study, we tested the antinociceptive and drug high effects of an *S*-ketamine OTF. The OTF was safe and side effects were related to ketamine itself and not to the thin film. Despite low bioavailability (on average 26%), the *S*-ketamine OTF produced potent antinociceptive responses in all three assays lasting 2-6 h, effects that were related to *S*-ketamine and not to its two metabolites, *S*-norketamine and *S*-hydroxynorketamine. The clinical indication of the OTF is primarily treatment of acute pain, for example in the emergency room, in the ambulance following acute trauma or for wound dressing. Additionally, we see a place for the *S*-ketamine OTF in the treatment of severe (cancer and non-cancer) breakthrough pain. However, further clinical studies are needed to address this issue.



## References

1. Kohtala S. Ketamine – 50 years in use: from anesthesia to rapid antidepressant effects and neurobiological mechanisms. *Pharmacol Rep.* 2021; **73**: 323–345  
DOI: 10.1007/s43440-021-00232-4.
2. Simons P, Olofsen E, Velzen M van, Lemmen M van, Mooren R, Dasselaar T van. S-ketamine oral thin film – Part 1: population pharmacokinetics of S-ketamine, S-norketamine and S-hydroxynorketamine. *Front Pain Res.* 2022;  
DOI: 10.3389/fpain.2022.946486.
3. Kamp J, Velzen M van, Olofsen E, Boon M, Dahan A, Niesters M. Pharmacokinetic and pharmacodynamic considerations for NMDA-receptor antagonist ketamine in the treatment of chronic neuropathic pain: an update of the most recent literature. *Exp Opin Drug Metab Toxicol.* 2019; **15**: 1033–1041  
DOI: 10.1080/17425255.2019.1689958.
4. Kamp J, Jonkman K, Velzen M van, Aarts L, Niesters M, Dahan A, al. et. Pharmacokinetics of ketamine and its major metabolites norketamine, hydroxynorketamine and dehydronorketamine: a model-based analysis. *Br J Anaesth.* 2020; **125**: 750–761  
DOI: 10.1016/j.bja.2020.06.067.
5. Olofsen E, Noppers I, Niesters M, Kharasch E, Aarts L, Sarton E, al. et. Estimation of the contribution of norketamine to ketamine-induced acute pain relief and neurocognitive impairment in healthy volunteers. *Anesthesiology.* 2012; **117**: 353–364  
DOI: 10.1097/ALN.0b013e31825b6c91.
6. Zanos P, Moaddel R, Morris PJ, Georgiou P, Fischell J, Elmer GI, al. et. NMDAR inhibition-independent antidepressant actions of ketamine metabolites. *Nature.* 2016; **533**: 481–486  
DOI: 10.1038/nature17998.



## References

---

7. Kroin JS, Das V, Moric M, Buvanendran A. Efficacy of ketamine metabolite (2R,6R)-hydroxynorketamine in mice models of pain. *Reg Anesth Pain Med.* 2019; **44**: 111–117  
DOI: 10.1136/rapm-2018-000013.
8. Simons P, Olofsen E, Velzen M van, Lemmen M van, Dasselaar T van, Mohr P, Hammes F, Schrier R van der, Niesters M, Dahan A. S-Ketamine oral thin film-Part 2: Population pharmacodynamics of S-ketamine, S-norketamine and S-hydroxynorketamine. *Front Pain Res (Lausanne).* 2022; **3**: 946487  
DOI: 10.3389/fpain.2022.946487.
9. Olofsen E, Romberg R, Bijl H, Mooren R, Engbers F, Kest B, al. et. Alfentanil and placebo analgesia: no sex differences detected in models of experimental pain. *Anesthesiology.* 2005; **103**: 130–139  
DOI: 10.1097/00000542-200507000-00020.
10. Martini C, Proto P, Olofsen E, Velzen M van, Aarts L, Dahan A, al. et. A randomized controlled trial and novel mathematical analysis of the analgesic effect of oxycodone versus paracetamol orodispersible tablets. *Eur J Pain.* 2015; **19**: 295–304  
DOI: 10.1002/ejp.546.
11. Bowdle TA, Radant AD, Cowley DS, Kharasch ED, Strassman RJ, Roy-Byrne PP. Psychedelic effects of ketamine in healthy volunteers: relationship to steady-state plasma concentrations. *Anesthesiology.* 1998; **88**: 82–88  
DOI: 10.1097/00000542-199801000-00015.
12. Sarton E, Olofsen E, Romberg R, Hartigh J den, Kest B, Nieuwenhuijs D, al. et. Sex differences in morphine analgesia: An experimental study in healthy volunteers. *Anesthesiology.* 2000; **93**: 1245–1254  
DOI: 10.1097/00000542-200011000-00018.
13. Oudejans LCJ, Velzen M van, Olofsen E, Beun R, Dahan A, Niesters M. Translation of random painful stimuli into numerical responses in fibromyalgia and perioperative patients. *Pain.* 2016; **157**: 128–136  
.
14. Velzen M van, Dahan A, Swartjes M, Noppers I, Fillingim RB, Aarts L, al. et. Efficacy of ketamine in relieving neuropathic pain: a systematic review and meta-analysis of animal studies. *Pain.* 2021; **162**: 2320–2330  
DOI: 10.1097/j.pain.0000000000002231.
15. Holtman Jr JR, Crooks PA, Johnson-Hardy JK, Hojomat M, Kleven M, Wala EP. Effects of norketamine enantiomers in rodent models of persistent pain. *Pharmacol Biochem Behav.* 2008; **90**: 676–685  
.

16. Mitchell AC. Generalized hyperalgesia and allodynia following abrupt cessation of subcutaneous ketamine infusion. *Palliat Med.* 1999; **13**: 427–428  
DOI: 10.1191/026921699667559279.
17. Niesters M, Dahan A, Swartjes M, Noppers I, Fillingim RB, Aarts L, al. et. Effect of ketamine on endogenous pain modulation in healthy volunteers. *Pain.* 2011; **152**: 656–663  
DOI: 10.1016/j.pain.2010.12.015.
18. Schmidt AP, Tort ABL, Silveira PP, Böhmer AE, Hansel G, Knorr L, al. et. The NMDA antagonist MK-801 induces hyperalgesia and increases CSF excitatory amino acids in rats: reversal by guanosine. *Pharmacol Biochem Behav.* 2009; **91**: 549–553  
DOI: 10.1016/j.pbb.2008.09.009.
19. Bonaventura J, Gomez JL, Carlom ML, Lam S, Sanchez-Soto M, Morris PJ, al. et. Target deconvolution studies of (2R,6R)-dehydroxynorketamine: an elusive search. *Mol Psychiatry.* 2022;  
DOI: 10.1038/s41380-022-01673-w.
20. Olofsen E, Kamp J, Henthorn TK, Velzen M van, Niesters M, Sarton E, al. et. Ketamine psychedelic and analgesic effects are connected. *Anesthesiology.* 2022; **136**: 792–801  
DOI: 10.1097/ALN.0000000000004176.
21. Oye I, Paulsen O, Maurset A. Effects of ketamine on sensory perception: Evidence for a role of N-methyl-D-aspartate receptors. *J Pharmacol Exp Ther.* 1992; **260**: 1209–1213  
.
22. Gitlin J, Chamadia S, Locascio JJ, Ethridge BR, Pedemonte JC, Hahm EY, al. et. Dissociative and analgesic properties of ketamine are independent. *Anesthesiology.* 2020; **133**: 1021–1028  
DOI: 10.1097/ALN.0000000000003529.



## Chapter 4

# Respiratory effects of biased-ligand oliceridine in older volunteers: a pharmacokinetic-pharmacodynamic comparison with morphine

Pieter Simons<sup>1</sup>, Rutger van der Schrier<sup>1</sup>, Maarten van Lemmen<sup>1</sup>, Simone Jansen<sup>1</sup>, Kiki WK Kuijpers<sup>1</sup>, Monique van Velzen<sup>1</sup>, Elise Sarton<sup>1</sup>, Todd Nicklas<sup>2</sup>, Cathy Michalsky<sup>2</sup>, Mark A Demitrack<sup>2</sup>, Michael Fossler<sup>2</sup>, Erik Olofsen<sup>1</sup>, Marieke Niesters<sup>1</sup>, Albert Dahan<sup>1,3</sup>

*Anesthesiology* 2023; 138:249–63

1. Department of Anesthesiology, Leiden University Medical Center, 2300 RC Leiden, The Netherlands
2. Trevena Inc., Chesterbrook, PA, USA
3. PainLess Foundation, Leiden, the Netherlands



---

## Introduction

In-hospital use of opioids is associated with multiple adverse events, prolonged length of stay and opioid-related readmissions.<sup>1,2,3,4</sup> Particularly respiratory depression from potent opioids is associated with not only respiratory depression but also cardiorespiratory collapse and death.<sup>5</sup> Despite these adverse effects, opioids remain the cornerstone of pharmacotherapy for moderate-to-severe acute pain because of their efficacy.<sup>6</sup> One strategy to mitigate opioid-induced adverse events is the development of safer opioids, *e.g.* opioids that produce less respiratory depression and lead to less addiction or abuse. One example of this strategy is the development of oliceridine that was recently approved by regulatory authorities in the United States for the treatment of postoperative pain.<sup>7</sup> It differs from other opioids in that it is assumed that after activation of the  $\mu$ -opioid receptor, oliceridine is biased toward the G-protein intracellular pathway which is predominantly associated with analgesia, and shows limited recruitment of the  $\beta$ -arrestin pathway, which is associated with opioid-related adverse events (*e.g.*<sup>7,8,9,10,11</sup> respiratory depression and tolerance).<sup>8,9,12</sup> Theoretically, this would suggest that oliceridine has a lower probability of respiratory depression than, for example, morphine a full  $\mu$ -opioid receptor agonist without biased toward the G-protein pathway. This was indeed observed in a study that examined the antinociceptive and respiratory effects of oliceridine *versus* morphine and showed a higher probability of antinociception *versus* respiratory depression for oliceridine while the reverse was true for morphine.<sup>13</sup> In that study, healthy young volunteers were studied. In the current study, we tested older and somewhat obese individuals (age range 55- to 90 years, body mass index up to 34 kg/m<sup>2</sup>) because such individuals are an increasing part of our clinical caseload and opioids in these older individuals possibly may have a higher potency for respiratory depression than in younger individuals. In the current sample of such older individuals, we performed a population pharmacokinetic-pharmacodynamic modeling study on the effect intravenous oliceridine *versus* morphine on ventilation at an extrapolated end-tidal carbon dioxide concentration of 55 mmHg ( $\dot{V}_{E55}$ ), the main endpoint of the study. We hypothesized that oliceridine and morphine differ in their pharmacodynamic behavior, measured as effect on ventilation at an extrapolated end-tidal  $PCO_2$  of 55 mmHg.



## Materials and Methods

### Ethics and Registration

The study was performed at a single site after approval of the protocol by the medical ethics committee of the Leiden University Medical Center, METC Leiden-Den Haag-Delft (under identifier P21.025) and the Central Committee on Research Involving Human Subjects (competent authority) in The Hague, The Netherlands (identifier NL75790.058.21). The study was performed from June 29, 2021, to January 4, 2022 in the Anesthesia & Pain Research Unit of the Department of Anesthesiology at Leiden University Medical Center. The study was registered in the trial register of the Dutch trial registry, currently available at the World Health Organization International Clinical Trials Registry Platform, under identifier NL9524 on June 2, 2021. The principal investigator of the study was Albert Dahan M.D. Ph.D. The study was conducted in accordance with current Good Clinical Practice Guidelines and adhered to the principles of the Declaration of Helsinki. Before enrollment, all subjects gave oral and written informed consent. Thereafter, their medical history was obtained and a physical examination was performed. The whole project was monitored by an independent data input monitor and a data safety monitoring committee.

### Participants

Healthy volunteers of either sex were recruited to participate in the study. Inclusion criteria were age 55 yr or older; body mass index in the range 19 to 35 kg/m<sup>2</sup> (inclusive); absence of any significant medical, neurologic, or psychiatric illness as determined by the investigators; and willing and able to sign a written informed consent. The inclusion process was aimed to include an equal number of men and women, include half of the participants with an age of 65 yr or older, and a third of subjects with a body mass index range of 30 to 35 kg/m<sup>2</sup>, to represent an average elective surgical population. The main exclusion criteria were intolerance, hypersensitivity, or recent (less than 1 month) exposure to opioids; a positive drug test or breath alcohol test on screening or subsequent study visits; inability to perform the study procedures as tested during screening; cognitive impairment as determined by the short version of the Mini Mental Status Examination (score less than 24); any clinically significant laboratory abnormality; abnormalities on the electrocardiogram including a corrected QT interval greater than 450 ms; alcohol intake of more than 4 units per day; participation in a drug trial in the 30 days before screening; or any other condition that in the opinion of the investigator would complicate or compromise the study or the well-being of the subject.

---

## Study Design

The following study drugs were administered on 4 separate study days, at least 1 week apart in a double-blind, randomized order: 0.5 mg low-dose oliceridine (Trevena Inc., USA), 2.0 mg high-dose oliceridine, 2.0 mg low-dose morphine hydrochloride (Centrafarm BV, Etten-Leur, The Netherlands), or 8.0 mg high-dose morphine hydrochloride. The study drugs were administered intravenously for over 60 s. The study drugs were prepared by the pharmacy and dispensed to the study team in identical, unmarked, numbered (subject and visit numbers) syringes on the morning of the experiment. Randomization was performed using a computer-generated randomization list; the list was available to the pharmacy and the data safety monitoring committee. Unblinding was only justified in case of drug-related serious adverse events.

The choice of the opioid doses was based on earlier clinical studies. Available oliceridine and morphine comparative data from the literature suggest that oliceridine is 6.7 times more potent than morphine in the cold pressor test and 3.3 times more potent in pupil constriction as derived from a phase 1 study obtained in younger adults (less than 50 yr),<sup>14</sup> and 4 times more potent in decreasing pain intensity as derived from a phase 2 study in 144 postoperative patients (age range 18 to 75 yr).<sup>15</sup> Based on these observations, we consider that the doses used in our study (2.0 mg and 8.0 mg morphine and 0.5 and 2.0 mg oliceridine) are equianalgesic.

Before each visit, participants were asked to fast for at least 8 h. Upon arrival in the research unit, the subjects were screened for the use of illicit substances by using a urine dipstick (Alere Toxicology Plc., Oxfordshire, United Kingdom), and screened for alcohol use with a breath analysis test (AlcoHawk CA-120, USA). Thereafter, the participants received an intravenous catheter in the median cubital vein of the left or right arm and an arterial line in the left or right radial artery. The arterial line was connected to a FloTrac Sensor and HemoSphere (Edwards Lifesciences, USA) for hemodynamic monitoring. Finally, a 3-lead electrocardiogram (Datex Cardiocap, Helsinki, Finland) and a finger probe for pulse oximetry (Masimo Corporation, USA) were placed.

## Respiratory Measurements

After a short period of relaxation, the ventilatory response to hypercapnia was measured by using a modified rebreathing method.<sup>16,17,18</sup> During respiratory testing, the subjects were semirecumbent and breathed through a face mask positioned over the mouth and nose. The face mask was connected to a pneumotachograph and pressure transducer system (Hans Rudolph Inc., USA) to measure ventilation on a breath-to-breath basis. Inspired and expired carbon dioxide concentrations were measured at the mouth using a Datex Capnomac (Datex, Finland). After a 4-min period of relaxed breathing of room air,

the subjects were coached to hyperventilate for 2 to 3 min while breathing a hyperoxic gas mixture ( $F_I O_2 \approx 1.0$ ), followed by normal breathing for 30 s of the hyperoxic gas mixture, after which rebreathing from a 6-l balloon containing 7% carbon dioxide in 93% oxygen was initiated. The rebreathing period lasted for 3 to 4 min. We obtained eight responses, one before any drug administration, and 30 min, 1, 2, 3, 4, 5, and 6 h after drug infusion. The following breath-to-breath data were collected: minute ventilation, end-tidal oxygen and carbon dioxide concentration, and oxygen saturation.

## Blood Sampling and Analysis

At the following time points, 2 ml blood was drawn from the arterial line for determination of oliceridine or morphine and morphine-6-glucuronide concentrations: 0 (predose) 2, 5, 10, 15, 30, and 45 min, and 1, 1.5, 2, 3, 4, 5, and 6 h (postdose). Plasma samples were shipped to Labcorp Bioanalytical Services LLC, Indianapolis, Indiana, for analysis.

Oliceridine plasma concentrations were quantified using a validated high-performance liquid chromatography with tandem mass spectrometry bioanalytical assay.<sup>7,13</sup> Oliceridine and the internal standard TRV0110813A:2 (tri-deutero <sup>13</sup>C-labeled oliceridine) were extracted from human plasma containing K<sub>2</sub>EDTA by supported-liquid extraction. The lower limit of quantitation for oliceridine in human plasma was 0.05 ng/ml, with linearity demonstrable up to 50 ng/ml (upper limit of quantitation), using a 50- $\mu$ l sample volume. Mean coefficient of variation among the various analytical runs ranged from 5.9 to 7.1% with bias ranging from 0.5 to 5.5% and accuracy from 100.5 to 105.5%. Oliceridine metabolites were not measured because none of them are pharmacologically active.

Morphine and morphine-6-glucuronide concentrations were determined by a validated high-performance liquid chromatography with tandem mass spectrometry method, after solid-phase extraction of morphine and internal standard morphine-d<sub>3</sub> and morphine-6-glucuronide and internal standard morphine-6-D-glucuronide-d<sub>3</sub> from human plasma containing K<sub>2</sub>EDTA. The lower limits of quantitation for morphine and morphine-6-glucuronide in human plasma were both 0.5 ng/ml, with linearity demonstrable up to 250 ng/ml (upper limit of quantitation), using a 50- $\mu$ l sample volume. For morphine, the mean coefficient of variations among the analytical runs ranged from 5.2 to 7.5% with bias ranging from 0.5 to 3.2% and accuracy from 100.5 to 103.2%. For morphine-6-glucuronide, the mean coefficient of variations ranged from 5.2 to 6.8% with bias ranging from 0.5 to 5.6% and accuracy from 100.5 to 105.6%. The assay has not been published previously, but see Dahan *et al.*<sup>13</sup>

To determine the drug metabolizer status of the participants, one additional blood sample was drawn for determination of the *CYP2D6* genotype. Genotyping was performed by the ISO15189-accredited laboratory of the

---

Leiden University Medical Center Pharmacy and Toxicology Department using the TAG CYP2D6 Kit v3 (Luminex Corporation, Den Bosch, The Netherlands). *CYP2D6*-haplotypes and copy number variants were determined.<sup>19</sup>

## Adverse Events

Side effects were evaluated on an 11-point visual analog scale (0 to 10) for the following items: nausea (none to severe), sedation (none to most intense), dizziness (none to most severe), lightheadedness (none to most severe), drug likability (5 was equivocal, under 5 was do not like, over 5 was like). Additionally, we scored occurrence vomiting (yes/no). These items were queried at baseline,  $t = 45$  min, and subsequently at 1-h intervals until  $t = 345$  min after drug administration. Also, adverse effects spontaneously reported by the participant or observed by the investigators were recorded.

## Data Analysis

Data analysis was performed in several steps. First,  $\dot{V}_{E55}$  or ventilation at an extrapolated end-tidal  $PCO_2$  of 55 mmHg (units l/min) was calculated from the slope of the ventilatory response to hypercapnia. The slope was determined in R (the R-Foundation for Statistical Computing, [www.r-project.org](http://www.r-project.org)) by fitting all ventilation-end-tidal  $PCO_2$  data points of the linear part of the ventilatory response to hypercapnia curve to the equation  $S = \text{Ventilation}(t)/[\text{end-tidal } PCO_2(t) - B]$ , where  $S$  is the slope of the ventilatory response to hypercapnia and  $B$  the apneic threshold or extrapolated end-tidal  $PCO_2$  at zero ventilation; this process was automated in R.<sup>20</sup> Next, the population pharmacokinetic data were analyzed, followed by a population pharmacokinetic–pharmacodynamic analysis using  $\dot{V}_{E55}$ , the main endpoint of the study, as pharmacodynamic input to the model.

## Pharmacokinetic-Pharmacodynamic Analysis

The pharmacokinetics and pharmacodynamics of oliceridine and morphine were analyzed with NONMEM VII (Icon Plc., USA), a software package for nonlinear mixed-effects modeling, using a population approach. Although measured in plasma, morphine-6-glucuronide was not included in the analyses, because previous studies indicated a rather low potency of morphine-6-glucuronide on generating respiratory effects in individuals with a normal renal function with a potency ratio of approximately 1:20 for depression of isohypercapnic ventilation and 1:50 for isocapnic hypoxic ventilation.<sup>21</sup> The pharmacokinetic data were analyzed using three-compartment models. The following analysis sequence was applied: initialization using iterative two-stage, parameter

estimation using stochastic approximation expectation maximization, objective function evaluation using importance sampling, and a final No U-Turn sampling Bayesian step using noninformative priors to visualize and quantify parameter uncertainty.

The early samples at 2 min after infusion showed considerable variability. Because infusion was done manually for 1 min, it was hypothesized that this could be caused, at least in part, by variability of the infusion duration. Therefore, NONMEM's parameter of the infusion duration ( $D_1$ ) was set up to be an estimable parameter.

Body weight and, for oliceridine, the metabolizer status based on the genotype of the *CYP2D6* gene, were incorporated as covariates in the pharmacokinetic analyses. The change in NONMEM's objective function value was tested to assess whether weight *via* allometric scaling improved the fit (because this requires no extra parameters, incorporating allometric scaling would be preferable with any decrease in the objective function value). For metabolizer status, the clearance for each nonnormal status was tested for statistically significant difference from the clearance for the normal status (change in objective function value of at least 6.63;  $p < 0.01$ ).

Allometric scaling using standard powers of weight (1 for volumes and 0.75 for clearances) was assumed *a priori* and implemented in the pharmacokinetic models.<sup>22</sup> During model evaluation, it was checked that incorporating allometric scaling indeed reduced NONMEM's objective function value and that it decreased the dependence of interindividual variability terms on weight. To quantify the hysteresis between the arterial drug concentration and effect, an effect site is postulated characterized by a first-order process with rate constant  $k_{e0}$  and half-life  $t_{1/2k_{e0}} (= \ln 2/k_{e0})$ . The ventilatory effects of oliceridine and morphine were modeled using an inhibitory sigmoid  $E_{MAX}$  model. Ventilation at an extrapolated isohypercapnic level of 55 mmHg ( $\dot{V}_{E55}$ ) was modeled as follows:

$$\dot{V}_{E55}(t) = \dot{V}_{E55} \text{ at baseline} - \dot{V}_{E55} \text{ at baseline} \times \frac{\left[ \frac{CE(t)^\gamma}{C_{50}^\gamma} \right]}{\left[ 1 + \frac{CE(t)^\gamma}{C_{50}^\gamma} \right]}$$

where baseline is the value before any drug administration,  $CE(t)$  is the effect-site concentration at time  $t$ ,  $C_{50}$  the effect-site concentration causing a 50% depression of  $\dot{V}_{E55}$ , and  $\gamma$  a shape parameter, which was fixed to 1 in the analyses. The same estimation steps were followed as was done for the pharmacokinetic analyses. To determine whether the models adequately described the data, Goodness-of-Fit plots were created and inspected. To allow a visual predictive check of the final pharmacokinetic or pharmacodynamic models, the normalized prediction discrepancies were estimated. Parameter estimates are reported as median  $\pm$  standard error of the estimate;  $p < 0.01$  was considered

---

significant.

No formal sample size analysis was performed. A previous study from our laboratory enrolled 15 subjects and was able to detect a significant difference between two opioids (oxycodone and tapentadol) on  $\dot{V}_{E55}$  in a young healthy population (mean difference 5 l/min, 95% CI -7 to -3 l/min).<sup>23</sup> In the current study, we planned to enroll 18 subjects to consider some variability in the data obtained from an older sample and possible withdrawal of up to 3 subjects.

The time to peak effect after a bolus dose is determined by both the blood-effect-site equilibration half-life and the pharmacokinetics.<sup>24</sup> This composite measure may be useful for the design of target-controlled infusion systems where the available models from the literature are evaluated. From the estimated parameters for both oliceridine and morphine, we calculated the time to peak effect using the method described in Minto *et al.*<sup>24</sup> implemented in R (the root of the derivative of the effect-site concentration function of time after a unit bolus dose).

## Simulations

We simulated the effect of multiple doses to reach a level of respiration depression of maximal 65% of isohypercapnic baseline ventilation in a typical 70-kg patient. The simulations were performed in R using implementation of the final models and estimated typical population parameters with simulated data obtained at 1-min intervals. After a bolus dose, a subsequent sequence of doses, three to four per hour, mimicking patient-controlled analgesia, was simulated while advancing simulated time considering a lockout time of 6 min. Three runs were done: one for morphine and two for oliceridine with normal and low elimination clearance. The bolus dose was 10 times and 3 times higher than the subsequent repetitive dose (10:1 and 1.5:0.5), for morphine and oliceridine, respectively, as applied clinically.<sup>14,15</sup>

## Results

A total of 341 individuals responded to an online mailing for participation in our study. Twenty-two were assessed for eligibility of which four were excluded because they did not show up on the first study day ( $n = 1$ ), they met exclusion criteria ( $n = 2$ ), or they declined to participate ( $n = 1$ ). Eighteen subjects (9 men and 9 women) were enrolled in the study and randomly assigned; seventeen subjects successfully completed the trial. One male subject withdrew consent after the second visit because of a (transient) painful hematoma that developed at the location of the vascular access line after the subject returned home; his data are included in the analyses. All other subjects completed the study without any serious or unexpected adverse effects. The mean age of the participants was 71 yr (range 56 to 87 yr), height 170 cm (155 to 189 cm), and body mass index 26 kg/m<sup>2</sup> (20 to 34 kg/m<sup>2</sup>). Five subjects, with age range 69 to 75 yr, had a body mass index greater than 30 kg/m<sup>2</sup> (mean value 33 kg/m<sup>2</sup>, with range 32 to 34 kg/m<sup>2</sup>); the other subjects (age range 56 to 87 yr) had a mean body mass index of 24 kg/m<sup>2</sup> (20 to 29 kg/m<sup>2</sup>).

### Primary Endpoint: Opioid Effect on $\dot{V}_{E55}$

The effect of oliceridine and morphine on mean isohypercapnic ventilation,  $\dot{V}_{E55}$ , are given in Figure 4.1 on page 74. The dynamic patterns observed after the opioid infusions were different for the two opioids. High-dose oliceridine and high- and low-dose morphine showed a rapid drop in  $\dot{V}_{E55}$ , an indication of rapid onset of respiratory depression, *i.e.*, within 30 min of administration. High-dose oliceridine and low-dose morphine returned toward baseline within 3 h, and high-dose morphine lagged behind, and a slow return toward baseline (more than 6 h) was observed. Low-dose oliceridine did not produce any significant respiratory depression. In contrast to  $\dot{V}_{E55}$  after high-dose morphine,  $\dot{V}_{E55}$  after low- and high-dose oliceridine infusion had mean values greater than predrug baseline values from  $t = 4$  h on.

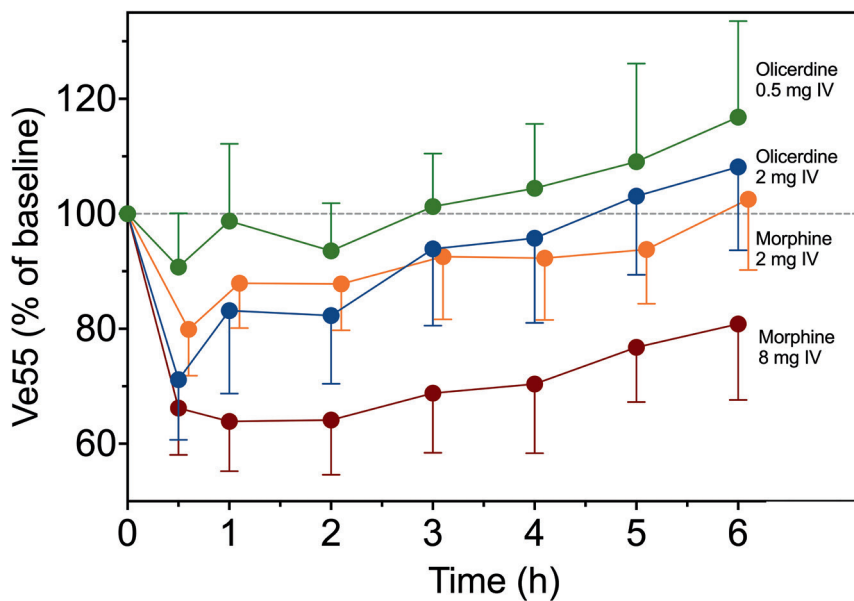


**Figure 4.1:**  $\dot{V}_{E55}$  change from baseline (%) after dosing. Ventilation at an extrapolated carbon dioxide partial pressure of 55 mmHg,  $\dot{V}_{E55}$ , during a hypercapnic ventilatory response, for the four treatment arms (green oliceridine 0.5 mg, blue oliceridine 2 mg, orange morphine 2 mg and red morphine 8 mg). Data are averaged percentage of baseline  $\pm$  95% confidence interval.



## Population Pharmacokinetic Analyses

The average plasma concentrations of oliceridine, morphine, and morphine-6-glucuronide are given in Figure 4.2 on page 76. Goodness-of-Fit plots (individual and population predicted *versus* measured data, conditional weighted residuals *versus* time, and normalized prediction discrepancy errors *versus* time) are given in Figure 4.3 on page 77; the population predicted pharmacokinetic outcomes and measured plasma concentrations of each individual of the four treatment arms are given in Figure 4.4 on page 78. Inspection of the data fits and Goodness-of-Fit plots indicate that the three-compartment models adequately described the data of both opioids. The estimated pharmacokinetic model parameter estimates are given in Table 4.1 on page 79. For all 4 treatment arms, the infusion rate parameter ( $D_1$ ) was not significantly different from 1, but its variability was significantly different from 0. Fixing it to zero had a marked effect on the remaining variability parameters and also on the population estimates. Therefore, including variability on  $D_1$  likely reduced the bias on all parameter estimates. The decrease in NONMEM's objective function value was 141 and 139 points for morphine and oliceridine, respectively. Weight had an effect on the pharmacokinetic parameters *via* allometric scaling, indicated by a decrease in objective function value of 43 and 24 points for morphine and oliceridine, respectively.

With respect to the CYP2D6 genotype, 10 subjects were classified as normal oliceridine metabolizers (2 functional alleles), 4 as intermediate metabolizer (heterozygous with one functional allele), 3 as poor metabolizer (with two alleles lacking activity due to  $*4/*4$ ,  $*3/*4$ , and  $*4/*4$  with  $*3 = 2549\text{delA}$  and  $*4 = 100\text{C}>\text{T}$ ,  $1661\text{G}>\text{T}$ ,  $1846\text{G}>\text{A}$ ,  $2850\text{C}>\text{T}$ , or  $4180\text{G}>\text{C}$ ) and 1 as ultrarapid metabolizer (more than two functional alleles).<sup>25</sup> A significant difference in clearance (CL1) by about 50% was observed in the three poor oliceridine metabolizers. This caused higher plasma concentrations in these three subjects after both low- and high-dose oliceridine compared with the other participants (Fig 4.4 C and D on page 78).

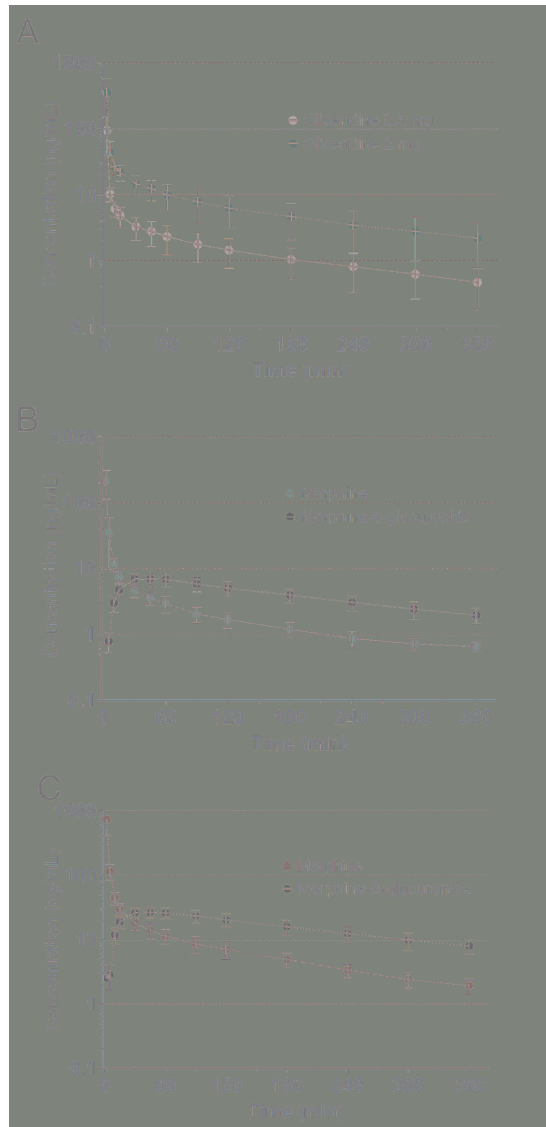


**Figure 4.2: Mean pharmacokinetic data** ( $\pm$  95% confidence interval) following intravenous administration of morphine and oliceridine. **A.** Oliceridine 0.5 mg (grey symbols) and oliceridine 2 mg (green symbols). **B.** Morphine 2 mg (red symbols) and morphine-6-glucuronide (blue symbols). **C.** Morphine 8 mg (red symbols) and morphine-6-glucuronide (blue symbols).

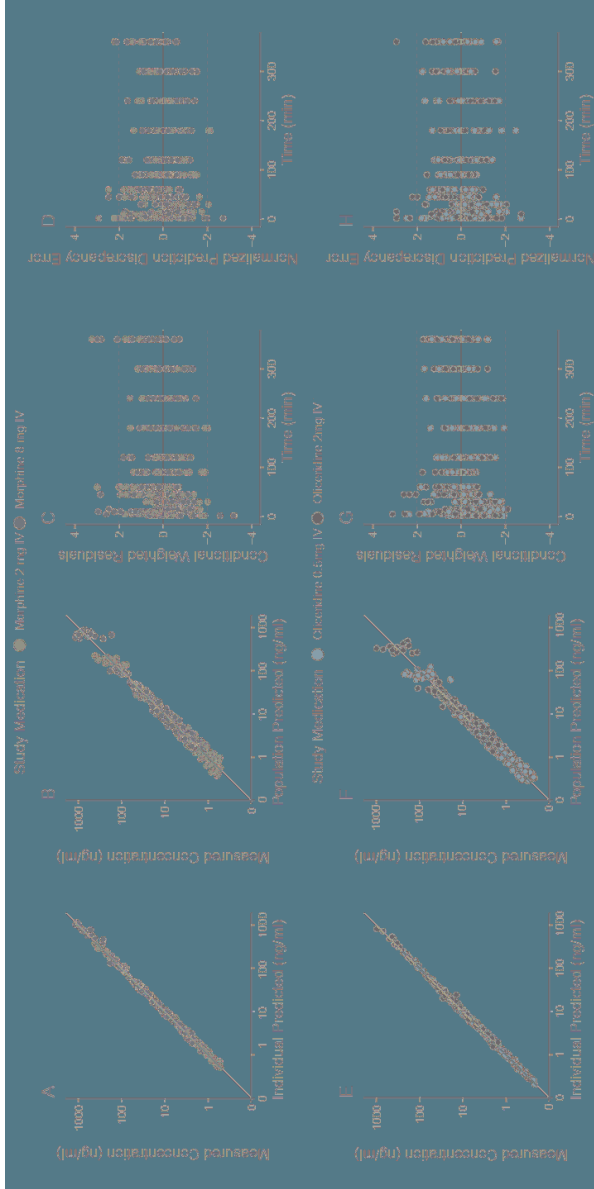


**Figure 4.3: Goodness-of-Fit PK data.** Goodness-of-Fit plots of the pharmacokinetic data analyses for morphine (panels A-D) and oliceridine (panels E-H). A and E. Measured concentration versus population predicted concentration. B and F. Measured concentration versus individual predicted concentration. C and G. Conditional weighted residuals versus time. D and H. Normalized prediction discrepancy error versus time. The dotted lines represent the upper and lower limits of the 95% confidence interval. Red symbols morphine 2 mg, green symbols morphine 8 mg, blue symbols oliceridine 0.5 mg, yellow symbols oliceridine 2 mg.

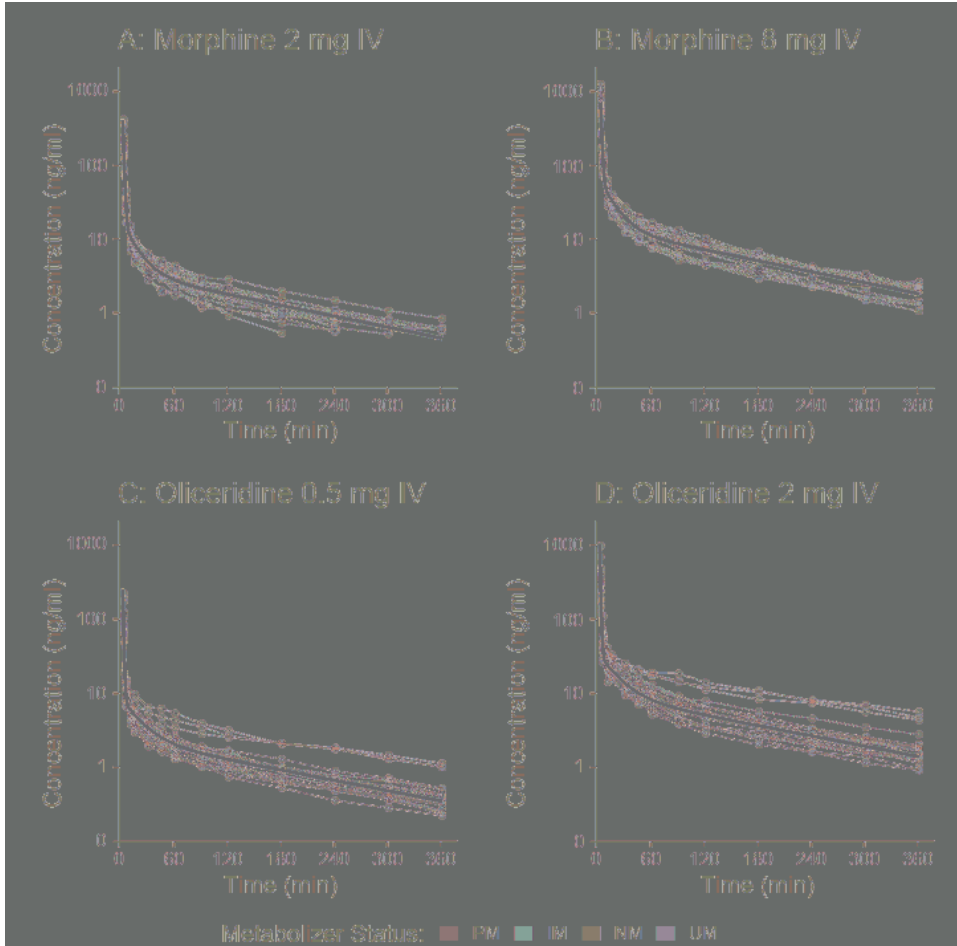


**Figure 4.4: Population pharmacokinetic model.** The population pharmacokinetic model outcome (red lines) and the observed pharmacokinetic data points of each individual versus time for morphine 2 mg (A), morphine 8 mg (B), oliceridine 0.5 mg (C) and oliceridine 2 mg (D). For oliceridine the status of the CYP2D6 genotype is given: poor metabolizer (green), intermediate metabolizer (dark yellow), normal metabolizer (blue) and ultra-rapid metabolizer (yellow).

**Table 4.1:** Pharmacokinetic parameter estimates

Oliceridine	Parameter ± SEE	Between-subject variability $\omega^2 \pm \text{SEE}$	Inter-occasion variability $\nu^2 \pm \text{SEE}$
V <sub>1</sub> (L/70 kg)	1.1 ± 0.1		0.07 ± 0.03
V <sub>2</sub> (L/70 kg)	5.6 ± 0.5		
V <sub>3</sub> (L/70 kg)	45.3 ± 1.8		0.01 ± 0.01
CL <sub>1</sub> (L/h at 70 kg)	33.1 ± 1.5	0.02 ± 0.01	0.006 ± 0.003
CL <sub>2</sub> (L/h at 70 kg)	22.8 ± 2.3	0.04 ± 0.02	0.02 ± 0.01
CL <sub>3</sub> (L/h at 70 kg)	27.6 ± 2.0	0.05 ± 0.03	
D <sub>1</sub> (min)	1		0.83 ± 0.43
CL <sub>1</sub> <sup>PM</sup> (L/h at 70 kg)	17.8 ± 1.5		
$\sigma^2$	0.009 ± 0.001		
<b>Morphine</b>			
V <sub>1</sub> (L/70 kg)	3.3 ± 0.3	0.05 ± 0.02	
V <sub>2</sub> (L/70 kg)	7.1 ± 0.6		
V <sub>3</sub> (L/70 kg)	90.2 ± 3.7	0.02 ± 0.01	
CL <sub>1</sub> (L/h at 70 kg)	80.1 ± 2.3	0.016 ± 0.004	
CL <sub>2</sub> (L/h at 70 kg)	35.8 ± 2.3		
CL <sub>3</sub> (L/h at 70 kg)	51.4 ± 2.4		
D <sub>1</sub> (min)	1.0	1.1 ± 0.5	
$\sigma^2$	0.012 ± 0.001		

SEE is standard error of the estimate,  $\omega^2$  inter-subject variability; V<sub>1</sub>, V<sub>2</sub> and V<sub>3</sub> are the volumes of compartments 1, 2 and 3, respectively; CL<sub>1</sub> is the clearance from compartment 1 with CL<sub>1</sub><sup>PM</sup> is CL<sub>1</sub> of the oliceridine poor metabolizer, CL<sub>2</sub> and CL<sub>3</sub> the intercompartmental clearances between compartments 1 and 2 and 1 and 3, respectively; D<sub>1</sub> is the infusion duration; and  $\sigma^2$  is a measure of residual variability.

---

## Pharmacodynamic Analyses

The population predicted pharmacodynamic outcomes and measured pharmacodynamic data points ( $\hat{V}_{E55}$ ) of each individual of the four treatment arms are illustrated in Figure 4.5 on page 81, and Goodness-of-Fit plots are given in Figure 4.6 on page 82. Inspection of the data fits and Goodness-of-Fit plots indicate that the pharmacodynamic model adequately described the data of both opioids. The estimated pharmacodynamic model parameter estimates are given in Table 4.2 on 83. Two relevant observations are that oliceridine displays a 39% higher  $C_{50}$  value than morphine, and the two drugs differ by a factor of 5 in their onset/offset times ( $t_{1/2ke0}$ ) with oliceridine being 5 times more rapid than morphine in the transition from plasma to effect site. The time to peak effect was 10.5 min and 56.0 min for oliceridine and morphine, respectively. For both drugs, parameter  $\gamma$  was not significantly different from 1 and therefore fixed to 1.

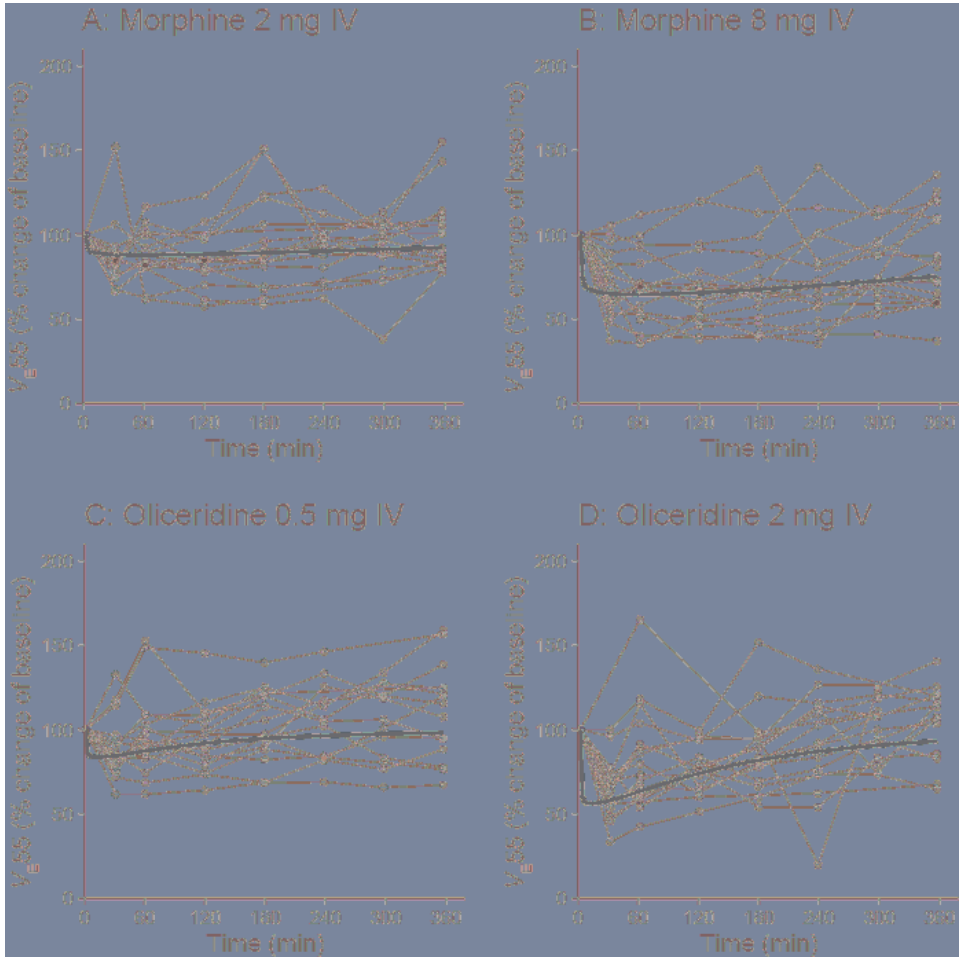


**Figure 4.5: Population pharmacodynamic model outcome.** The population pharmacodynamic model outcome (red lines) and the measured pharmacodynamic data points ( $\dot{V}_{E55}$ ) of each individual versus time for morphine 2 mg (A), morphine 8 mg (B), oliceridine 0.5 mg (C) and oliceridine 2 mg (D). Data are averaged percentage of baseline  $\pm$  95% confidence interval.

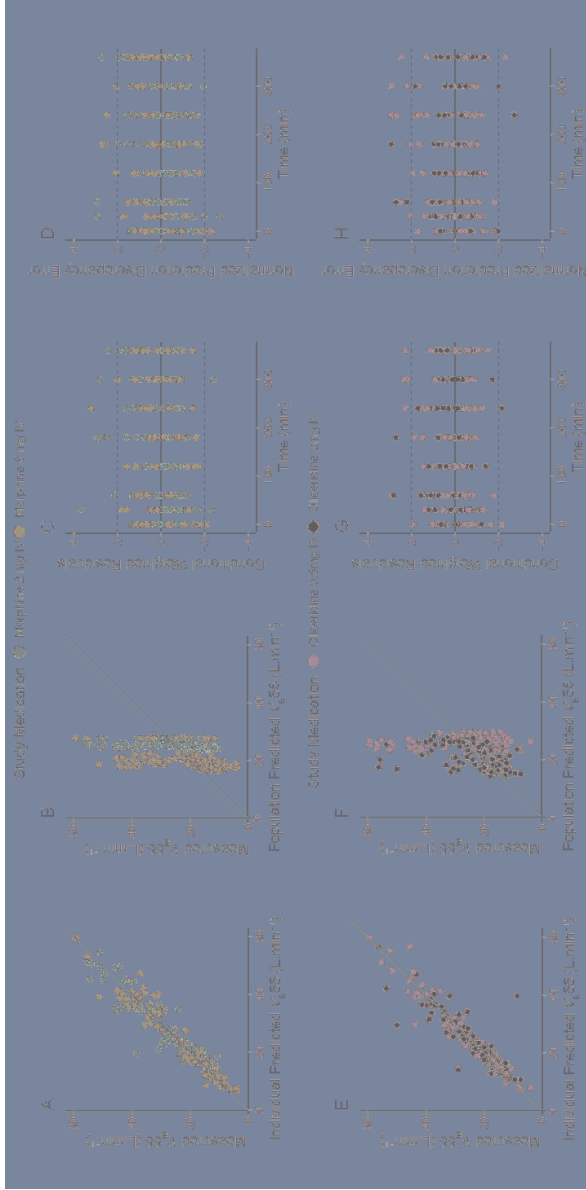


**Figure 4.6: Goodness-of-Fit PD data.** Goodness-of-Fit plots of the pharmacodynamic data analyses for morphine (panels A-D) and oliceridine (panels E-H). A and E. Measured concentration versus individual predicted concentration. B and F. Measured concentration versus population predicted concentration. C and G. Conditional weighted residuals versus time. D and H. Normalized prediction error versus time. The dotted lines represent the upper and lower limits of the 95% confidence interval. Top panels: red symbols morphine 2 mg, green symbols morphine 8 mg bottom panels: red symbols oliceridine 0.5 mg, green symbols oliceridine 2 mg.



**Table 4.2:** Pharmacodynamic parameter estimates

Oliceridine $\dot{V}_{E55}$	Parameter $\pm$ SEE	Between-subject variability $\omega^2 \pm$ SEE	Inter-occasion variability $\nu^2 \pm$ SEE
Baseline (L/min)	28.3 $\pm$ 3.3	0.21 $\pm$ 0.10	0.07 $\pm$ 0.03
$t_{1/2k_{e0}}$ (min)	44.3 $\pm$ 6.1		
$C_{50}$ (ng/mL)	29.9 $\pm$ 3.5		
$\sigma^2$	15.1 $\pm$ 5.7	1.95 $\pm$ 0.82	
<b>Morphine <math>\dot{V}_{E55}</math></b>			
Baseline (L/min)	27.8 $\pm$ 3.1	0.20 $\pm$ 0.08	0.05 $\pm$ 0.02
$t_{1/2k_{e0}}$ (min)	214 $\pm$ 27		
$C_{50}$ (ng/mL)	21.5 $\pm$ 4.6	0.49 $\pm$ 0.28	1.81 $\pm$ 0.55
$\sigma^2$	6.7 $\pm$ 1.7		

SEE is standard error of the estimate,  $\omega^2$  inter-subject variability;  $\dot{V}_{E55}$  is the extrapolated ventilation at an end-tidal  $PCO_2$  of 55 mmHg,  $t_{1/2k_{e0}}$  is the blood to effect-site equilibration half-life,  $C_{50}$  is the effect-site concentration causing 50% respiratory depression; and  $\sigma^2$  is a measure of residual variability.

---

## Simulations

The results of the simulation study are given in Figure 4.7 on page 85. They show the effect of multiple dosing aimed at a steady state in effect to maximal depression of 65% of baseline isohypercapnic ventilation. Irrespective of genotype (oliceridine), the differences in pharmacokinetic and pharmacodynamic properties result in less variation in the effect-site concentrations for morphine (difference between peaks and valleys 1 ng/ml) *versus* oliceridine (5 ng/ml) and variation in ventilation for morphine (difference between peaks and valleys 2% of baseline) *versus* oliceridine (7%). For morphine, in a 24-h period, the total drug dose given is 27 mg, which is made up of an initial bolus dose of 10 mg followed by 17 1-mg doses. For oliceridine in normal and poor metabolizers, the initial bolus dose was 1.5 mg followed by 20 doses of 0.5 mg in normal metabolizers (total dose given 11.5 mg) and 11 doses of 0.5 mg in poor metabolizers (total dose 7 mg). This indicates that less oliceridine was needed in poor than in normal metabolizers to induce a similar level of respiratory depression.

## Adverse Effects

All reported and observed adverse effects are given in Table 4.3 on page 86. At low dose and high dose, the total number of events was similar between opioids. Most frequently reported events were dizziness, lightheadedness, somnolence, and horizontal vertigo after oliceridine administration, and nausea, lightheadedness, dizziness, and somnolence following morphine (all occurring on at least 8 visits). The queried adverse events are given in Figure 4.8 on page 87. It shows the more protracted occurrence of events after morphine than oliceridine.

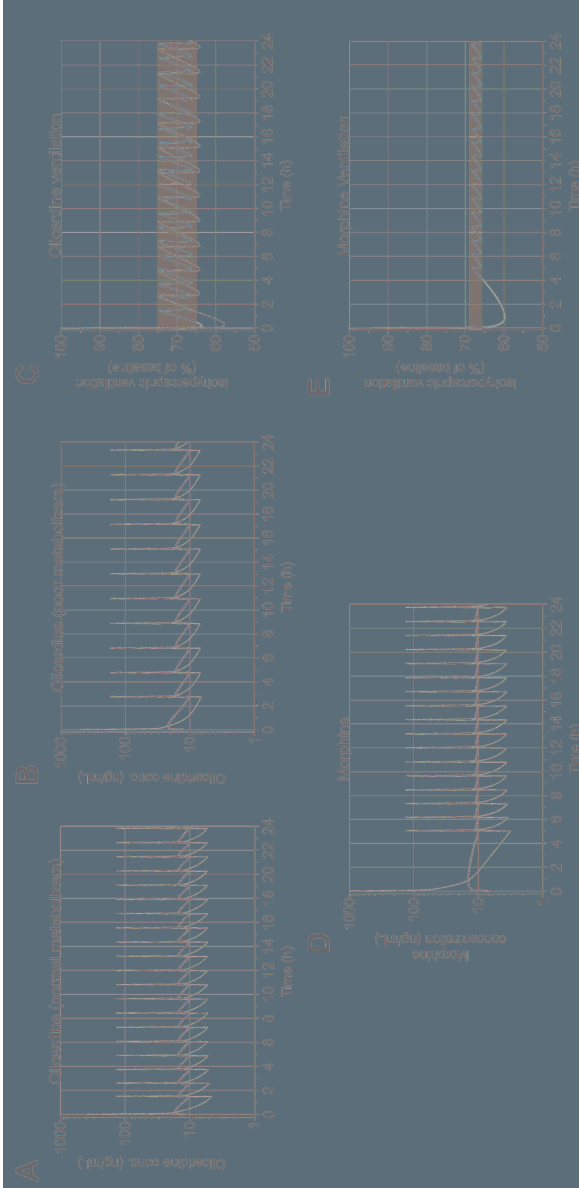


**Figure 4.7: Simulation of multiple dosing.** Simulation study of the effect of multiple doses oliceridine and morphine, mimicking patient-controlled analgesia and aimed at a maximum level of respiratory depression of 65% of baseline ventilation. **A.** Oliceridine pharmacokinetics in normal metabolizers. **B.** Oliceridine pharmacokinetics in poor metabolizers. **C.** Ventilation in normal (blue line) and poor oliceridine metabolizers (red broken line). The grey area indicates the ventilation variability. **D.** Morphine pharmacokinetics. **E.** Ventilation following morphine. Panels **A**, **B** and **D**: green lines depict plasma concentration, red lines effect-site concentrations. Panels **C** and **E**: grey areas depict the ventilation variability.

---

**Table 4.3:** Adverse effects

	Oliceridine		Morphine	
	0.5 mg	2 mg	2 mg	8 mg
Apnea*				1
Bradycardia			1	3
Dizziness	4	12	4	7
Drowsiness	1	1	1	2
Flushing		3	1	2
Headache	3	6	4	4
Hoarseness				1
Lightheadedness	5	8	3	8
Myalgia shoulders				1
Nausea (without vomiting)		6	2	10
Nausea and vomiting		1	2	5
Numbness shoulders			1	
Paresthesia extremities		1	1	3
Paresthesia whole body		1		
Pruritis at injection site		1	2	1
Rigidity of the thorax				1
Shivering			1	
Slurred speech		2		1
Somnolence	4	7	2	6
Syncope	1		1	1
Vertigo (horizontal)	2	6		3
Vertigo (vertical)		4		2
<b>Total</b>	<b>20</b>	<b>59</b>	<b>26</b>	<b>62</b>

Data are  $n$  (subjects); \*cessation of breathing for at least 30 s.

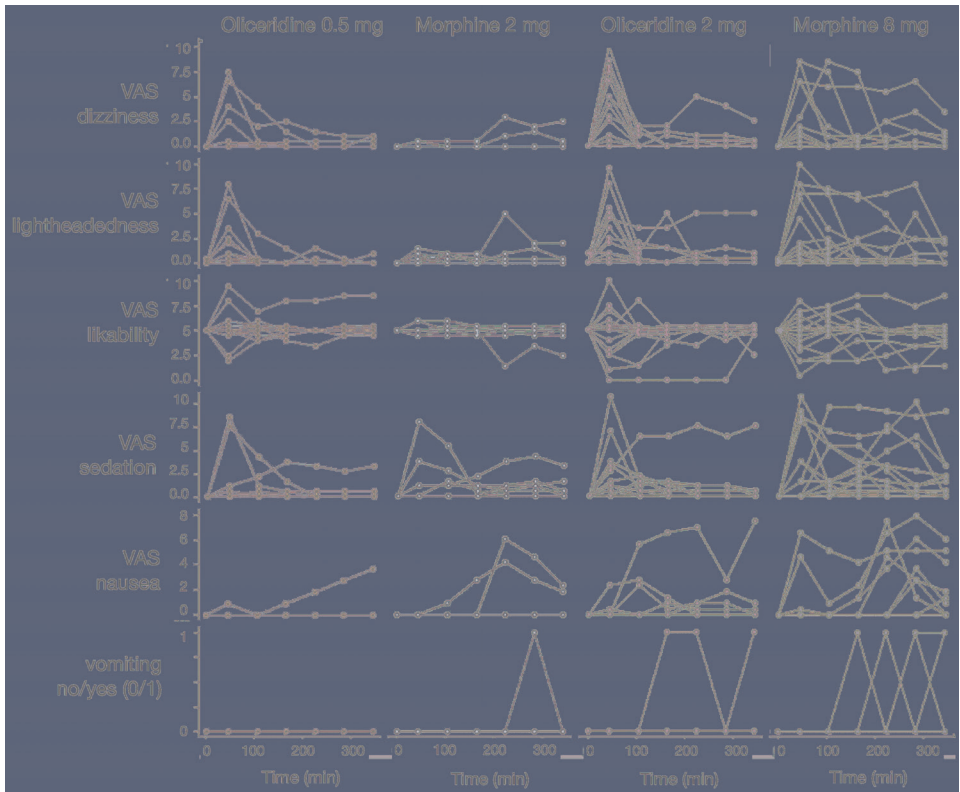


**Figure 4.8: Queried adverse events.** Adverse events, queried on a visual analog scale for dizziness, lightheadedness, drug likability, sedation, nausea and vomiting. For drug likability the score ranges from 0 = I do not like this drug to 10 = I do like this drug, with 5 an equivocal score = I do like/I do not like.

4

---

## Discussion

We studied oliceridine and morphine and measured isohypercapnic ventilation at an end-tidal  $PCO_2$  of 55 mmHg as a biomarker of drug effect in a sample of moderately overweight older men and women. Our main observations were as follows: (1) there was a 30% difference in respiratory potency between oliceridine and morphine with a 50% reduction of  $\dot{V}_E55$  ( $C_{50}$ ) observed at  $29.9 \pm 3.5$  ng/ml oliceridine and  $21.1 \pm 4.6$  ng/ml morphine; (2) oliceridine had a 5-times faster onset and offset of respiratory effect than morphine (blood-effect-site equilibration half-life,  $t_{1/2k_{e0}}$ ,  $44 \pm 6$  min for oliceridine *vs.*  $214 \pm 27$  min for morphine); and (3) oliceridine metabolism was dependent on the *CYP2D6* enzyme genotype. Simulations revealed that about 40% less oliceridine is needed to achieve the same level of respiratory depression in poor metabolizers compared with normal metabolizers over 24 h.

The study was conducted in older subjects as opposed to the more typically young and healthy study population. Previously, we studied healthy young volunteers (18 to 30 yr) to determine the respiratory effects of a range of opioids, including morphine, morphine-6-glucuronide, oxycodone, fentanyl, and buprenorphine.<sup>20,21,23,26</sup> Although these studies are of interest from a pharmacologic perspective, the current study sample is clinically more relevant, because patients aged 55 yr and older comprise the vast majority of patients in anesthetic practice. The differences in estimated model parameters indicate that, on bolus dose administration, oliceridine produces respiratory depression more rapidly than morphine, but the oliceridine effect wears off more quickly. In clinical practice, often higher opioid doses are administered than in our experimental study. This may be necessary, for example, to achieve rapid pain relief. Because we did not obtain pain data in our study (see next paragraph), we remain uninformed about how the ventilatory effects that we observed relate to the antinociceptive effects. This requires further study.

Previously, Dahan *et al.*<sup>13</sup> analyzed respiratory and antinociceptive oliceridine and morphine data in a younger cohort of healthy male volunteers (19 to 50 yr) to construct utility functions or therapeutic indices of the two opioids. They showed superiority for oliceridine compared with morphine in the utility  $U = P(A) - P(R)$ , where  $P(A)$  is the probability for analgesia and  $P(R)$  is the probability of respiratory depression. In the current study, we had planned to construct similar utility functions and therefore measured antinociceptive responses (cold pressor and electrical pain tests, data not shown) in our subjects. However, we experienced early on that the older subjects had difficulty scoring the applied noxious stimuli. They consistently were insensitive to the intense cold-water stimuli ( $1.5^\circ\text{C}$ ) and we did not detect a dose- or time-dependent effect in the electrical pain assay. We, therefore, discarded the antinociceptive

data obtained in the study. We demonstrated earlier that volunteers (mean age 37 yr, body mass index under 30 kg/m<sup>2</sup>) were not able to reliably score thermal or electrical stimuli after opioid administration.<sup>27</sup> This may be even worse in the elderly because the nociceptive fibers in the skin are affected by the normal aging process and there is also evidence for functional alterations in pain-processing regions in the brain of elderly individuals.<sup>28,29</sup> Additionally, we showed that a sample of predominantly women with morbid obesity (mean age 43 yr, body mass index range 43 kg/m<sup>2</sup>) were hypoalgesic to noxious stimuli and had difficulty grading thermal and electrical stimuli.<sup>30</sup> All of these factors could have impacted the pain measurement in our current study.

It was not possible to compare the respiratory safety of oliceridine and morphine in the older subjects of the present study because of our inability to construct utility functions. This is particularly so because respiratory depression is related to drug dose and plasma concentration, speed of drug infusion, timing of measurement and underlying pain, which are considered in the utility function. Similarly, a comparison with our previous study in younger volunteers should be made with caution given the many differences in protocol, such as the inclusion of only male subjects, venous sampling, and a different respiratory test in the earlier study.<sup>13</sup> Despite these differences, a comparison of respiratory potency ratios ( $C_{50}$  oliceridine)/( $C_{50}$  morphine) remains meaningful. The ratio equaled 1.4 in the current study and was 1.6 in the cohort of younger men.<sup>13</sup> This shows that the potency ratio is maintained over the age ranges studied (19 to 50 yr and 56 to 87 yr). Further, the estimated blood-effect site equilibration half-lives are in the same range as observed in earlier morphine and oliceridine respiratory studies.<sup>13,21,31,32</sup> Additional studies in preferably acute pain patients, comparing multiple age cohorts, on pain relief and respiration, are needed for definite conclusions.

The pharmacokinetic profile of oliceridine was altered in three poor metabolizers related to the *CYP2D6* genotype. All three had a significantly lower clearance ( $CL_1$ ) with higher plasma oliceridine concentrations than the other *CYP2D6* genotypes. Similar observations were reported earlier.<sup>33</sup> In reviewing the pharmacokinetic data, we also need to consider the effects of age and body mass index. Among other physiologic changes, at an increasing age, glomerular filtration rate is reduced and there is a shift in the distribution of fat and muscle mass.<sup>34,35</sup> The latter may account for the decreased morphine compartmental volumes compared with volumes reported in younger volunteers with mean age 26 yr.<sup>36</sup> Similar observations were made for remifentanyl showing reduced compartments volumes with increasing age.<sup>37</sup> Our oliceridine pharmacokinetic parameter estimates agree with the pooled analysis of seven oliceridine data sets in acute pain patients of which more than half had an age range of 40 to 65 yr.<sup>7</sup> For morphine, a possible age-related reduction in renal function may cause accumulation of morphine-6-glucuronide, morphine's

---

active metabolite, and subsequently enhance respiratory depression.<sup>38</sup> In our sample, all subjects had a glomerular filtration rate greater than 60 ml/min and a normal liver function.

The morphine and oliceridine  $C_{50}$  values (Table 4.2) are lower than previously reported in several studies in younger volunteers.<sup>32</sup> For example, we earlier observed a  $C_{50}$  for morphine respiratory effect of about 45 ng/ml in young volunteers in their twenties.<sup>39</sup> Although we did not perform a direct comparison among different age cohorts, these observations point toward an increase in respiratory potency with increasing age for the two tested opioids. Our findings are consistent with earlier studies showing enhanced desired and undesired opioid effect with increasing age.<sup>37,40,41,42</sup> For potent synthetic opioids, the age effect is well documented. For example, Scott *et al.*<sup>43</sup> found that the fentanyl dose requirements to produce a similar electroencephalographic effect decreases by 50% at an increasing age (from 20 to 89 yr) in male patients. Similar observations were made for remifentanyl.<sup>37</sup> Cepeda *et al.*<sup>42</sup> showed that the risk for postoperative respiratory depression rises with increasing age in 8,855 surgical patients receiving an opioid (fentanyl, meperidine, or morphine) for postoperative pain. Compared with younger patients (16 to 45 yr), those aged 61 to 70 yr, 71 to 80 yr, and 81 yr and older had, respectively, a 2.8, 5.4, and 8.7 times higher risk for the development of respiratory depression. The physiologic basis of the increased opioid respiratory sensitivity with age remains unknown but may be related to an age-dependent imbalance between excitatory and inhibitory neuronal pathways within the respiratory networks of the brainstem after opioid receptor activation.<sup>44</sup> Possibly excitatory pathways are less active in the elderly, leading to increased sensitivity of the ventilatory control system to opioids.



## $\dot{V}_{E55}$ versus Slope of the Hypercapnic Ventilatory Response

We measured the non-steady-state ventilatory response to carbon dioxide according to Read,<sup>16</sup> Rebuck,<sup>17</sup> and Florian *et al.*<sup>18</sup> Rather than using the slope of the response curve as our primary endpoint, we used ventilation at an end-tidal  $PCO_2$  of 55 mmHg ( $\dot{V}_{E55}$ ) calculated from the slope ( $S$ ) and the  $x$ -axis intercept ( $B$ ) as follows:  $\dot{V}_{E55} = [S \times (55 - B)]$ ;  $S$  and  $B$  are estimated from the regression of the breath-to-breath  $PCO_2$  ventilation data. As is apparent from the formula,  $\dot{V}_{E55}$  considers the slope and the position of the hypercapnic response curve. Opioids are known to decrease the slope and shift the response curve to the right, both of which are signs of respiratory depression. We and others earlier used  $\dot{V}_{E55}$  to reliably express opioid effects on ventilatory control.<sup>18,20,23</sup> We chose a rebreathing rather than a steady-state technique to quantify the opioid effect on the hypercapnic ventilatory response to enable rapid and frequent testing over time. The steady-state technique is more cumbersome and takes 30 to 40 min to complete.<sup>20</sup> We previously argued that, in contrast to the steady-state technique, the rebreathing technique causes a reduction of the response slope due to a decrease in the differences between end-tidal (and arterial)  $PCO_2$  and the content in the rebreathing balloon (7%) after opioid administration.<sup>45,46</sup> However, the opioid-induced rise in end-tidal is due to the opioid respiratory effect, and, consequently, the reduced slope is a sign of respiratory depression that becomes apparent because of methodologic issues. A reduced slope is often not observed using a nonrebreathing steady-state technique.<sup>47</sup> Interestingly, opioids cause a rightward shift of the steady-state hypercapnic response curve, but the effect of opioids on  $\dot{V}_{E55}$  seems independent of the method used to measure the hypercapnic ventilatory response.<sup>48</sup>

In conclusion, our population pharmacokinetic–pharmacodynamic analysis, performed in older individuals, shows that oliceridine has a more rapid onset/offset of respiratory depression, as defined by parameter  $t_{1/2k_{e0}}$ , combined with a 30% lesser potency for respiratory depression, as defined by parameter  $C_{50}$ , than morphine.



## References

1. Paul AK, Smith CG, Rahmattullah M, Nissapatorn V, Wilairatana P, Spetea M, Gueven N, Diteis N. Opioid analgesia and opioid-induced adverse effects: a review. *Pharmaceut (Basel)*. 2021; **14**: 1091  
DOI: 10.3390/ph14111091.
2. Shafi S, Collinsworth AW, Copeland LA, Ogola GO, Qiu T, Kouznetsova M, Liao IC, Mears N, Pham AT, Wan GJ, Masica AL. Association of Opioid-Related Adverse Drug Events With Clinical and Cost Outcomes Among Surgical Patients in a Large Integrated Health Care Delivery System. *Jama Surgery*. 2018; **153**: 757–763  
DOI: 10.1001/jamasurg.2018.1039.
3. Kessler ER, Shah M, Gruschkus SK, Raju A. Cost and quality implications of opioid-based postsurgical pain control using administrative claims data from a large health system: opioid-related adverse events and their impact on clinical and economic outcomes. *Pharmacother*. 2013; **33**: 383–91  
DOI: 10.1002/phar.2013.33.issue-4.
4. Boom M, Niesters M, Sarton E, Aarts L, Smith TW, Dahan A. Non-analgesic effects of opioids: opioid-induced respiratory depression. *Curr Pharm Des*. 2012; **18**: 5994–6004  
DOI: 10.2174/138161212803582469.
5. Mann J, Samieegohar M, Chaturbedi A, Zikle J, Han X, Ahmadi SF, Eshleman A, Janowsky A, Wolfrum K, Swanson T, Bloom S, Dahan A, Olofsen E, Florian J, Strauss D, Li Z. Development of a translational model to assess the impact of opioid overdose and naloxone dosing on respiratory depression and cardiac arrest. *Clin Pharmacol Ther*. 2022;  
DOI: 10.1002/cpt.v112.5.
6. Kharasch ED, Avram MJ, Clark JD. Rational perioperative opioid management in the era of the opioid epidemic. *Anesthesiology*. 2020; **132**: 603–5  
DOI: 10.1097/ALN.0000000000003166.

## References

---

7. Fossler MJ, Sadler BM, Farrell C, Burt DA, Pitsiu M, Skobieranda F, Soergel DG. Oliceridine (TRV130), a novel G protein-biased ligand at the mu-opioid receptor, a predictable relationship between plasma concentrations and pain relief. I: Development of pharmacokinetic/pharmacodynamic model. *J Clin Pharmacol*. 2018; **58**: 750–61  
DOI: 10.1002/jcph.1076.
8. Dewire SM, Yamashita DS, Rominger DH, Liu G, Cowan CL, Graczyk TM, Chen XT, Pitis PM, Gotchev D, Yuan C, Koblish M, Lark MW, Violoin JD. A G protein-biased ligand at the  $\mu$ -opioid receptor is potently analgesic with reduced gastrointestinal and respiratory dysfunction compared with morphine. *J Pharmacol Exp Ther*. 2013; **344**: 708–17  
DOI: 10.1124/jpet.112.201616.
9. Manglik A et al. Structure-based discovery of opioid analgesics with reduced side effects. *Nature*. 2016; **537**: 185–90  
DOI: 10.1038/nature19112.
10. Raehal KM, Walker JKL, Bohn LM. Morphine side effects in  $\beta$ -arrestin 2 knockout mice. *J Pharmacol Ther*. 2005; **314**: 1195–2001  
DOI: 10.1124/jpet.105.087254.
11. Gillis A et al. Low intrinsic efficacy for G protein activation can explain the improved side effect profiles of new opioid agonists. *Sci Signal*. 2020; **13**: eaaz3140  
DOI: 10.1126/scisignal.aaz3140.
12. Stahl EL, Bohn LM. Low intrinsic efficacy alone cannot explain the improved side effect profiles of new opioid agonists. *Biochem*. 2021;  
DOI: 10.1021/acs.biochem.1c00466.
13. Dahan A, Dam CJ van, Niesters M, Velzen M van, Fossler MJ, Demitrack MA, Olofsen E. Benefit and risk evaluation of biased  $\mu$ -receptor agonist oliceridine versus morphine. *Anesthesiology*. 2020; **133**: 559–568  
DOI: 10.1097/ALN.0000000000003441.
14. Soergel G, Subach RS, Burnam N, Lark MW, James IE, Sadler BM, Skobieranda F, Violin JD, Webster LR. Biased agonism of the  $\mu$ -opioid receptor by TRV130 increases analgesia and reduces on-target adverse effects vs. morphine: a randomized, double-blind, placebo-controlled, crossover study in healthy volunteers. *Pain*. 2014; **155**: 1829–1835  
DOI: 10.1016/j.pain.2014.06.011.
15. Viscussi ER, Webster I, Kuss M, Daniels S, Bolognese JA, Zuckerman S, Soergel DG, Subach RA, Cook E, Skobieranda F. A randomized, phase-2 study investigating TRV130, a biased-ligand of the mu-opioid receptor, for intravenous treatment of pain. *Pain*. 2016; **157**: 264–272  
DOI: 10.1097/j.pain.0000000000000363.

16. Read DJ. A clinical method for assessing the ventilatory response to carbon dioxide. *Australas Ann Med.* 1967; **16**: 20–32  
DOI: 10.1111/imj.1967.16.issue-1.
17. Rebuck AS. Measurement of ventilatory response to CO<sub>2</sub> by rebreathing. *Chest.* 1976; **70**: 118–121  
DOI: 10.1378/chest.70.1'Supplement.118.
18. Florian J et al. Effect of paroxetine or quetiapine combined with oxycodone on ventilation: a randomized clinical trial. *JAMA.* 2022; **328**: 1405–1414  
DOI: 10.1001/jama.2022.17735.
19. Henriques BC et al. Methodology for clinical genotyping of CYP2D6 and CYP2C19. *Transl Psychiatry.* 2021; **11**: 596 (2022 corrected version)  
DOI: 10.1038/s41398-021-01717-9.
20. Schrier R van der, Roozkrans M, Olofsen E, Aarts L, Velzen M van, Jong M de, Dahan A, Niesters M. Influence of ethanol on oxycodone-induced respiratory depression: a dose-escalating study in young and elderly volunteers. *Anesthesiology.* 2017; **126**: 534–542  
DOI: 10.1097/ALN.0000000000001505.
21. Romberg R, Olofsen E, Sarton E, Teppema L, Dahan A. Pharmacodynamic effect of morphine-6-glucuronide versus morphine on hypoxic and hypercapnic breathing in healthy volunteers. *Anesthesiology.* 2003; **99**: 788–789  
DOI: 10.1097/0000542-200310000-00008.
22. Holford NH. A size standard for pharmacokinetics. *Clin Pharmacokinet.* 1996; **30**: 329–332  
DOI: 10.2165/00003088-199630050-00001.
23. Schrier Rvd, Jonkman K, Velzen Mv, Olofsen E, Drewes AM, Dahan A, Niesters M. An experimental study comparing the respiratory effects of tapentadol and oxycodone in healthy volunteers. *Br J Anaesth.* 2017; **119**: 1169–1177  
DOI: 10.1093/bja/aex295.
24. Minto CF, Schnider TW, Gregg KM, Henthorn TK, Shafer SL. Using the maximum effect site concentration to combine pharmacokinetics and dynamics. *Anesthesiology.* 2003; **99**: 324–333  
DOI: 10.1097/0000542-200308000-00014.
25. Caudle KE, Sangkuhl K, Whirl-Carrillo M, Swen JJ, Haider CE, Klein TE, Gammal RS, Relling MV, Scott SA, Hertz DL, Guchelaar HJ, Gaedigk A. Standardizing CYP2D6 genotype to phenotype translation: consensus recommendations from the clinical pharmacogenetics implementation consortium and Dutch pharmacogenetics working group. *Clin Transl Sci.*

## References

---

- 2020; **13**: 116–124  
DOI: 10.1111/cts.v13.1.
26. Olofsen E, Algera M, Moss L, Dobbins RL, Groeneveld GJ, Velzen M van, Niesters M, Dahan A, Laffont C. Modelling buprenorphine reduction of fentanyl-induced respiratory depression. *JCI Insight*. 2022; **7**: e156973  
DOI: 10.1172/jci.insight.156973.
27. Oudejans LCJ, Velzen M van, Olofsen E, Beun R, Dahan A, Niesters M. Translation of random painful stimuli into numerical responses in fibromyalgia and perioperative patients. *Pain*. 2016; **157**: 128–136  
DOI: 10.1016/j.pain.2016.06.041.
28. Kemp J, Després O, Pabayle T, Dufour A. Differences in Age-Related Effects on Myelinated and Unmyelinated Peripheral Fibres: A Sensitivity and Evoked Potential Study. *European Journal of Pain*. 2014; **18**: 482–488  
DOI: 10.1002/ejp.2014.18.issue-4.
29. Tseng M, Chiang M, Yazhuo K, Chao C, Tseng W, Hsieh S. Effect of Aging on the Cerebral Processing of Thermal Pain in the Human Brain. *Pain*. 2013; **154**: 2120–2129  
DOI: 10.1016/j.pain.2013.06.041.
30. Torensma B, Oudejans L, Velzen M van, Swank D, Niesters M, Dahan A. Pain Sensitivity and Pain Scoring in Patients with Morbid Obesity. *Surgery for Obesity and Related Diseases*. 2017; **13**: 788–795  
DOI: 10.1016/j.soard.2017.01.015.
31. Lötsch J, Skarke C, Schmidt H, Grösch S, Geisslinger G. The Transfer Half-life of Morphine-6-Glucuronide from Plasma to Effect Site Assessed by Pupil Size Measurement in Healthy Volunteers. *Anesthesiology*. 2001; **95**: 1329–1338  
DOI: 10.1097/00000542-200112000-00009.
32. Martini CH, Olofsen E, Yassen A, Aarts L, Dahan A. Pharmacokinetic-Pharmacodynamic Modeling in Acute and Chronic Pain: An Overview of the Recent Literature. *Expert Review of Clinical Pharmacology*. 2011; **4**: 719–732  
DOI: 10.1586/ecp.11.59.
33. Fossler MJ, Sadler BM, Farrell C, Burt DA, Pitsiu M, Skobieranda F, Soergel DG. Oliceridine, a Novel G Protein-Biased Ligand at the  $\mu$ -Opioid Receptor, Demonstrates a Predictable Relationship Between Plasma Concentrations and Pain Relief. II: Simulation of Potential Phase 3 Study Designs Using a Pharmacokinetic/Pharmacodynamic Model. *Journal of Clinical Pharmacology*. 2018; **58**: 762–770  
DOI: 10.1002/jcph.1075.

34. Boss GR, Seegmiller JE. Age-Related Physiological Changes and Their Clinical Significance. *The Western Journal of Medicine*. 1981; **135**: 434–440  
DOI: Not available.
35. Dodds CM, Kumar CM, Veering BT. *Oxford Textbook of Anaesthesia for the Elderly Patient*. Oxford University Press, 2014. DOI: Not available.
36. Lötsch J, Stockmann A, Kobal G, Brune K, Waibel R, Schmidt N, Geisslinger G. Pharmacokinetics of Morphine and Its Glucuronides After Intravenous Infusion of Morphine and Morphine-6-Glucuronide in Healthy Volunteers. *Clinical Pharmacology Therapeutics*. 1996; **60**: 316–325  
DOI: 10.1016/S0009-9236(96)90058-2.
37. Minto CF, Schnider TW, Shafer SL. Pharmacokinetics and Pharmacodynamics of Remifentanyl. II. Model Application. *Anesthesiology*. 1997; **86**: 24–33  
DOI: 10.1097/00000542-199701000-00005.
38. Crugten JT van, Somogyi AA, Nation RL, Reynolds GR. The Effect of Age on the Disposition and Antinociceptive Response of Morphine and Morphine-6-Glucuronide in the Rat. *Pain*. 1997; **71**: 199–205  
DOI: 10.1016/S0304-3959(97)03363-0.
39. Olofsen E, Dorp E van, Teppma L, Aarts L, Smith T, Dahan A, Sarton E. Naloxone Reversal of Morphine- and Morphine-6-Glucuronide-Induced Respiratory Depression in Humans. *Anesthesiology*. 2010; **212**: 1417–1427  
DOI: 10.1097/ALN.0b013e3181d5e29d.
40. Vuyk J. Pharmacodynamics in the Elderly. *Best Practice Research Clinical Anaesthesiology*. 2003; **17**: 207–218  
DOI: 10.1016/S1521-6896(03)00008-9.
41. Bowie MW, Slattum PW. Pharmacodynamics in Older Adults: A Review. *The American Journal of Geriatric Pharmacotherapy*. 2007; **5**: 263–303  
DOI: 10.1016/j.amjopharm.2007.10.001.
42. Cepeda MS, Farrar JT, Baumgarten M, Boston R, Carr DB, Strom BL. Side Effects of Opioids During Short-Term Administration: Effect of Age, Gender, and Race. *Clinical Pharmacology Therapeutics*. 2003; **74**: 102–112  
DOI: 10.1016/S0009-9236(03)00152-8.
43. Scott JC, Stanski DR. Decreased Fentanyl and Alfentanil Dose Requirements with Age: A Simultaneous Pharmacokinetic and Pharmacodynamic Evaluation. *Journal of Pharmacology and Experimental Therapeutics*. 1987; **240**: 159–166  
DOI: PMID 3100765.

## References

---

44. Dahan A, Schrier R van der, Smith T, Aarts L, Velzen M van, Niesters M. Averting Opioid-Induced Respiratory Depression Without Affecting Analgesia. *Anesthesiology*. 2018; **128**: 1027–1037  
DOI: 10.1097/ALN.0000000000002184.
45. Dahan A, Berkenbosch A, DeGoede J, Olievier ICW, Bovill JG. On a Pseudo-rebreathing Technique to Assess the Ventilatory Sensitivity to Carbon Dioxide in Man. *The Journal of Physiology*. 1990; **423**: 615–629  
DOI: 10.1113/jphysiol.1990.sp018043.
46. Berkenbosch A, DeGoede J, Olievier CN, Schuitmaker JJ. A Pseudo-Rebreathing Technique for Assessing the Ventilatory Response to Carbon Dioxide in Cats. *The Journal of Physiology*. 1986; **381**: 483–495  
DOI: 10.1113/jphysiol.1986.sp016340.
47. Berkenbosch A, Bovill JG, Dahan A, DeGoede J, Olievier ICW. The Ventilatory CO<sub>2</sub> Sensitivities from Read's Rebreathing Method and the Steady-State Method Are Not Equal in Man. *The Journal of Physiology*. 1989; **411**: 367–377  
DOI: 10.1113/jphysiol.1989.sp017578.
48. Bourke DL, Warley A. The Steady-State and Rebreathing Methods Compared During Morphine Administration in Humans. *The Journal of Physiology*. 1989; **419**: 509–517  
DOI: 10.1113/jphysiol.1989.sp017883.



## Chapter 5

# Effects of insulin on the acute hypoxic ventilatory response: an exploratory study in patients with non-insulin dependent diabetes mellitus versus healthy controls

Pieter Simons<sup>1</sup>, Rutger van der Schrier<sup>1</sup>, Maarten van Lemmen<sup>1</sup>, Albert Dahan<sup>1,2</sup>

*Submitted*

1. Department of Anesthesiology, Leiden University Medical Center, 2300 RC Leiden, The Netherlands
2. PainLess Foundation, Leiden, the Netherlands

---

## Introduction

Type 2 diabetes mellitus (T2DM) is a heterogeneous disease characterized by hyperinsulinemia, absolute or relative insulin deficiency due to  $\beta$ -cell secretory dysfunction, insulin resistance, glucose intolerance, and fasting hyperglycemia.<sup>1</sup> With a projected prevalence of 1.3 billion people with T2DM in 2050, it is one of the leading causes of morbidity and mortality worldwide.<sup>2</sup> Understanding the pathogenesis of T2DM is essential for the development of new therapeutic approaches and for improving the health status of afflicted individuals.

Augmentation of autonomic nervous system activity *via* the carotid bodies is a proposed mechanism for the initiation and progression of insulin resistance.<sup>3,4,5</sup> Increased sympathetic outflow results in a cascade of effects, including lipolysis, vasoconstriction, increased gluconeogenesis, impaired glucose uptake, and reduced insulin release.<sup>5</sup> Insulin, a sympathoexcitatory hormone, activates the sympathetic nervous system through pathways that are not fully understood. While previous research focused on the central nervous system as a source of sympathetic nervous system activation, recent studies support a role for peripheral sensors as well, including the carotid bodies.<sup>6,7,8,4,9</sup> Chronic exposure to high levels of insulin could result in long-term facilitation of the carotid bodies (CB), similar to changes observed in the CB during chronic intermittent hypoxia.<sup>10,11</sup> The carotid bodies are small organs located above the bifurcation of the common carotid arteries that contain specialized chemosensory type I glomus cells. In addition to their ability to cause hyperventilation in response to hypoxia, the so-called acute hypoxic ventilatory response or HVR, the carotid bodies detect glucose, insulin, lactate, leptin, and GLP1, indicative of their role in metabolic homeostasis.<sup>12,13,14,4,15</sup>

Hypertrophy of the carotid bodies is observed in T2DM,<sup>16,17</sup> an observation also made in animals and humans exposed to chronic or intermittent hypoxia (*e.g.* in children with congenital heart disease).<sup>10,18</sup> These changes are associated with an increased glomus cell excitability, hypersensitivity, and long-lasting carotid body afferent activity that persists even after termination of the underlying causes of CB hypertrophy.<sup>19</sup> Interestingly, hyperbaric oxygen therapy, silencing the carotid bodies, improves glucose homeostasis in T2DM patients.<sup>20,21</sup>

The carotid bodies contain insulin receptors and the sympathoexcitatory effect of insulin on the carotid bodies has been demonstrated before.<sup>4</sup> *In vivo* experiments demonstrated a dose-dependent insulin-induced increase in ventilation while maintaining euglycemia, which was abolished by carotid sinus nerve denervation.<sup>4</sup> During euglycemia, increasing insulin levels in human volunteers increased muscle sympathetic nerve activity and ventilation.<sup>22,23</sup>

## Diabetes, hyperinsulinemia, and the hypoxic ventilatory response

Since the carotid bodies sense insulin in humans, it is plausible that insulin influences hypoxic chemosensitivity, potentially leading to changes in the HVR. Moreover, the carotid body might serve as a conduit through which insulin mediates shifts in autonomic balance and metabolic control.

This exploratory and hypothesis-generating investigation aims to increase our understanding of the intricate interplay between insulin, carotid body function, and the autonomic response to insulin in both T2DM patients and HC. To discern the genuine effects of insulin, free from hypoglycemia's or hyperglycemia's confounding influences, we measured the HVR during a hyperinsulinemic-euglycemic clamp (HEC).

---

## Methods

### Ethics and Registration

The protocol and subsequent amendment were approved by the local Institutional Review Board (IRB; The Medical Ethics Committee Leiden, The Hague, Delft, The Netherlands) and the Central Committee on Research Involving Human Participants (CCMO) in The Hague, The Netherlands. The trial was registered at the International Clinical Trials Registry Platform (identifier: NCT05237076) All participants gave written informed consent before enrollment in the study and all experiments and procedures conformed to the Declaration of Helsinki. The study was performed from December 2021 to August 2022. All participants gave written informed consent prior to enrollment in the study.

### Study Design

#### Participants

Participants aged 18 and older were recruited. The T2DM group had to be diagnosed with non-insulin-dependent diabetes without any diabetic autonomous neuropathy-related symptoms and needed to use antidiabetic medication. Healthy Controls (HC) were enrolled if they had no known history of pre-diabetes or any other significant disease. Main exclusion criteria for both groups were any clinically significant concomitant disease, smoking, pregnancy, vital parameters outside the normal range (systolic blood pressure between 90 and 150 mmHg, diastolic blood pressure between 40 and 95 mmHg, pulse rate between 40 and 100 breaths/min and body mass index of 35 m<sup>2</sup>/kg or less). See appendix A for all inclusion and exclusion criteria.

#### Intervention

All participants fasted overnight before arrival in the laboratory. T2DM patients refrained from antidiabetic drugs for 24 hrs. All participants received a venous access line and a radial arterial line for blood sampling. Thereafter, ventilatory measurements were performed during fasting and subsequently during a hyperinsulinemic-euglycemic clamp. All measurements were performed at room temperature (20–22 °C), at sea level, in a semi-recumbent position.

#### Ventilatory Apparatus

Participants breathed through a face mask over mouth and nose that was attached to a gas-mixer (The Leiden Gas Mixer, LUMC, Leiden, the Netherlands). Computer-driven (RESREG/ACQ software, Leiden, the

## Diabetes, hyperinsulinemia, and the hypoxic ventilatory response

Netherlands) mass-flow controllers (EL-Flow, Bronkhorst High Tech, the Netherlands) provided a gas mixture consisting of nitrogen, carbon dioxide, and oxygen as desired. The software allows for the steering of the end-tidal gas concentrations (by varying the inspired concentration) and the collection of respiratory variables. Airflow was measured with a pneumotachograph/pressure transducer system (#4813, Hans Rudolph, Shawnee, Kansas). Both inspiratory and expiratory concentrations for O<sub>2</sub> and CO<sub>2</sub> were continuously measured (ISA OR<sup>+</sup> Masimo Root Platform, Irvine, CA). Heart rate and oxygen saturation were obtained by pulse oximetry at the finger (Radical-7 Masimo Root Platform, Irvine, CA). Ventilation data were collected on a breath-to-breath basis.

### Respiratory Measurements

**Isocapnic ventilatory response to hypoxia** The HVR was obtained at isocapnia (end-tidal PCO<sub>2</sub> 0.3-0.4 kPa above resting PCO<sub>2</sub>) by a rapid decrease in inspired oxygen fraction to 0.08 that was maintained for 5 min. Thereafter, the subjects were made hyperoxic (inspired oxygen fraction 0.4) for another 5 min. The HVR was calculated as  $V_E/SpO_2$ . Modified Dejour Test. The ventilatory response to 5 breaths of hyperoxia (inspired oxygen fraction 1.0) was obtained after 5 min of room air breathing. The decrease in ventilation in response to hyperoxia provides an indirect assessment of carotid sinus afferent nerve activity, which, in this context, is considered an indicator of carotid body activity or the carotid body's influence on resting ventilation.

**Modified Dejour** The ventilatory response to 5 breaths of hyperoxia (inspired oxygen fraction 1.0) was obtained after 5 min of room air breathing. The decrease in ventilation in response to hyperoxia provides an indirect assessment of carotid sinus afferent nerve activity, which, in this context, is considered an indicator of carotid body activity or the carotid body's influence on resting ventilation.

### Hyperinsulemic-euglycemic clamp

A manual hyperinsulinemic-euglycemic clamp was applied as described by de Fronzo *et al.*<sup>24</sup> Insulin (100 IU/ml, Novorapid) was infused intravenously at 40 mU/body surface area (m<sup>2</sup>)/min, to achieve steady-state insulin levels (plasma levels ~ 700 mU/mL). The body surface was calculated using Du Bois equation. Glucose 40% was infused to maintain blood glucose at a predetermined target level (fasting arterial blood glucose). Adjustments were performed at 5 min intervals, using arterial samples to determine glucose level using a blood gas analyzer (RAPID point 500e, Siemens Healthineers, Erlangen, Germany) for a total duration of 120 min. Respiratory measurements were performed during steady-state glucose infusion rates (coefficient of variation in blood glucose  $\leq$

---

10%).

### **Hemodynamic parameters**

Pulse rate, blood pressure (diastolic, mean, systolic), and stroke volume were continuously monitored with the FloTrac system (HemoSphere, Edwards Lifesciences, Irvine, CA, U.S.) connected to the arterial cannula..

### **Heart Rate Variability**

The electrocardiogram was sampled at 200 Hz (IntelliVue MX850, Philips, Eindhoven, the Netherlands), and interbeat interval data were extracted. With specific software (Kubios HRV v3.1, Kuopio, Finland) cardiac autonomic activity was analyzed.<sup>25</sup> The parasympathetic (PNS) index was computed using the following parameters: mean RR interval, root mean square of successive RR interval differences (RMSSD), and Poincaré plot index SD1 in normalized units. The sympathetic (SNS) index was computed using the following parameters: mean RR interval, Baevsky's stress index, and Poincaré plot index SD2 in normalized units. An association between a low heart rate variability and autonomic imbalance, whether symptomatic or asymptomatic, has been described in patients with T2DM compared to HC.<sup>26,27</sup>

### **Statistical analysis**

Based on prior studies assessing changes in hypoxic sensitivity, a sample size calculation was performed targeting a statistical power of 90%. It was determined that a sample size of  $n = 28$  would be sufficient to detect significant changes in HVR. We planned to enroll fifteen individuals with T2DM with a balanced gender distribution. Additionally, fifteen age, sex, and weight-matched HC were enrolled.

Data were compared between T2DM and HC using linear mixed-effects models using packages lme4 and lmerTest in R (version 4.2.2, R Foundation for Statistical Computing, Vienna, Austria). Data are represented as means  $\pm$  95% CI, unless otherwise stated.

## Results

A total of 32 participants was enrolled (Figure 5.1). Data from five subjects were excluded from the analysis due to insufficient quality of the hyperinsulinemic-clamp and data from three subjects were excluded due to insufficient quality of the HVR. Table 5.1 on page 106 summarizes baseline demographics and patient characteristics. Mean fasting glucose levels were higher in T2DM individuals compared to HC ( $8.6 \pm 0.8$  vs.  $5.4 \pm 0.2$  mmol.L<sup>-1</sup>).

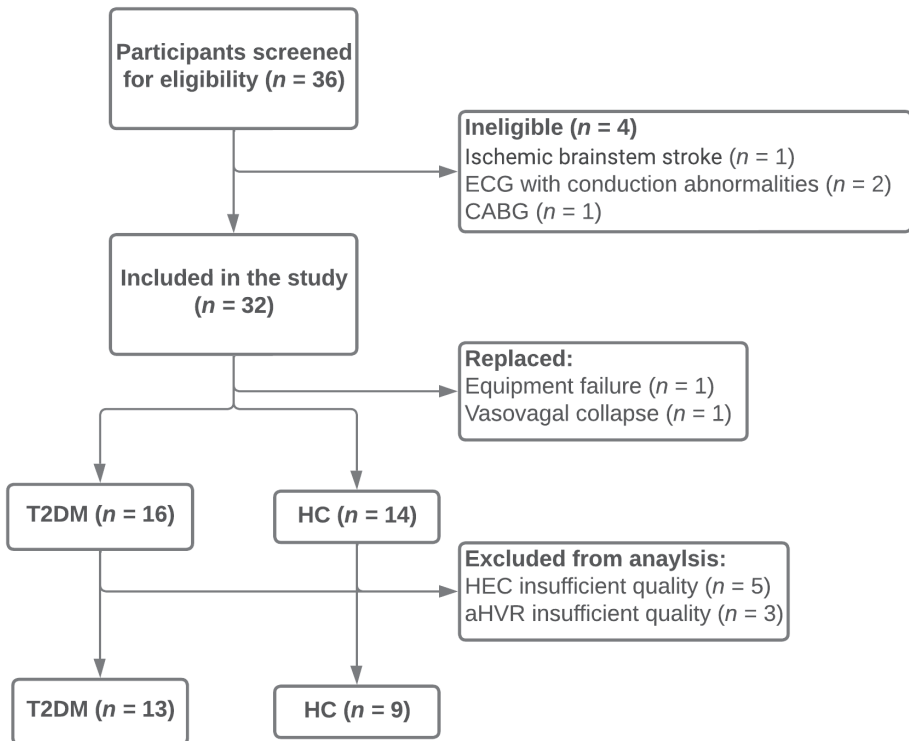


**Figure 5.1:** Study enrollment. ECG = electrocardiogram, CABG = coronary artery bypass graft, T2DM = diabetes mellitus type 2, HC = healthy control, HEC = hyperinsulinemic-euglycemic clamp.

**Table 5.1:** Subject characteristics

	<b>T2DM</b> <b>(n = 13)</b>	<b>Healthy controls</b> <b>(n = 9)</b>	<b>Mean difference</b> <b>(mean ± 95% CI)</b>
<b>Demographics</b>			
Age (years)	62 ± 13	70 ± 7	7 ± 9
Female, n (%)	7 (54)	4 (44)	3
Height (m)	1.7 ± 0.1	1.7 ± 0.1	0 ± 0.1
Weight (kg)	81.9 ± 13.6	73.8 ± 20.4	8.2 ± 16.8
Body surface area (m <sup>2</sup> )	2.0 ± 0.2	1.9 ± 0.3	0.1 ± 0.2
Body mass index (kg/m <sup>2</sup> )	26.9 ± 3.6	24.2 ± 4.1	2.7 ± 3.6
<b>Metabolic</b>			
Fasting plasma glucose (mmol.l <sup>-1</sup> )	8.6 ± 1.4	5.4 ± 0.3	3.2 ± 0.8
<b>Respiratory</b>			
Respiratory rate (min <sup>-1</sup> )	16.2 ± 2.3	15.1 ± 0.9	1.5 ± 1.6
Tidal volume (ml)	505 ± 37	490 ± 58	4.1 ± 53.1
Minute Ventilation (l.min <sup>-1</sup> )	7.6 ± 0.8	6.9 ± 0.9	0.6 ± 0.7
<b>Cardiovascular</b>			
Heart rate (beats.min <sup>-1</sup> )	67 ± 10	59 ± 7	8 ± 7
Systolic blood pressure (mmHg)	143 ± 15	140 ± 16	3 ± 14
Diastolic blood pressure (mmHg)	77 ± 9	79 ± 13	2 ± 11
Cardiac index (l.min <sup>-1</sup> .m <sup>-2</sup> )	2.5 ± 0.3	2.8 ± 0.3	0.2 ± 0.4



Table 5.1 continued from previous page

	NIDDM ( <i>n</i> = 13)	Healthy controls ( <i>n</i> = 9)	Mean difference (mean ± 95% CI)
<b>Comorbidities</b>			
Time since diagnosis NIDDM (yrs.)	10 ± 6		
Anti-diabetic medication			
Metformin, <i>n</i> (%)	13 (100%)		
Sulfonylureas, <i>n</i> (%)	4 (31%)		
SGLT2 inhibitors, <i>n</i> (%)	1 (7%)		

Values are means ± SD unless otherwise noted. NIDDM = non-insulin dependent diabetes.

---

## Isocapnic HVR

Going from a fasting state to euglycemic-hyperinsulinemic conditions, the HVR exhibited distinct patterns in the two groups. In HC, the HVR increased from  $0.56 \pm 0.11$  to  $0.77 \pm 0.11$   $\text{L}\cdot\text{min}^{-1}\cdot\%^{-1}$  ( $p = 0.04$ ). In contrast, individuals with T2DM showed minimal changes, with the HVR shifting from  $0.69 \pm 0.10$  to  $0.67 \pm 0.10$   $\text{L}\cdot\text{min}^{-1}\cdot\%^{-1}$  ( $p = 0.78$ ). Notably, the interaction between diagnosis (T2DM or HC) and the intervention (HEC) was statistically significant ( $p = 0.02$ ). A visual representation of the HVR for both groups during fasting and hyperinsulinemia is provided in Figure 5.2.

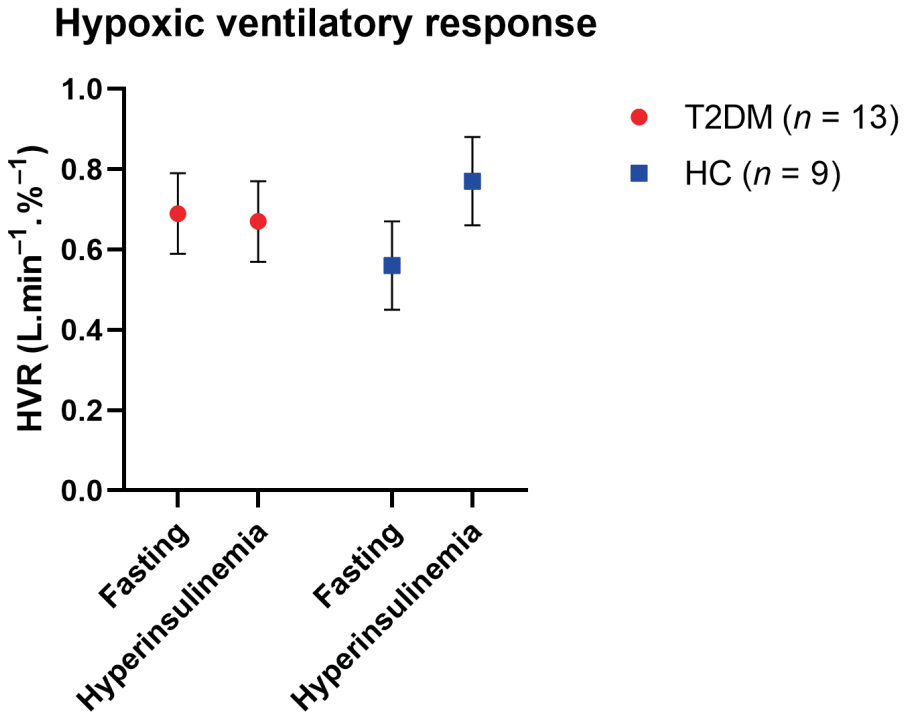


**Figure 5.2:** Hypoxic ventilatory response during baseline and hyperinsulinemia, for T2DM and HC. The effect of hypersinsulinemia on HC and the interaction between diagnosis and intervention was significantly different. This suggests that the effect of the intervention (hyperinsulinemia) on the HVR differs depending on the diagnosis of the participant.

## Dejour test

A representative tracing of the modified Dejours test is given in Figure 5.3 on page 109, illustrating the effects of a brief period of hyperoxia. The reduction in minute ventilation during and following hyperoxia (*i.e.* hyperoxic inhibition, a measure of reduced carotid body discharge), showed notable differences in T2DM individuals between fasting and hyperinsulinemic conditions, respectively  $-1.13 \pm 0.42$  and  $-1.88 \pm 0.49$  ( $p = 0.039$ ). The same effect was not observed in HC, respectively  $-1.41 \pm 0.59$  and  $-1.62 \pm 0.49$  ( $p > 0.05$ ).

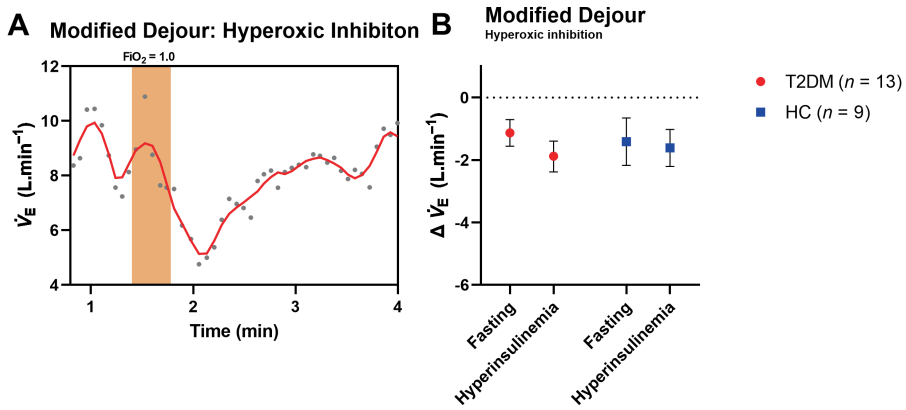


**Figure 5.3:** Hyperoxic inhibition of minute ventilation (Modified Dejour test). Representative tracing (A) and absolute hyperoxic-induced decrease in minute ventilation for NIDDM and HC during fasting and hyperinsulinemia (B). Inhibition increased in the NIDDM group during hypersinsulinemia.

## Heart rate variability

Distinct patterns emerged based on the intervention (baseline, HEC, and hypoxia) and diagnosis (T2DM or HC). In the baseline condition, T2DM patients had higher sympathetic activity compared to HC (SNS indices of  $7.2 \pm 5.7$  and  $4.0 \pm 5.1$ , respectively). Parasympathetic activity was lower for T2DM compared to HC ( $-3.2 \pm 4.7$  and  $9.4 \pm 7.4$ , respectively). During hyperinsulinemia, the SNS index increased in T2DM ( $9.7 \pm 5.4$ ), but not in HC ( $0.2 \pm 6.4$ ). During hypoxia, both groups showed increased sympathetic responses, with a slight rise in T2DM's sympathetic index ( $12.6 \pm 4.0$ ). In HC, hyperinsulinemia reduced sympathetic activity (SNS index:  $0.3 \pm 6.3$ ) and slightly reduced

---

parasympathetic activity (PNS index:  $4.2 \pm 6.5$ ), while T2DM's autonomic response remained largely unchanged (PNS and SNS index were  $-4.7 \pm 2.3$  and  $9.7 \pm 5.4$ , respectively). Combining hyperinsulinemia and hypoxia intensified the sympathetic surge, especially in HC (SNS index:  $7.4 \pm 6.4$ ). T2DM showed further parasympathetic suppression ( $-3.6 \pm 5.2$ ), while HC experienced increased parasympathetic activity ( $6.6 \pm 7.2$ ).

These autonomic changes, assessed via heart rate variability metrics, may impact the HVR. T2DM disrupted autonomic balance, leaning towards sympathetic dominance, and attenuated the hypoxic response. Conversely, HC maintained or enhanced their autonomic equilibrium and hypoxic sensitivity during hyperinsulinemia. These findings highlight T2DM's significant influence on autonomic regulation and physiological responses to hyperinsulinemia and hypoxia.

## Hemodynamic parameters

The effects of hyperinsulinemia on hemodynamic variables are given in Figure 5.4 on page 111. Sympathetic effects of hyperinsulinemia and hypoxia are reflected by an increase in diastolic blood pressure, systolic blood pressure, and cardiac index. The most distinguishing characteristic of T2DM is the elevated cardiac index (T2DM  $2.71 \pm 0.19$  L.min<sup>-1</sup>.m<sup>-2</sup> *vs.* HC  $2.42 \pm 0.13$  L.min<sup>-1</sup>.m<sup>-2</sup>), which was most pronounced during the combination of hyperinsulinemia and hypoxia (T2DM  $3.44 \pm 0.18$  L.min<sup>-1</sup>.m<sup>-2</sup> *vs.* HC  $2.67 \pm 0.10$  L.min<sup>-1</sup>.m<sup>-2</sup>; interaction diagnosis (T2DM or HC) and intervention (baseline or hyperinsulinemic hypoxia)  $p = 0.002$ ).

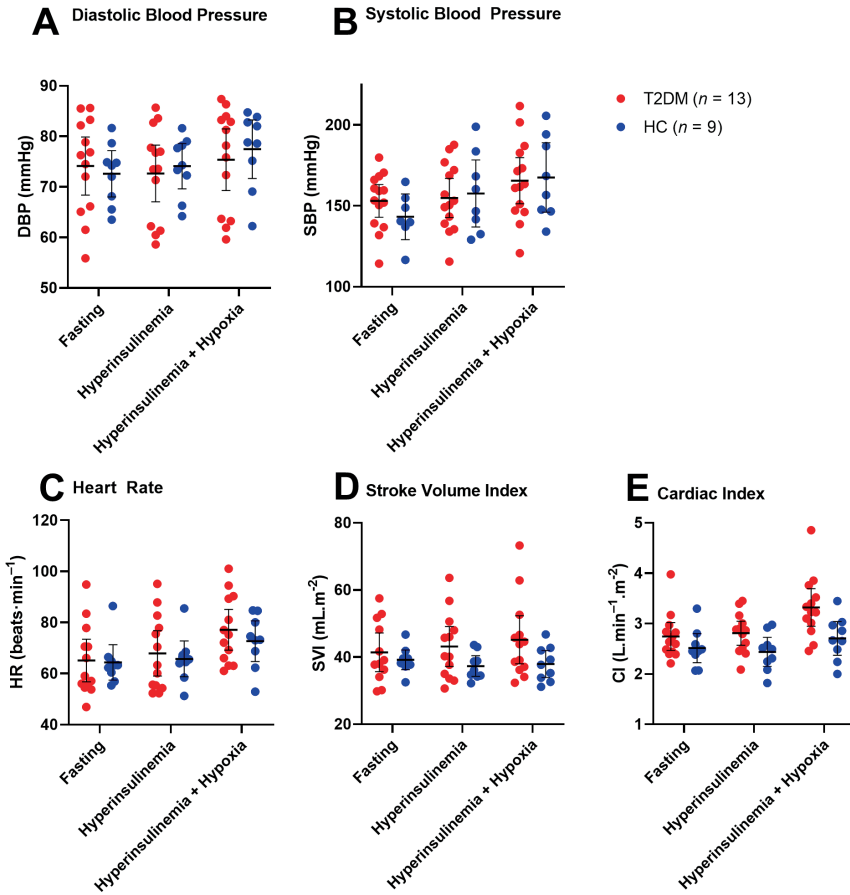


**Figure 5.4:** Hemodynamic parameters in the course of fasting, hyperinsulinemia, and hyperinsulinemia and hypoxia combined. Diastolic blood pressure (A), Systolic Blood Pressure (B), Heart Rate (C), Stroke Volume Index (D), and Cardiac Index (E).

---

## Discussion

The present study reveals the effects of insulin on the HVR in individuals with non-insulin dependent diabetes mellitus. While HC showed that insulin increases the isocapnic HVR, no such effect was observed in individuals with T2DM. Additionally, under fasting conditions the effect of hyperoxia on ventilation was less in T2DM compared to HC, a sign of carotid body excitation. Finally, sympathetic excitation was noted in T2DM. These data indicate an impaired carotid body function in T2DM with signs of insulin resistance coupled with impaired autonomic function regulation of the carotid body.

Previous studies, both in animal models and humans, exploring the effects of insulin on the CB and ventilation showed that insulin increases CB activation and increases ventilation.<sup>22,4,28</sup> Ward *et al.* performed isocapnic HVR in healthy humans during hypoglycemia and hyperglycemia, and found increased hypoxic sensitivity during hyperglycemia and more so during hypoglycemia.<sup>29</sup> Our study is the first, to our knowledge, to assess the effects of hypoxia under influence of hyperinsulinemic-euglycemia in humans. Our finding of an enhanced HVR in HC in a state of hyperinsulemic-euglycemia is a new finding, which agrees with earlier studies.

Data on the effect of T2DM on the HVR, both in animal models and in man, is conflicting. Some studies indicate an increased response,<sup>3,4</sup> while other found no difference,<sup>28</sup> or diminished responses.<sup>30,31,32</sup> The heterogeneity of these results could potentially be explained by the metabolic state of the control group (fasting or euglycemic hyperinsulinemia), a factor that is either not mentioned or considered in the aforementioned studies. Our study's observation of an unaltered HVR during HEC (mimicking a postprandial state) in T2DM contributes to our understanding of these differences.

Our observations point towards (1) carotid body insulin resistance in T2DM (no effect of insulin on the HVR) and (2) a hyperactive carotid body (reduced depression of ventilation during hyperoxia), coupled to a general state of sympathicoexcitation, as observed from the heart variability data and the enhanced cardiac index in T2DM. The latter was particularly observed for the parasympathetic tone, where the T2DM groups showed pronounced suppression, in contrast to the heightened activity in HC. Such autonomic shifts, as observed from the heart rate variability metrics may be instrumental in shaping the HVR.<sup>33</sup>

We argue that the heightened sympathetic tone in T2DM affects the HVR response to insulin. In agreement with this statement, we observed that HC exhibited a resilience in maintaining, or perhaps even enhancing, their autonomic

## Diabetes, hyperinsulinemia, and the hypoxic ventilatory response

balance and hypoxic reactivity during hyperinsulinemia. Sympathetic excitation may also explain the observed changes in hemodynamic response to hyperinsulinemia and hypoxia, due to different levels of attenuation of peripheral  $\alpha$ -adrenergic mediated vasoconstriction, peripheral  $\beta$ -adrenergic vasodilation, myocardial glucose uptake, and  $\beta$ -adrenergic cardiac stimulation.<sup>34,35</sup>

Apart from the observation of a substantial influence of T2DM on autonomic regulation, our findings suggest a dynamic interaction between the metabolic and respiratory systems, with effects of diabetes on respiratory physiology in the presence of hyperinsulinemia and hypoxia. The carotid body, a primary oxygen-sensing organ, plays an integral role in ventilatory adjustments to hypoxia. Prolonged hyperinsulinemia might exert modulatory effects on the carotid body, potentially altering its sensitivity and responsiveness to hypoxic challenges. Such alterations could, in turn, impact the overall functionality of the autonomic nervous system, given the close interplay between carotid body activity and autonomic regulation.

### **Limitations**

Our study has several limitations: (1) While the T2DM group refrained from antidiabetic drugs for 24 h, prolonged effects of various medications cannot be ruled out. (2) Data of subjects with poor HEC was disregarded and data of three subjects with insufficient quality HVR was excluded from analysis, resulting in missing data in both groups that affected our sample size. (3) Furthermore, there was significant variability in insulin resistance in both patients with T2DM and HC. This suggests undiagnosed insulin resistance in the “healthy” population, which cannot be detected from fasting glucose measurements, and heterogeneity in T2DM phenotype, with different progression, severity, and drug response.<sup>36</sup> A stronger demarcation between patients with and without insulin resistance, irrespective of their diagnosis, could have increased the observed differences.

### **Conclusion**

In an experimental paradigm, we observed that individuals with T2DM display significant differences in their carotid body function that affects ventilatory and metabolic control and is possibly an important factor in sympathetic tone-related hemodynamic changes. This study should be considered exploratory and hypothesis-generating. Our study may be used to power future studies on the intricate interaction between metabolic, hemodynamic and ventilatory control.





## References

1. James DE, Stockli J, Birnbaum MJ. The aetiology and molecular landscape of insulin resistance. *Nature Reviews Molecular Cell Biology*. 2021; **22**: 751–771  
DOI: 10.1038/s41580-021-00390-6.
2. Collaborators G2D. Global, regional, and national burden of diabetes from 1990 to 2021, with projections of prevalence to 2050: a systematic analysis for the Global Burden of Disease Study 2021. *The Lancet*. 2023; **402**: 203–234  
DOI: 10.1016/s0140-6736(23)01301-6.
3. Cunha-Guimaraes JP, Guarino MP, Timoteo AT, Caires I, Sacramento JF, Ribeiro MJ, Selas M, Santiago JCP, Mota-Carmo M, Conde SV. Carotid body chemosensitivity: early biomarker of dysmetabolism in humans. *European Journal of Endocrinology*. 2020; **182**: 549–557  
DOI: 10.1530/EJE-19-0976.
4. Ribeiro MJ, Sacramento JF, Gonzalez C, Guarino MP, Monteiro EC, Conde SV. Carotid body denervation prevents the development of insulin resistance and hypertension induced by hypercaloric diets. *Diabetes*. 2013; **62**: 2905–16  
DOI: 10.2337/db12-1463.
5. Schlaich M, Straznicky N, Lambert E, Lambert G. Metabolic syndrome: a sympathetic disease? *The Lancet Diabetes Endocrinology*. 2015; **3**: 148–57  
DOI: 10.1016/S2213-8587(14)70033-6.
6. Kumar P, Prabhakar NR. Peripheral chemoreceptors: function and plasticity of the carotid body. 2012; **2**: 141–219  
DOI: 10.1002/cphy.c100069.
7. Limberg JK. Glucose, insulin, and the carotid body chemoreceptors in humans. *Physiological Genomics*. 2018; **50**: 504–509  
DOI: 10.1152/physiolgenomics.00032.2018.

## References

---

8. Luckett BS, Frielle JL, Wolfgang L, Stocker SD. Arcuate nucleus injection of an anti-insulin affibody prevents the sympathetic response to insulin. *American Journal of Physiology-Heart and Circulatory Physiology*. 2013; **304**: H1538–H1546  
DOI: 10.1152/ajpheart.00081.2013.
9. Ward KR, Bardgett JF, Wolfgang L, Stocker SD. Sympathetic Response to Insulin Is Mediated by Melanocortin 3/4 Receptors in the Hypothalamic Paraventricular Nucleus. *Hypertension*. 2011; **57**: 435–441  
DOI: 10.1161/hypertensionaha.110.160671.
10. Caballero-Eraso C, Colinas O, Sobrino V, González-Montelongo R, Cabeza JM, Gao L, Pardal R, López-Barneo J, Ortega-Sáenz P. Rearrangement of cell types in the rat carotid body neurogenic niche induced by chronic intermittent hypoxia. *The Journal of Physiology*. 2023; **601**: 1017–1036  
DOI: 10.1113/jp283897.
11. Limberg JK, Curry TB, Prabhakar NR, Joyner MJ. Is insulin the new intermittent hypoxia? *Med Hypotheses*. 2014; **82**: 730–735  
DOI: 10.1016/j.mehy.2014.03.014.
12. Caballero-Eraso C, Shin MK, Pho H, Kim LJ, Pichard LE, Wu ZJ, Gu C, Berger S, Pham L, Yeung HY, Shirahata M, Schwartz AR, Tang WY, Sham JSK, Polotsky VY. Leptin acts in the carotid bodies to increase minute ventilation during wakefulness and sleep and augment the hypoxic ventilatory response. *J Physiol*. 2019; **597**: 151–172  
DOI: 10.1113/JP276900.
13. Pardal R, López-Barneo J. Low glucose-sensing cells in the carotid body. *Nat Neurosci*. 2002; **5**: 197–198  
DOI: 10.1038/nm812.
14. Pauza AG, Thakkar P, Tasic T, Felipe I, Bishop P, Greenwood MP, Rysevaite-Kyguoliene K, Ast J, Broichhagen J, Hodson DJ, Salgado HC, Pauza DH, Japundzic-Zigon N, Paton JFR, Murphy D. GLP1R Attenuates Sympathetic Response to High Glucose via Carotid Body Inhibition. *Circ Res*. 2022; **130**: 694–707  
DOI: 10.1161/CIRCRESAHA.121.319874.
15. Torres-Torrel H, Ortega-Sáenz P, Gao L, López-Barneo J. Lactate Sensing Mechanisms in Arterial Chemoreceptor Cells. *Nature Communications*. 2021; **12**: 4166  
DOI: 10.1038/s41467-021-24450-4.
16. Cramer JA, Wiggins RH, Fudim M, Engelman ZJ, Sobotka PA, Shah LM. Carotid body size on CTA: correlation with comorbidities. *Clinical Radiology*. 2014; **69**: e33–6  
DOI: 10.1016/j.crad.2013.08.016.

17. Santos ED, Sacramento JF, Melo BF, Conde SV. Carotid Body Dysfunction in Diet-Induced Insulin Resistance Is Associated with Alterations in Its Morphology. *Advances in Experimental Medicine and Biology*. 2018; 103–108  
DOI: 10.1007/978-3-319-91137-3\_13.
18. Lack EE. Carotid body hypertrophy in patients with cystic fibrosis and cyanotic congenital heart disease. *Human Pathology*. 1977; **8**: 39–51  
DOI: 10.1016/s0046-8177(77)80064-6.
19. Peng YJ, Overholt JL, Kline D, Kumar GK, Prabhakar NR. Induction of sensory long-term facilitation in the carotid body by intermittent hypoxia: Implications for recurrent apneas. *Proceedings of the National Academy of Sciences of the United States of America (PNAS)*. 2003; **100**: 10073–10078  
DOI: 10.1073/pnas.1734109100.
20. Sarabhai T, Mastrototaro L, Kahl S, Bönhof GJ, Jonuscheit M, Bobrov P, Katsuyama H, Guthoff R, Wolkersdorfer M, Herder C, Meuth SG, Dreyer S, Roden M. Hyperbaric oxygen rapidly improves tissue-specific insulin sensitivity and mitochondrial capacity in humans with type 2 diabetes: a randomised placebo-controlled crossover trial. *Diabetologia*. 2022; **66**: 57–69  
DOI: 10.1007/s00125-022-05797-0.
21. Vera-Cruz P, Guerreiro F, Ribeiro MJ, Guarino MP, Conde SV. Hyperbaric Oxygen Therapy Improves Glucose Homeostasis in Type 2 Diabetes Patients: A Likely Involvement of the Carotid Bodies. *Arterial Chemoreceptors in Physiology and Pathophysiology*. 2015; **860**: 221–5  
DOI: 10.1007/978-3-319-18440-1\_24.
22. Barbosa TC, Kaur J, Holwerda SW, Young CN, Curry TB, Thyfault JP, Joyner MJ, Limberg JK, Fadel PJ. Insulin increases ventilation during euglycemia in humans. *Regulatory, Integrative and Comparative Physiology*. 2018; **315**: R84–R89  
DOI: 10.1152/ajpregu.00039.2018.
23. Borne PVD, Hausberg M, Hoffman RP, Mark AL, Anderson EA. Hyperinsulinemia produces cardiac vagal withdrawal and nonuniform sympathetic activation in normal subjects. *American Journal of Physiology-Regulatory, Integrative and Comparative Physiology*. 1999; **276**: R178–R183  
DOI: 10.1152/ajpregu.1999.276.1.r178.
24. DeFronzo RA, Ferrannini E. Insulin resistance. A multifaceted syndrome responsible for NIDDM, obesity, hypertension, dyslipidemia, and atherosclerotic cardiovascular disease. *Diabetes Care*. 1991; **14**: 173–94  
DOI: 10.2337/diacare.14.3.173.

## References

---

25. Tarvainen MP, Niskanen JP, Lipponen JA, Ranta-aho PO, Karjalainen PA. Kubios HRV – Heart rate variability analysis software. *Computer Methods and Programs in Biomedicine*. 2014; **113**: 210–220  
DOI: 10.1016/j.cmpb.2013.07.024.
26. Azulay N, Olsen RB, Nielsen CS, Stubhaug A, Jenssen TG, Schirmer H, Frigessi A, Rosseland LA, Tronstad C. Reduced heart rate variability is related to the number of metabolic syndrome components and manifest diabetes in the sixth Tromsø study 2007–2008. *Scientific Reports*. 2022; **12**:  
DOI: 10.1038/s41598-022-15824-0.
27. Benichou T, Pereira B, Mermillod M, Tauveron I, Pfabigan D, Maqdasy S, Dutheil F. Heart rate variability in type 2 diabetes mellitus: A systematic review and meta-analysis. *PLOS ONE*. 2018; **13**: e0195166  
DOI: 10.1371/journal.pone.0195166.
28. Saiki C, Seki N, Furuya H, Matsumoto S. The acute effects of insulin on the cardiorespiratory responses to hypoxia in streptozotocin-induced diabetic rats. *Acta Physiologica Scandinavica*. 2005; **183**: 107–115  
DOI: 10.1111/j.1365-201x.2004.01375.x.
29. Ward DS, Voter WA, Karan S. The effects of hypo- and hyperglycaemia on the hypoxic ventilatory response in humans. *The Journal of Physiology*. 2007; **582**: 859–69  
DOI: 10.1113/jphysiol.2007.130112.
30. Nishimura M, Miyamoto K, Suzuki A, Yamamoto H, Tsuji M, Kishi F, Kawakami Y. Ventilatory and heart rate responses to hypoxia and hypercapnia in patients with diabetes mellitus. *Thorax*. 1989; **44**: 251–257  
DOI: 10.1136/thx.44.4.251.
31. Pokorski M, Pozdzik M, Antosiewicz J, Dymecka A, Mazzatenta A, Giulio CD. Hypoxic Ventilatory Reactivity in Experimental Diabetes. 2015; 123–132  
DOI: 10.1007/978-3-319-18440-1\_14.
32. Weisbrod CJ, Eastwood PR, O'Driscoll G, Green DJ. Abnormal ventilatory responses to hypoxia in Type 2 diabetes. *Diabetic Medicine*. 2005; **22**: 563–568  
DOI: 10.1111/j.1464-5491.2005.01458.x.
33. Bernardi L, Bianchi L. Integrated Cardio-Respiratory Control: Insight in Diabetes. *Current Diabetes Reports*. 2016; **16**:  
DOI: 10.1007/s11892-016-0804-9.
34. Fu Q, Wang Q, Xiang YK. Insulin and Adrenergic Receptor Signaling: Crosstalk in Heart. *Trends in Endocrinology & Metabolism*. 2017; **28**: 416–427  
DOI: 10.1016/j.tem.2017.02.002.

35. Limberg JK, Soares RN, Padilla J. Role of the Autonomic Nervous System in the Hemodynamic Response to Hyperinsulinemia—Implications for Obesity and Insulin Resistance. *Current Diabetes Reports*. 2022; **22**: 169–175  
DOI: 10.1007/s11892-022-01456-1.
36. Nair ATN, Wesolowska-Andersen A, Brorsson C, Rajendrakumar AL, Hapca S, Gan S, Dawed AY, Donnelly LA, McCrimmon R, Doney ASF, Palmer CNA, Mohan V, Anjana RM, Hattersley AT, Dennis JM, Pearson ER. Heterogeneity in phenotype, disease progression and drug response in type 2 diabetes. *Nature Medicine*. 2022; **28**: 982–988  
DOI: 10.1038/s41591-022-01790-7.



## Chapter 6

# Summary, conclusions, and perspectives

---

This thesis represents the intricate journey between physiology and pharmacology. Our primary aim was to investigate the effects of different pharmacotherapies on antinociception and ventilatory control. Additionally, we delved into the inherent variabilities in patient phenotypes within the population to gain a deeper understanding of the individual effects of analgesics and the ventilatory effects of disease, particularly type 2 diabetes mellitus (T2DM).

## Summary of the main findings

In **chapter 1**, we briefly introduce the reader to recent advancements in the use of ketamine in clinical practice (for pain management and depression), and the ventilatory depressant effect of opioids and alterations in ventilatory control in T2DM are discussed. Our goal was to highlight current challenges in pain management, emphasize the importance of considering risk factors and side effects, and propose strategies for investigating new or alternative therapies.

In **chapter 2**, we examined the pharmacokinetics of oral-thin-film (OTF) administration of 50 mg and 100 mg *S*-ketamine and its major metabolites. These films were rapidly absorbed, with bioavailabilities of 26% and 29%, respectively, and exhibited relatively small variability in their pharmacokinetics. Therapeutic plasma concentrations for antinociception were achieved. The majority of *S*-ketamine was metabolized into *S*-norketamine, with about half further metabolized into *S*-hydroxynorketamine. These findings were attributed to the swallowing of the active substance, gastrointestinal absorption of the majority of *S*-ketamine, and a significant first-pass effect.

In the complementary **chapter 3**, we investigated the pharmacodynamics of the aforementioned oral-thin-film. Both dosages exhibited antinociceptive effects with a rapid onset (approximately 30 minutes) and lasting effects of at least two hours. Psychotomimetic side effects, such as drug-high, followed a similar pattern. Our model did not detect contributions of *S*-norketamine and *S*-hydroxynorketamine to the antinociceptive or drug-high effects. We conclude that this administration form of *S*-ketamine may be suitable for the treatment of acute pain and breakthrough pain, a proposition that warrants further clinical studies.

Moving on to **chapter 4**, where we examined the respiratory effects of a biased ligand at the  $\mu$ -opioid receptor, oliceridine. We observed a lower potency of the respiratory depressant effect induced by oliceridine compared to morphine, a lower  $C_{50}$  for respiratory depression for both opioids in the elderly population, a shortened onset/offset of respiratory depression with oliceridine, and differences in oliceridine's pharmacokinetic profiles due to *CYP2D6* polymorphisms



and phenotype variations. We could not relate the ventilatory effects to the antinociceptive effects, a critical aspect for evaluating the harm-benefit profile of this pharmacologic compound. We relate our inability to generate opioid-induced antinociception to the specific patient population that was examined by us (our population was insensitive to cold water stimuli). Elderly individuals have difficulty scoring nociception, particularly when exposed to opioids. This may be related to a series of age-related changes in physiology, such as reduced C-fiber density in the skin, alterations in central pain processing as well as cognitive changes. Additionally, obesity negatively affects the proper scoring of nociceptive stimuli.

Finally, in **chapter 5**, we compared hypoxic sensitivity between patients with T2DM with healthy controls and studied the effects of hyperinsulinemia on hypoxic sensitivity. During fasting, we observed no differences between these two groups, however, intriguingly, during euglycemic-hyperinsulinemia significant changes emerged. Heightened hypoxic sensitivity was observed in healthy controls, but not in insulin-resistant individuals. Moreover, during hyperinsulinemia, hyperoxic inhibition increased in patients with T2DM, indicating increased carotid body discharge in this group. This suggests that T2DM negatively affects the carotid bodies with an indication of insulin resistance of that particular organ, albeit the carotid system seems to be in a hyper-excitable state.

### Clinical perspectives

All topics discussed above merit further studies. Regarding **chapter 2** and **chapter 3**, it is important to start clinical trials with the *S*-ketamine oral-thin-film in patients, either in patients in acute pain (including breakthrough pain) as well as with therapy-resistant depression. The high levels of *S*-hydroxynorketamine may hold promise for the management of the latter, as it has been identified as an active substance following (*R,S*)-ketamine administration.<sup>1,2</sup> Besides a possible benefit of this particular administration form, we need to explore the ideal ketamine compositions (pure enantiomer or racemic ratio), efficacy and safety of different dosing regimens, which are expected to differ depending on the indication.<sup>3,4,5</sup> Equally important is to determine the side effect profile for each indication. This may, for example, be done using utility function analysis, an approach that calculates the likelihood of benefit *versus* the likelihood of harm, as a function of effect-site concentration.<sup>6</sup> We expect that due to the production of high concentrations of the hydroxynorketamine the utility function may be particularly positive when the *S*-ketamine OTF is used in the treatment of depression, while a lesser positive function, or even a negative function, may be expected in the treatment of acute pain, an effect that relies mostly on the ketamine concentrations in the

---

brain and spinal cord.<sup>7</sup> Finally, we need to be aware of the fact that we recently showed that ketamine benefit and harm (*i.e.* its schizotypal adverse effects) are intricately connected, and when none of these adverse effects occur the likelihood of a benefit (pain relief or anti-depressive effects) is reduced.<sup>8</sup>

The results of **chapter 4**, the effect of the biased ligand oliceridine on ventilatory control in elderly volunteers, agrees with evidence in animal models that shows the reduced duration and magnitude of respiratory depressant effect of oliceridine, compared to morphine.<sup>9</sup> Also, clinical studies in postoperative patients point in that direction.<sup>10</sup> Whether these underlying features can be attributed to biased agonism or low intrinsic efficacy remains disputed among molecular researchers.<sup>11</sup> Considering the burden of perioperative respiratory effects, we need to realize that with proper monitoring the number of serious respiratory depression events following surgery is limited. For example, the PRODIGY trial, an observational study in more than 1,300 postoperative patients on opioids, showed that while 46% of patients had at least one respiratory event, there were just very rare incidences of the need for naloxone reversal, reintubation, or admittance to the intensive care unit because of opioid treatment.<sup>12</sup> Still, less than 20% of patients exclusively treated with oliceridine in the postoperative period have a respiratory event, and most of such events are not related to the opioid treatment per se, but relate to ventilation/perfusion ( $\dot{V}_A/\dot{Q}$ ) mismatch and concomitant hypoxemia.<sup>12</sup> Further studies are needed to determine what the pharmacoeconomic advantage is of treatment with oliceridine in comparison to commonly used opioids and other analgesics such as morphine or hydromorphone. These generic opioids are cheap, effective, and albeit with a higher tendency to affect the ventilatory control system than oliceridine, are considered a safe drug when used appropriately in the perioperative setting. Furthermore, while outside the scope of this thesis, other actions are necessary beyond innovations in biomedical research, to reduce deaths and prevent further escalation of the opioid crisis around the globe. These include reforming regulatory systems, informed prescribing, and advancements in opioid stewardship. Additionally, efforts should be put towards preventing chronic pain and preventing substance use disorder by modification of risk factors at both individual and population levels.

Finally, in **chapter 5**, the effect of insulin on ventilatory control is examined. The two main observations, carotid body insulin resistance in T2DM coupled with a carotid body that seems to be in a basal hyper-excitable state are important findings that have important health-related effects.<sup>13,14</sup> The lack of increase in hypoxic response upon exposure to insulin in patients with T2DM, is relevant although an appreciable hypoxic response remained; the magnitude of the hypoxic response is quite variable among individuals. Still, the inability to enhance the response is a clear sign of insulin resistance. The carotid body

is considered the watchdog of the brain and a proper insulin response is needed to control the glucose exposure to the brain. Carotid body insulin resistance falls within the general concept of insulin resistance in T2DM. However, the hyperexcitability of the carotid body in T2DM is an important observation that may be linked to health outcome measures such as hypertension, cardiac arrhythmias, and heart failure.<sup>15</sup> Carotid body denervation or destruction has earlier been suggested as a treatment of a hyperexcitable carotid body related diseases, such as treatment-resistant hypertension, heart failure, myocardial infarction, and ventricular tachycardia.<sup>16,17</sup> Hence, our data suggest that patients with T2DM might be at an increased risk for such adverse health issues. While carotid sinus nerve denervation in T2DM may be a bridge too far due to adverse effects, electronic modulation has been shown to restore metabolic homeostasis in animal models.<sup>18</sup> Given the high prevalence of T2DM, further studies are warranted to determine the risks of a hyperexcitable carotid body in T2DM, determine how this is associated with alterations in ventilatory control, and evaluate preclinical therapeutic approaches.

In conclusion, the research conducted in this thesis has expanded our knowledge of pharmacology and pathophysiology on the control of breathing, both in health and disease. We anticipate that these findings will contribute to improved health outcomes and enhanced safety in pain management and foster further research.



## References

1. Abdallah CG, Sanacora G, Duman RS, Krystal JH. Ketamine and rapid-acting antidepressants: a window into a new neurobiology for mood disorder therapeutics. *Annu Rev Med.* 2015; **66**: 509–523  
DOI: 10.1146/annurev-med-053013-062946.
2. Highland JN, Zanos P, Riggs LM, Georgiou P, Clark SM, Morris PJ, al. et. Hydroxynorketamine: pharmacology and potential therapeutic applications. *Pharmacol Rev.* 2021; **73**: 763–791  
DOI: 10.1124/pharmrev.120.000149.
3. Fjendbo Galili S, Nikolajsen L, Papadomanolakis-Pakis N. Subanaesthetic single-dose ketamine as an adjunct to opioid analgesics for acute pain management in the emergency department: a systematic review and meta-analysis. *BMJ Open.* 2023; **13**: e066444  
DOI: 10.1136/bmjopen-2022-066444.
4. Jonkman K, Dahan A, Donk T van de, Aarts L, Niesters M, Velzen M van. Ketamine for pain. *F1000Research.* 2017;  
DOI: 10.12688/f1000research.11372.1.
5. Nikolin S, Rodgers A, Schwaab A, Bahji A, Zarate C. J, Vazquez G, Loo C. Ketamine for the treatment of major depression: a systematic review and meta-analysis. *eClinicalMedicine.* 2023; **62**: 102127  
DOI: 10.1016/j.eclinm.2023.102127.
6. Boom M, Olofsen E, Neukirchen M, Fussen R, Hay J, Groeneveld GJ, Aarts L, Sarton E, Dahan A. Fentanyl utility function: a risk-benefit composite of pain relief and breathing responses. *Anesthesiology.* 2013; **119**: 663–674  
DOI: 10.1097/ALN.0b013e31829ce4cb.
7. Sleigh J, Harvey M, Voss L, Denny B. Ketamine - More mechanisms of action than just NMDA blockade. *Trends in Anaesthesia & Critical Care.* 2014; **4**: 76–81  
DOI: 10.1016/j.tacc.2014.03.002.

## References

---

8. Olofsen E, Kamp J, Henthorn TK, Velzen M van, Niesters M, Sarton E, al. et. Ketamine psychedelic and analgesic effects are connected. *Anesthesiology*. 2022; **136**: 792–801  
DOI: 10.1097/ALN.0000000000004176.
9. Hill R, Sanchez J, Lemel L, Antonijevic M, Hosking Y, Mistry SN, Kruegel AC, Javitch JA, Lane JR, Canals M. Assessment of the potential of novel and classical opioids to induce respiratory depression in mice. *British Journal of Pharmacology*. 2023;  
DOI: 10.1111/bph.16199.
10. Ayad S, Demitrack MA, Burt DA, Michalsky C, Wase L, Fossler MJ, Khanna AK. Evaluating the Incidence of Opioid-Induced Respiratory Depression Associated with Oliceridine and Morphine as Measured by the Frequency and Average Cumulative Duration of Dosing Interruption in Patients Treated for Acute Postoperative Pain. *Clinical Pharmacokinetics*. 2020; **59**: 755–764  
DOI: 10.1007/s40261-020-00936-0.
11. Stahl EL, Bohn LM. Low intrinsic efficacy alone cannot explain the improved side effect profiles of new opioid agonists. *Biochem*. 2021;  
DOI: 10.1021/acs.biochem.1c00466.
12. Karcz M, Papadakos PJ. Respiratory complications in the postanesthesia care unit: A review of pathophysiological mechanisms. *Journal of Clinical Medicine Research*. 2013; **5**: 21–29  
DOI: PMID:26078599.
13. Kim LJ, Polotsky VY. Carotid Body and Metabolic Syndrome: Mechanisms and Potential Therapeutic Targets. *International Journal of Molecular Sciences*. 2020; **21**:  
DOI: 10.3390/ijms21145117.
14. Sacramento JF, Andrzejewski K, Melo BF, Ribeiro MJ, Obeso A, Conde SV. Exploring the Mediators that Promote Carotid Body Dysfunction in Type 2 Diabetes and Obesity Related Syndromes. *International Journal of Molecular Sciences*. 2020; **21**:  
DOI: 10.3390/ijms21155545.
15. Iturriaga R. Translating carotid body function into clinical medicine. *The Journal of Physiology*. 2018; **596**: 3067–3077  
DOI: 10.1113/JP275335.
16. Dahan A, Nieuwenhuijs D, Teppema L. Plasticity of central chemoreceptors: effect of bilateral carotid body resection on central CO<sub>2</sub> sensitivity. *PLOS Medicine*. 2007; **4**: e239  
DOI: 10.1371/journal.pmed.0040239.

17. Timmers HJ, Wieling W, Karemaker JM, Lenders JW. Denervation of carotid baro- and chemoreceptors in humans. *The Journal of Physiology*. 2003; **553**: 3–11  
DOI: 10.1113/jphysiol.2003.052415.
18. Sacramento JF, Chew DJ, Melo BF, Donega M, Dopson W, Guarino MP, Robinson A, Prieto-Lloret J, Patel S, Holinski BJ, Ramnarain N, Pikov V, Famm K, Conde SV. Bioelectronic modulation of carotid sinus nerve activity in the rat: a potential therapeutic approach for type 2 diabetes. *Diabetologia*. 2018; **61**: 700–710  
DOI: 10.1007/s00125-017-4533-7.





## Hoofdstuk 7

### Nederlandse samenvatting

---

Dit proefschrift toont het effect aan van verschillende farmaca op pijnstilling en ademhalingsregulatie. Daarnaast werd het effect van verschillende fenotypes onderzocht, om meer inzicht te verkrijgen in de individuele effecten van analgetica en de ventilatoire effecten van bepaalde aandoeningen op ventilatoire regulatie, zoals diabetes type 2.

## Samenvatting van de belangrijkste bevindingen

In **chapter 1**, introduceren we de lezer in de stand van zaken in de anesthesiologie. Het klinisch gebruik van ketamine wordt besproken (voor pijnbestrijding en depressie), alsook het ademhalingsdepressieve effect van opioïden en veranderingen in ademhalingsregulatie bij diabetes type 2. De huidige uitdagingen in pijnbestrijding worden benoemd, evenals het belang om effect tegen bijwerkingen te wegen. Tot slot worden de belangrijkste meetmethoden besproken van belang in dit proefschrift.

In **chapter 2**, onderzochten we de farmacokinetiek van 50 mg en 100 mg OTF *S*-ketamine en de belangrijkste metabolieten. Deze *films* werden snel geabsorbeerd, met een biobeschikbaarheid van respectievelijk 26% en 29%, met relatief kleine variabiliteit in hun farmacokinetiek. Therapeutische plasmaconcentraties voor antinociceptie werden bereikt. De meerderheid van de *S*-ketamine werd gemetaboliseerd tot *S*-norketamine en ongeveer de helft werd verder gemetaboliseerd tot *S*-hydroxynorketamine. Deze bevindingen werden toegeschreven aan het inslikken van de actieve werkzame stof, gastro-intestinale absorptie van de meerderheid van *S*-ketamine en een aanzienlijk first-pass effect.

In het aanvullende **chapter 3**, onderzochten we de farmacodynamiek van de eerder genoemde OTF. Beide doseringen vertoonden antinociceptieve effecten met een snelle aanvang (ongeveer 30 minuten) en langdurige effecten van minstens twee uur. Psychotomimetische bijwerkingen, zoals drug-high, volgden een vergelijkbaar patroon. Ons model detecteerde geen bijdrage van *S*-norketamine en *S*-hydroxynorketamine aan de antinociceptieve of drug-high effecten. We concluderen dat deze toedieningsvorm van *S*-ketamine geschikt kan zijn voor de behandeling van acute pijn en doorbraakpijn, dat verder klinisch onderzoek rechtvaardigt.

In **chapter 4** werden de respiratoire effecten van een biased ligand van de  $\mu$ -opioïde receptor, oliceridine onderzocht. We observeerden een lagere potentie van het ademhalingsdepressieve effect dat werd veroorzaakt door oliceridine in vergelijking met morfine, een lagere  $C_{50}$  voor respiratoire depressie voor beide opioïden bij de oudere bevolking, een verkorte periode van ontstaan/verdwijnen van de respiratoire depressie met oliceridine, en verschillen in het farmaco-

kinetisch profiel van oliceridine als gevolg van *CYP2D6* polymorfismen en fenotypevariaties. We konden de ventilatoire effecten niet in verband brengen met de antinociceptieve effecten, een cruciaal aspect voor de evaluatie van harm/benefit van dit farmacologische middel. We relateren deze tekortkoming om opioïd-geïnduceerde antinociceptie te kwantificeren aan de specifieke patiëntenpopulatie die we hebben onderzocht (onze populatie was ongevoelig voor koud waterprikkel). Oudere personen hebben moeite met het scoren van nociceptie, vooral wanneer ze worden blootgesteld aan opioïden. Dit kan te maken hebben met een reeks leeftijdsgebonden veranderingen in de fysiologie, zoals verminderde C-vezeldichtheid in de huid, veranderingen in centrale pijnverwerking en cognitieve veranderingen. Bovendien beïnvloedt obesitas het juist beoordelen van nociceptieve prikkels negatief.

Ten slotte, in **chapter 5**, vergeleken we de hypoxische gevoeligheid tussen patiënten met diabetes type 2 (T2DM) en gezonde vrijwilligers en bestudeerden we de effecten van hyperinsulinemie op hypoxische gevoeligheid. Tijdens vasten zagen we geen verschillen tussen deze twee groepen, maar opvallend genoeg kwamen er tijdens euglycemische-hyperinsulinemie significante veranderingen naar voren. Verhoogde hypoxische gevoeligheid werd waargenomen bij gezonde controles, maar niet bij insulineresistente individuen. Bovendien nam tijdens hyperinsulinemie de hyperoxische inhibitie toe bij patiënten met T2DM, wat mogelijk wijst op een verhoogde excitatie van de carotislichaampjes. Dit duidt op een negatief effect van T2DM op de carotislichaampjes, met een indicatie van insulineresistentie van dat specifieke orgaan, hoewel het carotissysteem lijkt te verkeren in een staat van hyperexcitatie.



# Addenda

---

## Curriculum Vitae

Pieter Simons werd geboren op 6 december 1991 in Enschede. Als jongste kind van Paul en Maria Simons, groeide hij samen met Anneriek op tussen het groen. De eerste bouwstenen van zijn onderwijs werden gelegd op Montessorischool de Wielerbaan en later op het Stedelijk Lyceum Zuid, waar een sterke interesse voor biologie, scheikunde en sport werd aangewakkerd.

Deze interesse kon hij kwijt in de studie geneeskunde aan de Rijksuniversiteit Groningen, waar hij in 2010 aan begon. Tijdens zijn studie deed hij onderzoekservaring op bij het studententraumateam onder leiding van prof. dr. Jan Hulscher en later bij de SICS Study Group onder leiding van prof. dr. Iwan van der Horst. Ter verdieping volgde hij een minor Philosophy of the Life Sciences. Buiten zijn studie was hij actief bij de studievereniging en de Groninger Studenten Kitesurf Vereniging. De coschappen in binnen- en buitenland, werden opgevolgd door periodes als arts-assistent op de spoedeisende hulp in Emmen en later tijdens de COVID-19-pandemie in het Rode Kruis Ziekenhuis in Beverwijk, afgewisseld met werk als scheepsarts. Na de eerste stappen in de kliniek, mocht hij in het najaar van 2020 starten met een promotietraject bij de Anesthesia & Pain Research Unit in het LUMC, waaruit het werk voortvloeide beschreven in dit proefschrift.

Buiten het ziekenhuis is Pieter actief bij Outdoor Medicine, dat een platform biedt voor geïnteresseerden in expeditie geneeskunde, wildernisgeneeskunde of geneeskunde in extreme omstandigheden. Deze interesse kwam samen met onderzoek tijdens de laatste fase van zijn promotietraject, waar hij meewerkte aan een onderzoek naar de determinanten van hoogteziekte bij het EURAC Institute of Mountain Emergency Medicine. In de toekomst wil Pieter actief blijven meewerken aan onderzoek en kennisoverdracht op het gebied van respiratoire (patho)fysiologie, zowel binnen - als buiten het ziekenhuis.

---

## Portfolio

Phd Training	Year
<b>Courses</b>	
Taking control of your academic career	2024
Storytelling Lab (Graduate School Leiden)	2024
Scientific Conduct for PhD's (Graduate School Leiden)	2023
Clinical Epidemiology (Boerhaave CME)	2023
Academic Writing for PhDs (Graduate School Leiden)	2022
BROK - Good Clinical Practice (Boerhaave CME)	2022
Communication in Science (Graduate School Leiden)	2022
Basic Methods and Reasoning in Biostatistics (Boerhaave CME)	2021
R for Data Analysis (Boerhaave CME)	2020
<b>Presentations and conferences</b>	
Insulin and the Carotid Body <i>Oral presentation, NVA Wetenschapsdag 2023, Utrecht, the Netherlands</i>	2023
Insulin and the Carotid Body <i>Oral presentation, LUMC Anesthesiologie/IC Wetenschapsdag 2023, Leiden, the Netherlands</i>	2023
A randomized, double-blind crossover trial comparing oliceridine and morphine on ventilatory control in an elderly population <i>Oral presentation ASA 2022 annual meeting - Best of Abstracts: Clinical Science Session, New Orleans, United States</i>	2022
Respiratory Effects of Biased Ligand Oliceridine in Older Volunteers <i>NVA Wetenschapsdag 2022, Amersfoort, the Netherlands</i>	2022
Why prick, when you can lick? Sublingual Esketamine OTF <i>Oral presentation, LUMC Anesthesiologie/IC Wetenschapsdag 2022, Leiden, the Netherlands</i>	2022

---

---

## List of Publications

1. **Simons, P.**, Schrier, R. van der, Lemmen, M. van, Jansen, S., Kuijpers, K., Velzen, M. van, Sarton, E., Nicklas, T., Michalsky, C., Demitrack, M., Fossler, M., Olofsen, E., Niesters, M., Dahan, A. (2023). Respiratory Effects of Biased Ligand Oliceridine in Older Volunteers: A Pharmacokinetic-Pharmacodynamic Comparison with Morphine. *Anesthesiology*, 138, 249–263.
2. Dam, C. van, Schrier, R. van der, Velzen, M. van, Lemmen, M. van, **Simons, P.**, Kuijpers, K., Jansen, S., Kowal, M., Olofsen, E., Kramers, C., Dahan, A., Niesters, M. (2023). Inhaled Delta(9)-tetrahydrocannabinol does not enhance oxycodone-induced respiratory depression: randomised controlled trial in healthy volunteers. *Br J Anaesth*, 130, 485–493.
3. **Simons, P.**, Olofsen, E., Velzen, M. van, Lemmen, M. van, Mooren, R., Dasselaar, T. van, Mohr, P., Hammes, F., Schrier, R. van der, Niesters, M., Dahan, A. (2022). S-Ketamine Oral Thin Film-Part 1: Population Pharmacokinetics of S-Ketamine, S-Norketamine and S-Hydroxynorketamine. *Front Pain Res (Lausanne)*, 3, 946486.
4. **Simons, P.**, Olofsen, E., Velzen, M. van, Lemmen, M. van, Dasselaar, T. van, Mohr, P., Hammes, F., Schrier, R. van der, Niesters, M., Dahan, A. (2022). S-Ketamine oral thin film-Part 2: Population pharmacodynamics of S-ketamine, S-norketamine and S-hydroxynorketamine. *Front Pain Res (Lausanne)*, 3, 946487.
5. Diepen, A. van, **Simons, P.**, Bos, J., Kramers, C. Metamizol: current status in Dutch practice. (2022) *Ned Tijdschr Geneeskd*, 166.
6. Dahan, A., Lemmen, M. van, Jansen, S., **Simons, P.**, Schrier, R. van der. (2022). Buprenorphine: a treatment and cause of opioid-induced respiratory depression. *Br J Anaesth*, 128, 402–404.



## Dankwoord

Na bijna vier jaar promoveren zijn enkele woorden van waardering op zijn plaats. De totstandkoming van dit proefschrift is mede door de bijdrage en samenwerking van vele anderen.

Allereerst, naar mijn promotor prof. dr. A. Dahan en copromotores dr. M. Niesters en dr. M. van Velzen.

Beste Albert, bedankt voor het vertrouwen en de energie om samen met mij een promotietraject aan te gaan. Jouw kennis, kunde en drive zijn een bron van inspiratie. Ik heb veel kunnen leren en je zette vaart achter mijn promotie. Beste Monique, bedankt voor de korte lijntjes, je kordaatheid en hulp bij het opzetten van de studies.

Beste Marieke, op de fundamenten van de lijn ketamineonderzoek in het LUMC, waar jij belangrijke bijdrage aan hebt geleverd, mocht ik mijn eerste studies opzetten. Jullie allen bedankt voor de begeleiding en mijn ontwikkeling als wetenschapper.

Aan prof. dr. L.P.H.J. Aarts en prof. dr. E.Y. Sarton, bedankt voor het navigeren van het schip.

Beste Rutger, dank voor het begeleiden van ademhalingsstudies. Jouw kroonjuweel, de nieuwe mixer, kwam op precies het goede moment tijdens de eerste proefpersoon van de Oliceridine studie. Beter had ik niet kunnen wensen. Ik heb genoten van je humor, relativiseringsvermogen en interesse in het onderzoek.

Beste Erik, bedankt voor jouw kunde en aandeel. De geïntegreerde PK-PD modellen zijn een drijvende kracht achter ons onderzoek.

Naar René, alle stafleden, in het bijzonder op de 99543, wetenschapsstudenten en latere promovendi, Tom, Maarten, Kiki en Anita bedankt voor jullie bijdrage.

Beste mede-promovendi, we hebben samen heel wat uurtjes in J5-37 en het grote lab doorgebracht. Dikke dankjewel voor de samenwerking en goede tijd. Let's go, Pels!

Sebas, een grand merci voor je hulp tijdens de fietstrip Maastricht-Basel. Ondanks een detour naar Troisvierges, werd er vanuit Hôtel Europe te Saverne op tijd een brief verstuurd.

Anneriek en Arne, mijn bruidsmeisje en bruidsjonker, succes met het verdedigen van dit proefschrift als ik van een berg val.

---

Verder wil ik alle vrienden uit Groningen, Den Haag, van Outdoor Medicine en de (schoon)familie bedanken voor het sparren en de ontspanning tussendoor.

Pa en Ma, onmeinig bedankt voor het aanwakkeren van mijn nieuwsgierigheid en eigenfilosofie.

Lieve Manouk, wij leerden elkaar halverwege dit promotietraject kennen, tijdens pieken en dalen. Je geeft mijn leven kleur. Bedankt voor je begrip, steun en fijne tijd samen.



